Body Composition Analysis using Air Displacement Plethysmography

Chuan-Hsiao Peter Ma

University of Cape Town

A dissertation submitted to the Faculty of Health Science at the University of Cape Town in partial fulfillment of the requirements for the degree of Master of Science in medicine in the field of Biomedical Engineering.

August 2004

The copyright of this thesis vests in the author. No quotation from it or information derived from it is to be published without full acknowledgement of the source. The thesis is to be used for private study or non-commercial research purposes only.

Published by the University of Cape Town (UCT) in terms of the non-exclusive license granted to UCT by the author.

University of Cape Town

Acknowledgements

I would like to thank the following people for their contributions toward this thesis:

My family, for their endless love.

Dr. W. Capper, for serving as my supervisor, for technical advice and for sourcing equipment for this project, as well as for editing the manuscript.

Harry, John and Charles, for their professional advice on designing and constructing the device.

Kit, for his encouragement and faith.

Rafal, for his time reading and editing this thesis. For his constant support and valid points given for this.

Elias, Bruce, Nazir ,Rex for their support through the whole three years

Libra Bathware for the donation of the bath tube used in the construction of the chamber.

Respiratory ICU C27 Groote Schuur hospital for their donation of ventilator and plunger calibrator used in this project.

The University of Cape Town research committee for funding this project.

DECLARATION

I, _____, hereby declare that the work on which this thesis is based is my original work (except where acknowledgements indicate otherwise), and that neither the whole work nor any part of it has been, is being, or is to be submitted for another degree in this or any other university.

I empower the University of Cape Town to reproduce for the purpose of research either the whole or any portion of the contents in any manner whatsoever.

_____

Signature

_____

Date

Synopsis

In modern times, preventative medicine has become a major international focus. Body composition analysis and in particular the estimation of the percentage of body fat is an important tool for disease management. The percentage of body fat has the potential to be a tool health practitioners can use to suggest lifestyle and dietary changes that can help prevent disease.

The approach taken in devising a low cost body composition measuring device is the principle of plethysmography. This approach measures the density of an object by measuring the volume of air the object displaces as well as the objects mass.

A principle assumption of this approach is the validity of the Two Component Model of body composition (2C Model). The model states that the human body can be split into two components of constant density: Fat (which has a measured density of $0.9\,g/cm^3$) and Non-fat tissue (which has a measured density of $1.1\,g/cm^3$). The validity of the 2C model allows an individual's body fat percentage to be determined following the calculation of that individual's body density. According to the 2C model, a person who has a density of $1.06\ g/cm^3$ (according to the 2C Model) has 15% of body fat.

This dissertation investigates other methods of body fat determination and suggests why air displacement plethysmography (ADP) is the best solution for the aims of the project. A theoretical analysis of ADP has indicated that the volume needs to be determined to an accuracy of within 200 ml for a ±2% precision in body fat estimation.

This model also demonstrates how this initial goal can be achieved with in vivo studies. The various parameters of the model are examined to determine the sensitivity of % body fat estimation to various errors of measurement in each respective parameter.

A low cost ADP device that measures the volume of an unknown test object has been constructed based on the theoretical model. This device consists of a measuring chamber and a reference chamber. Each connects to a motor driven piston pump. The pressure difference between the chambers is sensed and calibrated with known test volumes in the measuring chamber. After callbration the volume of unknown objects can be determined from the pressure differential using the correlation equation. The constructed ADP device provides repeatable ± 300ml precision on inanimate objects. Using the 2C model, this accuracy in volume measurement results in a 3% inaccuracy in the determination of body fat percentage.

Although this error is not low enough for a biologically meaningful result in body composition analysis, the major factors that cause error have been identified and investigated. In particular, it has been found that the piston pump frequency must be stable and constant within 0.06rpm. The recommendation for further development therefore is that a stepper motor driven piston or a precision loud speaker system be used to compress the air in the chambers, at a precise and constant frequency. Theoretical investigations reveal that these will allow accuracy of the volume measurement to be within 200 ml.

A solid foundation has been established for a low cost device. The total cost of this device including future development is estimated to be less than 10% of the existing commercial devices. This will provide a practical tool for medical practitioners involved in preventative medicine, and will also allow interventional procedures to be monitored and assessed.

Table of Contents

List of Figures

List of Tables

1. Introduction

1.1. What is body composition

The term is often used to describe the proportion of total body mass that is composed of adipose tissue. Body composition is the true definition of an individual's weight status.

The body can be represented by the molecules that constitute the whole. A broader definition is to specify the components of the human body in terms of:

- Total body fat
- Total body water
- Total body mineral
- Total body protein

As such, the human body can be seen as a multi component model by defining the composition in terms of the various components.

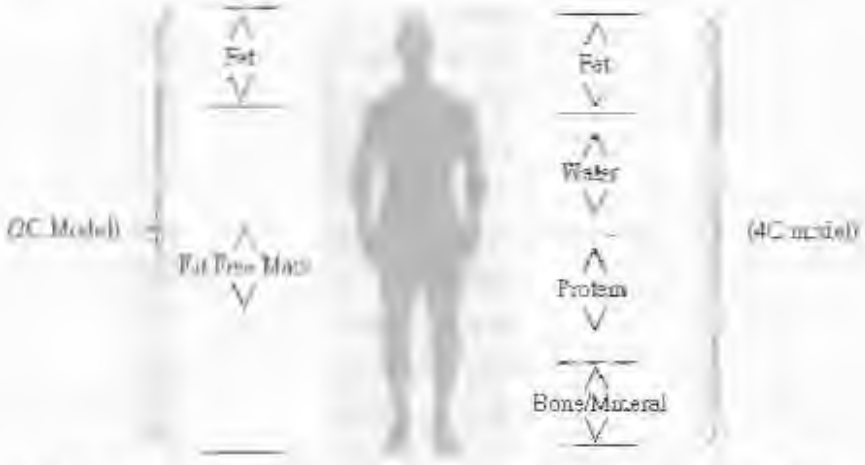

Figure 1.1 Different compartment models of the human body

1.2. How to determine body composition

Body composition analysis is the process of estimating the composition of the human body. Researchers often use models comprising two, three or four compartments to represent the human body, abbreviated as 2C, 3C, 4C respectively.

With each additional measurement it may possible to extend the number of compartments in the body composition model. Each measurement must be compositionally independent of the other measurements. The assumption has to be made that these compartments have well defined properties.

However, some of the approaches are costly, time consuming and often not practical. Therefore many researchers and clinicians continue to rely on a basic two-compartment (2C) model to assess body composition. The classic 2C model of body composition divides body weight into fat mass (FM) and fat free mass (FFM). These two components have well defined properties which can be measured. In particular, the density of FM and the density of FFM can each be taken as constant. A limitation of the 2C model is that the FFM and FM densities are not universally constant and exhibit small variations.

1.3. The importance of understanding body composition

Statistics indicate that obesity in both children and adults have increased in the past 20 years. There is a strong relationship between obesity in children and adult obesity. Using the body mass index (BMI) as a reference, readings above 25 in males and above 32 in females are associated with higher levels of cardiovascular disease (Williams *et al* 1992).

The link between excess body fat and conditions such as:

- coronary heart disease
- hypertension
- hyperlipidemia
- hypercholesterolemia
- myocardial infarction
- type II diabetes

has been observed in studies where subjects are obese and blood lipid levels and blood pressure are high, and glucose tolerance is low compared with an individual with less body fat (Aristimuno *et al* 1984; Berenson *et al* 1980).

The above motivates the use of the knowledge of fat mass as an important tool for doctors in health assessment.

It is important to note that a lack of fat can also be an important issue. Adolescents, elderly patrons and malnourished infants can suffer vascular conditions related to a low level of fat mass (Evans *et al* 1993). There is an increased awareness of the role that fat plays in the body, with a widespread understanding that a level of fat is required in order to live healthily and can decrease the incidence of eating disorders such as Binge and Bulimia in adolescents (Fairburn *et al* 1993). While prevalence of anorexia nervosa has been relatively stable in the past decade, (Fairburn, *et al* 1993) a high prevalence of body weight dissatisfaction is observed, especially in female adolescents. It is important to educate people to avoid the emphasis on low weight that is strongly pervasive in western culture. The aim is that society places less emphasis on body weight and more on body fat, which is more important in body perception. This is to stop people from losing body water and lean muscle mass in an attempt to weigh less (imagining they are shedding fat) which has the ultimate effect of slowing down metabolism and retarding the body from natural fat burning.

Body composition analysis can also help sport science researchers to optimize the training programs of their athletes. It provides useful information such as basal metabolic rate (BMR) for athletes to make necessary adjustments to their training programs. BMR is defined as the total calories burnt in 24 hours when at complete rest. A person's total caloric energy requirement can be estimated from the results of body composition analysis.

1.3.1. The Wellness Principle

The advantages of a healthy range of body fat percentage are well documented. However few people are able to or have measured their own body composition to estimate their own percentage body fat.

Wellness is a collective term for adequate nutrition, sleep, low alcohol intake, stress management and exercise. The collective effect of these elements is to keep the body in harmony, which can greatly reduce the chances of disease occurring.

Wellness is the principle that prevention is cheaper and quicker than treatment and that this prevention is achieved from following a wellness strategy.

Professor Tim Noakes of the Sports Science Institute South Africa (SSISA) has long been a proponent of the Wellness Principle for many years. He concluded "Exercise is the cheapest and the most effective preventive medicine yet discovered." Exercise brings down the percentage of body fat and hence that reduces the risk of stroke as well as other peripheral arterial disease (Noakes 2001).

Scale weight alone does not necessarily mean an individual is lean or fat. Only body composition analysis can determine how much muscle and fat are lost or gained as a result of any nutritional, exercise or pharmaceutical program.

The knowledge of one's body fat will help to promote permanent successful fat loss. Focusing on losing fat and maintaining or increasing lean muscle is a much healthier way to increase longevity and fat loss. This leads to my mantra catch phrase: Get people to talk about the fat content rather than weight!

1.4. Aims of the thesis

- Review the principal findings related to body composition analysis
- Investigate potential field methods
- Develop a low cost body composition analysis system
- Determine the accuracy of this device
- Identify the sources of error and quantify these errors

1.5. Method

This thesis is divided into the following parts:

Background studies

- History of body composition analysis
- Literature review on different body composition methods
- Comparison between these methods
- Discussing the cost and practical constraints of these methods

Determining the most appropriate body composition analysis method for use in the field

- Selecting a method of analysis for the project and a global standard with which it can be compared
- Theoretical analysis of these methods
- Identifying and commenting on the impact of assumptions made in these methods.

Design and Construction of the system

- Design of the device
- Evaluation of the design based on the available materials before construction
- Construction of the device

Trial Studies

- Studies on inanimate subjects
- Comments on the trial studies using the constructed system
- Evaluation of the device

Discussion, conclusions and further recommendations

2. Literature Review

2.1. Introduction

The literature review covers the background study of the development of body composition analysis. The various methods to measure body composition are briefly reviewed and compared with one another. The comparison shows why air displacement plethysmography (ADP) is the most suitable method and why the DEXA method is the best available reference method for this project.

The DEXA method of body composition is then reviewed in greater detail in the following chapter.

2.2. Historical review of body composition

At the turn of the twentieth century the study of gross body composition was pioneered by agriculture. Physiologists and scientists would take samples of the body's components directly from living subjects. Dissections on human cadavers were also performed (Haecker 1920, Moultion *et al* 1922, Pitts 1963). These researches focused mainly on the weight of the organs. The research showed that the chemical composition of humans is constant among individuals. Data obtained from the direct dissection of the cadaver has served as a reference for human body composition.

The method of dissection allows for direct measurement of the density, mass and size of tissues and organs. However, the inherent difficulties in retrieving samples are that the environment is not hygienic and dissection is not practically straightforward. Assumptions are made when only part of the tissue from an organ can be obtained. It is difficult to extrapolate from a sample of tissue to a complete organ, and more so to the whole body (Ellis 2000).

The difficulties mentioned above result in measurement error and hence the difficulty in drawing conclusions about the density of tissue in the human body.

Keys and Brozek (1953) measured the density of fat at 0.9007g/cc and the density of other fat-free mass at about 1.100g/cc. They observed that the density of fat is constant between individuals and that there is a significant difference in the density of fat mass and fat free mass. This observation resulted in the two component model (2C Model) to analyze body fat percentage.

Densitometric formulas have been developed by Siri (1961) and Keys and Brozek (1963). The densitometric formulas are:

Siri: Body Fat = 495 / Db – 450 (2.1)

Brozek: Body Fat = 457 /Db – 414.2 (2.2)

Db is the total body density; see section 9.4 for the discussion of these derived formulas and appendix A1 for the derivation of the two compartment model.

The fundamental difference between FM (Fat mass) and FFM (Fat-free mass) and the consistency of the density of both FM and FFM have led to the widespread acceptance of these formulas. This methodology has been recognized as the "gold standard" for 2C non-invasive body composition assessment. The determination of the percentage of body fat (%BF) follows from the measurement of body density.

Body density (Db) is the ratio of total body mass to body volume. Body mass can be obtained from a calibrated mass scale. Hence Db and %BF can be derived from measurement of the total body volume.

2.3. Body composition methods

The review covers most of the practical body composition methods. Other methods such as Helium Dilution (Edelman *et al* 1952) to measure body volume have not been included as they do not have the potential to be practical field methods and can only be used as reference methods.

The following methods are reviewed:

- Anthropometry-Based models
  - Body mass index (BMI)
  - Skinfold calliper
- Bioelectrical and conductance methods
  - Bioelectrical impedance analysis (BIA)
  - Near Infrared Interactance (NII)
- Body Volumetry
  - Hydrodensitometry (HW)
  - Air displacement plethysmography (ADP)
  - Three dimensional Photonic scanning
- Body imaging model
  - Dual –energy X-Ray absorptiometry (DEXA)
  - Computer Tomography (CT) and Magnetic Resonance imaging (MRI)

2.4. Anthropometry-based models

2.4.1. Body mass index (BMI)

Body mass index is the ratio of mass to the height squared (kg/m^2). It is one of the most common ways to give an indication of the body status.

The main weakness of the model is that it makes inference about body fat without taking fat into consideration. Different organizations suggest different standards of BMI although this subjectivity can confuse the interpretation of body status. See appendix A2 for the interpretation from the World health Organization (WHO).

2.4.2. Skinfold calliper

Skinfold calliper is one of the most widely used field methods in body composition measurement due to its cost and availability.

Skinfold calliper assumes that 50% of an individual's body fat is under the skin and 50% is inside the muscle. This is the major assumption and source of error in this method. It measures the thickness of skin and fat at various points on the body (bicep, triceps, scapula, and hip) and with the knowledge of anthropometric data; the body composition is predicted using equations derived for each age group.

Some shortcomings are:

- A true skinfold assessment requires trained experts
- Results can vary between different experts doing the assessment
- Different types of callipers use different formulas to interpret their results

2.5. Bioelectrical and conductance methods

2.5.1. Bioelectrical impedance analysis (BIA)

The basic principle of BIA is that fat has high impedance (which refers to the degree to which the passage of charged particles is obstructed) compared to muscle. Therefore charge flows with less resistance through muscle than it does through fat. This is because lean tissue is ¾ water, and water is a good conductor (National Institutes of health 1996).

BIA measures the impedance of the body using small electrical currents. The method assumes that the body is approximately cylindrical and of uniform cross section. In this case body volume can be calculated, since it is proportional to body length squared divided by impedance. This measurement is performed using four electrodes: usually two are attached at the wrist and two at the ankle. A constant current is injected between the wrist and ankle, and the resultant voltage between these sites is measured, with Z=V/I. The leaner and shorter the individual, the lower the observed voltage. Body composition is then estimated from the impedance and the height.

BIA is probably the most frequently used laboratory method (Ellis 2000) due to the relatively inexpensive cost of the basic instruments, its ease of operation, and its portability. There are no risks or side effects with this procedure (Ellis 2000).

The downside of the BIA includes the following points:

- Hydration level
- Distribution of water in the body
- Tissue orientation
- Body temperature

The results are very sensitive to hydration levels. High levels of hydration reduce the impedance and lower the body fat reading. Exercise can cause such a problem. An individual's exercise level, alcohol intake and hydration levels will vary during the day and over time. (National Institutes of health 1996, Ellis 1999 *et al*, Body composition Lab. Univ. of Vermont) reducing the validity of BIA.

The distribution of water through the body varies when the subject lies down for more than a few minutes. The fluids tend to settle and this changes the distribution of the body water, hence results are unpredictable due to the change in impedance. The end result is a volatile body composition result. (Body composition Lab. Univ. of Vermont)

If the tissue is oriented perpendicular to the current flow, the current is slowed by the increased number of membranes. If the tissue is oriented parallel to the current flow, the impedance is reduced.

Variations in body temperature also have an effect on the precision of the result. As a warm tube of solution has a higher conductivity than a cold tube, an increase in body temperature can underestimate the body fat.

The accuracy of the result should be used with caution ((National institutes of health 1996, Ellis *et al* 1999) considering the complications discussed above.

2.5.2. Near infrared interactance (NII)

Near Infrared Interactance measures the subcutaneous fat at a single site only e.g. the dominant arm's bicep (Schreiner *et al* 1995).

The method is considered relatively easy and convenient with good repeatability. Testing consists of a fibre optic probe positioned over the bicep. Two infrared beams of slightly different frequency are transmitted into the bicep and the reflections monitored (Schreiner *et al* 1995). The proportion of the reflections determines the percentage of the body fat, since the reflections from muscle are different from those from fat.

The biggest weakness is that it can measure subcutaneous fat at a single point only and does not take the whole body into consideration. This is similar to BMI where individuals with varying fat distribution on the body will have large errors of measurement.

The results are sensitive to skin colour and hydration levels, which are sources of measurement error. The method also requires careful instruction as the readings can be distorted by incorrect bicep positioning.

This method tends to overestimate body fat in lean individuals and underestimate body fat in obese individuals.

2.6. Body volumetry

2.6.1. Hydrodensitometry (HW)

Hydrodensitometry (HW) is an established method for measuring body volume based on Archimedes' principle (see appendix A3). The accuracy, its early development and consistency have resulted in HW being the most commonly used method for determining total body volume.

HW requires the subject to be completely submerged in temperature controlled water and then weighed (Behnke, *et al* 1942). As the density of water is known, the person's loss of weight in the water (due to buoyancy) is equal to the weight of the volume of water displaced.

The lung volume is measured by helium dilution while the subject is in water. The size of the lung varies from person to person so it is necessary to know the lung volume. Body volume can be calculated by subtracting the lung volume from the total volume.

- The approach is cumbersome (figure 2.1.)
- Not practical
- Requires cooperation
- Time consuming (usually over 30minutes)
- Requires a well trained field worker
- This task is more complex for the handicapped
- Not suitable for elderly or unwell individuals.

modern medicine, this method has been considered as a reference ethod rather than a practical field method.

gure 2.1 Photograph of underwater weighing apparatus
ehnke, *et al* 1942)

2.6.2. Air displacement plethysmography (ADP)

Plethysmography refers to the measurement of volume. In air displacement plethysmography, the subject is placed in a plethysmograph. The human body will displace a volume of air that is equal his or her body volume. The volume of the subject can therefore be measured indirectly by measuring the volume of the remaining air in the plethysmograph.

This can be calculated by applying Boyle's law which states pressure (P) and volume (V) are inversely related when the temperature is constant (i.e. isothermal condition).

$$P \times V = \text{constant} \qquad (2.3)$$

The advantages of ADP are:

- The patient will not need to be submerged into water, which will increase the acceptability of the method by subjects.

- The air in the cavities is compressed with the rest of the air in the chamber and therefore does not contribute to the apparent body volume (Taylor *et al* 1985).

The weakness of the method is caused by distorting effects such as humidity, temperature and breathing, which are all related and have a sizeable impact on the accuracy of body volume estimations.

Development of Air Displacement Plethysmography

The principle of air displacement plethysmography was first described by Jaeger around 1878 (quoted in Wedgewood 1953). In the early 1900's research focused on measuring the volume of infants, (Murlin *et al* 1913, Pfaundler 1916) where child cadavers and reference materials of known volume were used in the studies.

Studies have been performed on living dogs by Kohlrausch (1929) where the following issues were identified:

- Humidity effect
- Temperature effect
- Respiratory effect

The humidity affects the Boyle's constant in a closed system. The chamber of the plethysmograph was filled with saturated water vapour to counter the effect of changing humidity. Other researchers such as Bohnenkamp and Schmah, (1931) used similar techniques to address the humidity issue. In addition they used fans and a cooling system to maintain a constant temperature. To date, however, the respiratory effect has not been solved.

Noyons (1935) and Jongbloed (1938) had a different approach to measure volume. They altered the ambient pressure in their plethysmograph. As air density varied, the body weight was obtained from the variation in the density of air. No further studies have been done in this direction because of the discomfort claimed by subjects during the procedure. It was also difficult to seal the chamber. This approach did not address the issues raised by Kohlrausch.

New Generation Development in ADP

In a later development, a sinusoidal displacement volume was proposed by Wedgewood (1963). The volume in the chamber was altered by a displacement tool, which changed the volume in a pre-determined manner serving to overcome the difficulty of changing variables with in vivo studies (the temperature, humidity and breathing effect).

A stable system (with more robust results) was only developed around 1960 (Friis-Hansen 1963). This system required one to two hours of calibration and an additional two to three hours of measuring time due to rapid fluctuations in temperature, humidity and pressure. Gnaedinger (1963) concluded that the error in volume measurement was due to these three terms.

The systems would be considered impractical and not suitable for body composition analysis if these errors could not be removed (Gnaedinger 1963).

Developments in the last 20 years

Modern and quick improvements in technology developed during the 1980's, such as the advent of a motor driven pump (Petty *et al*, 1984) and a two chambered dynamic pressure differential system, improved the use of plethysmographs (Taylor *et al* 1985).

A sinusoidal moving piston was placed between the two chambers (a reference chamber and a test chamber). This allowed for the pressure in the test chamber to be compared with the pressure in the reference chamber and this reduced the effects of temperature and humidity. Harmonic analysis was used to process the pressure signals in order to measure body volume.

Another advancement in the method of ADP was the compensation for the effect of the body surface area and isothermal heat emission. In particular, Gundlach and Visscher (1986) had subjects wrapped in blankets and instructed to hold their breath during the measurement, in order to maintain isothermal conditions.

Their system also used the pump and the pressure drive mentioned above. They added consideration of isothermal air. It provides a better result than underwater weighing but the difficult preparation makes this method impractical for daily use.

Development in the last 10 years

In the mid 1990's BOD POD (life measurement, Inc. Concord, CA) was the first commercial product to use air displacement plethysmography (ADP).

Description of BOD POD

It consists of a single structure containing two chambers. A fiberglass seat is placed in one of the chambers. A diaphragm is placed between the two chambers which generates pressure changes (figure 2.2). Fourier coefficients are used to calculate pressure amplitude at the frequency of oscillation. Temperature changes during the measurement period are monitored and taken into account. (Dempster and Aitkens 1995)

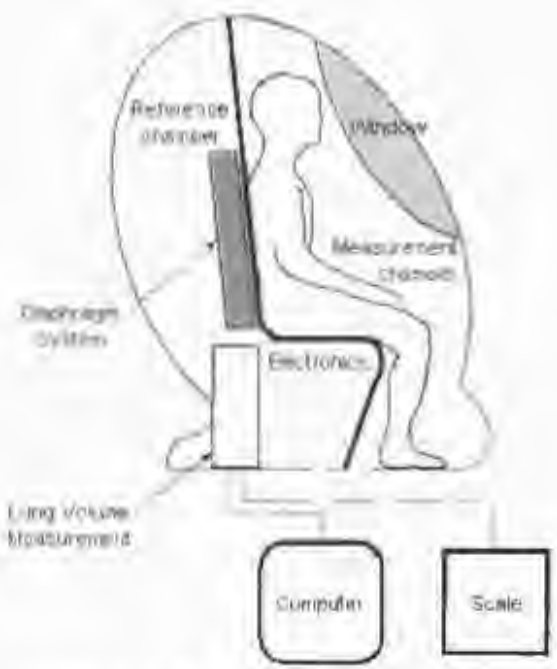

Figure 2.2 BodPod (www.bodpod.com)

Many studies compared the differences between BOD POD and HW. Some studies showed no significant differences between the two methods (%BF < 0.5) (McCrory *et al* 1995, Biaggi *et al* 1999, Collins *et al* 1999, Levenhagen *et al* 1999, Field *et al* 2002); while others showed a mean difference from –4.0% to 1.9% (Iwaoka *et al* 1998, Dewit *et al* 2000, Wells *et al* 2000, Millard-Stafford *et al* 2001).

The largest difference (-4.0% and 3.3%) occurred in the 2 studies (Iwaoka *et al* 1998, Dewit *et al* 2000) with the fewest subjects ($n < 10$). ADP has been suggested by many studies as the gold standard in body composition analysis.

2.6.3. Three dimensional photonic scanning

Three dimensional photonic scanning is an innovative approach to determine body volume. This technique is relatively fast (12 second scan period) and is of low cost. Originally used in the clothing industry, the system is made of eight imaging units, with each unit measuring the reflection from 32 infra-red LED's. This means that 256 points on the body can be obtained (left part of figure 2.3). The body surface (skin) can be reconstructed using a curve fitting algorithm from the data points obtained (right part of figure 2.3)

Figure 2.3 Scan configuration (left) and quadmesh representation for skin surface (right) (Wells *et al* 2000)

The precision for measuring body volume is ~3% which is too high to use in determining body composition. The main source of the error is in standardizing the thoracic volume during the scan (Wells *et al* 2000). The thoracic volume is not part of the volume of the subject while the scan includes thoracic volume, so will need to be subtracted.

2.7. Body imaging model

2.7.1. Dual energy X-Ray absorptiometry (DEXA)

Dual photon absorptiometry (DPA) became clinically available in the early 1980s. Photon absorptiometry required a photon source and a detector. The subject was placed between the photon source and the detector; and an image of the body was acquired. Radionuclide elements such as I, Am, Cd and Gd were used as the photon source.

Over the past decade, the radionuclide source photons was replaced by an X-ray source (hence DEXA.); it is a great advantage due to its low radiation.

Figure 2 4 A clinically used DEXA machine

The primary application of DEXA has been the measurement of the bone mineral content (BMC). DEXA has been suggested to be the best clinical diagnosis tool to measure bone loss in Osteopenia and osteoporosis.

More recently, DEXA techniques have been applied to body composition analysis (including in vivo studies). Many reviews (Brunton *et al* 1993, Svendsen *et al* 1993, Tothall *et al* 1994, Prior *et al* 1997, Kohrt 1998) have examined the validity of DEXA and these suggest it to be the latest gold standard in body composition. Such a device is also available in the Sport Science Institute South Africa (SSISA). It is felt that this is the best reference method available at present. Hence the theory and the assumptions of this method are discussed in more detail in the following chapter.

2.7.2. Computer Tomography (CT) & Magnetic resonance imaging (MRI)

Both CT and MRI can provide the basic anatomical image of the human body using reconstruction algorithms. Studies show both methods have excellent accuracy and precision (<1% error in body fat measurement). However, the cost of the studies is high for both of the methods. For MRI the measuring time is in excess of 30 minutes. In CT, the scan time is much shorter. The radiation doses required for a CT scan make this method unsuitable for daily use. These methods have good potential in determining body composition if the practical constraints can be overcome.

2.8. Comparison table of different measuring Methods

The methods reviewed above are compared in terms of

- Theoretical assumptions
- Pros
- Cons
- Accuracy
- Cost

Methods of body composition analysis can be inaccurate due to model error and/or parameter error. The theoretical assumptions bear the most importance as the results are largely influenced by model error, which is described by the theoretical assumptions. Cost, mentioned last, is important as it can limit the extent of usage, as low cost is a major aim of this project.

Table 2.1

Comparison of various methods for body composition analysis

Method	Principle Assumption	Advantage	Disadvantage	Accuracy for %BF	Cost
BMI	Over weight=Fat	Simple	Not directly related to %BF	Low	Inexpensive
Skinfold caliper	½ Body fat is under the skin surface	Fast, cheap	Inaccurate, require trained operator	Low	Inexpensive
BIA	Water is 3/4 of the total body	Relative fast and portable	Hydration effect	<5%	Inexpensive
NIR	Body composition can be determined at one point	Fast and portable	Not a whole body measurement	<10%	Inexpensive
HW	Fat and fat free mass are constant among race groups.	Accurate	Cumbersome	<4%	Inexpensive
ADP		Fast and accurate	Availability	<3%	Inexpensive
3D scan		Fast	Prediction of the lung volume required	<15%	Medium
DEXA	Body hydration is constant	Fast accuracy	Availability	<3%	Expensive
CT& MRI		Precision	Time consumption	<1%	Very Expensive

The table shows that the DEXA model has the advantage of being fast and accurate but expensive; the Skinfold calliper is fast and cheap (with good availability), however inaccurate. Likewise the ADP scores highly on cost, relative accuracy, and practical use.

As far as assumptions go, the assumption of constant density involves model errors which may limit their use for accurate measurement (i.e. ADP is better suited to measure changes in body fat from day to day, than as an accurate measurement at any given time).

2.9. Conclusion

Hydrodensitometry (HW), Air displacement plethysmography (ADP) and Dual energy X-ray absorptiometry (DEXA) have all been rated as gold standards at different times.

There are assumptions and uncertainty in all three methods. Thus none of these methods can be regarded as a perfect measure of body composition. ADP and DEXA are discussed in more detail because they have the following common advantages over HW: good repeatability, fast, convenient, high acceptance and relatively good accuracy. Because of these advantages and its low cost; ADP has been chosen as the method most suitable for implementation in this project. DEXA has been chosen as a reference method because DEXA is available for cross referencing at the Sports Science Institute South Africa (SSISA) and it is a significantly different method from ADP.

A detailed investigation of the theory of DEXA and ADP follow in the 3rd and 4th chapter. The errors (model and parameter) are identified and quantified.

3. Concept of dual energy X-Ray absorptiometry (DEXA)

3.1. Introduction

The human body can be regarded as a form with several different compartments. This chapter describes how DEXA can determine the mass of each of these compartments. Firstly, the concept of the x-ray and how it works is covered as it is a fundamental precursor to DEXA. We will see how x-ray can be used to determine the mass of a homogenous absorber; (such as a single element, or compound solution) then see how x-ray works on a heterogeneous absorber (such as the human body).

The aim of this chapter is to explain the fundamentals of DEXA to support its use as a reference method. As a reference method it will be used to validate the results of ADP analysis in future research.

The intention of having this chapter is not to discuss the details of DEXA or to clearly understand its methodology. It is sufficient for the aims of the project to identify the assumptions and its practical constraints.

3.2. Obtaining medical images using X-ray

It is essential to understand the basics of X-ray as it is a critical developmental factor in DEXA.

All X-ray systems consist of an X-ray source, a Collimator and an X-ray detector. X-rays are produced by a cathode ray tube that generates a beam of X-rays when excited by a high voltage power supply. This beam is shaped by a Collimator and passed though the patient, creating an image on the image detectors.

Figure 3.1 Illustration of the basic principle of an X-ray system

3.3. Basic concept of X-ray absorptiometry

3.3.1. Determining the mass of a three dimensional subject

DEXA determines the total mass of a three dimensional (3D) subject by scanning the 3D subject onto a two dimensional (2D) image using X-ray.

From the scan point of view, the higher the resolution the higher the accuracy. The 2D image is divided into small unit areas known as pixels. Using the pixel as the unit area, the total mass of a 3D subject can be expressed by the following form:

$$M_{total} = \sum M_{pixel} \quad (3.1)$$

Where

M_{total} = the total mass for the subject

M_{pixel} = the mass per pixel

The mass obtained in each pixel, is referred to as "mass per unit area." Therefore the total mass of the subject can be determined by adding up the masses in each pixel.

3.3.2. Determining the mass per unit area (*M*)

The mass per unit area (*M*) is linearly proportional to the thickness and the density of the 3-D subject. It can be expressed in the following form:

$$M = \sigma \times L \quad (3.2)$$

Where:

M is the mass per unit area

σ is the density

L is the thickness

3.3.3. Mass per unit area with X-ray absorptiometry

When the X-ray beam travels through an absorptive material, the mass per unit area is determined by measuring the amount of the X-Ray that is absorbed by the subject.

The X-ray beam is composed of photons that are projected in a straight line. When the photons travel though an absorptive material, they may be partially absorbed or scattered. The level of absorption is inversely proportional to the intensity (I) of the beam. The absorption also varies with the thickness, density, and chemical composition of the absorptive material.

The physical interaction between the intensity of the beam and the absorption is referred to as attenuation. The higher the energy of the incident photon, the larger the attenuation would be. More specifically, the physical interaction of the photon with the orbital electrons of the absorber material is mainly effected by the Photoelectric Effect and Compton Scattering

Photoelectric collision refers to the photons that give up their energy and therefore cease to exist (and do not pass through the absorber material), because they collides with more tightly bound inner orbit electrons in the absorber.

Compton scattering refers to the photons that are deflected from their path due to colliding with the weakly bound outer orbital electrons in the absorber, which knock the electrons from their original positions.

Thus, as a result of these interactions of the x-ray photons with the absorber, the incident photon energy is exponentially reduced or attenuated, as it passes though the absorber (figure 3.2).

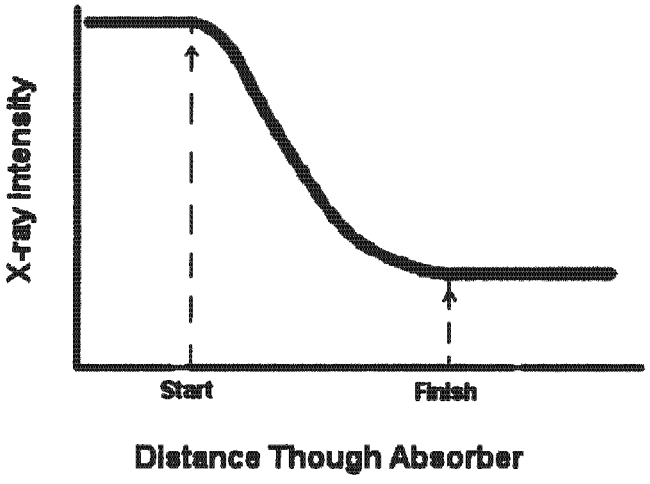

Figure 3.2 The attenuation phenomenon

Due to the nonlinearity of the attenuation, the response of the intensity of the photons can be expressed by the following exponential equation: (Coulam and Erickson 1981)

$$I = I_0 e^{-\mu L} \tag{3.3}$$

Where:

I_0 is the incident intensity

μ is the linear attenuation coefficient

L is the absorber's thickness

3.3.4. The use of a mass attenuation coefficient (μ_m)

Linear attenuation coefficient (μ) is a density (σ) dependent variable, therefore if we extract this density element, a new constant coefficient can be derived. This element is named "mass attenuation coefficient" (μ_m). μ_m is a constant for the particular absorber material at any given photon energy. (Hubbell, 1969, Rao and Gregg 1975, Roubenoff *et al* 1993))

The following table shows some homogenous absorbers and their corresponding μ_m values at the two photon energy levels:

Table 3.1
Typical homogenous absorbers contained in the body

	μ_m	
Component	40 keV	70 keV
Water	1.7920	0.5059
Protein	0.2363	0.1831
Bone Mineral	0.9039	0.3159
Fat (Oleic Acid)	0.2273	0.1872
Glycogen	0.2375	0.1825
Calcium	1.792	0.5059

(complied from Pietrobelli *et al* 1996)

Using $M = \sigma L$ (equation 3.2), the following equation can be obtained after rearranging:

$$I = I_0 e^{-\mu_m M} \qquad (3.4)$$

By further rearranging the formula, mass of the unit area can be interpreted as:

$$M = \frac{-\ln(I/I_0)}{\mu_m} \qquad (3.5)$$

Where

I = incident x-ray beam intensity

I_0 =emerging x-ray beam intensity

μ_m = Mass attenuation coefficient of the absorber material

M =mass per unit area which equals to σL

3.3.5. Mass per unit area for heterogeneous absorbers

The above equation holds for the case where the absorber is a homogenous material.

A homogenous absorber is defined as any single material for which μ_m is known for a specific incident x-ray photon energy. This can be a single element, compound or solution (Write *et al* 1980).

A signal energy beam can be used in determining the mass of a homogenous absorber. However, to determine the mass of a heterogeneous absorber, such as the human body, (which consists of several different homogeneous absorbers) , a dual energy x-ray beam must be used to distinguish between the different compartments.

3.4. DEXA in a 2C model

While a mono-energetic x-ray source is capable of measuring the real density of homogenous absorbers, a dual- energy x-ray source is required to determine the real densities of up to two components in a multi component absorber. Most of the DEXA systems have their two energy levels set at 40keV and 70keV.

Although stated above that a dual energy x-ray source can only measure two components, the DEXA methodology can measure the masses of 3 body components of interest.

The 3 body components of interest:

1. Bone mineral mass
2. Fat mass
3. Lean soft tissue mass

These 3 components are not all heterogeneous and are made up of the body's 6 main components; namely Fat, Water, Protein, Glycogen, Minerals and Bone Minerals. Their masses cannot be measured individually as DEXA can only measure the mass of 2 components or component groupings at any one measurement, so it combines these 6 main components of the body into component groups.

The 6 main components can be combined in several ways into distinct two-component groups, such as Fat and Lean tissue (Water, Glycogen, Minerals, Bone Minerals and Protein). According to their characteristics, the 6 main components are grouped into two component groupings in the following way (figure3.3):

1. Fat and lean
2. Soft tissue and bone mineral mass
3. Soft tissue can be divided into fat and lean soft tissue

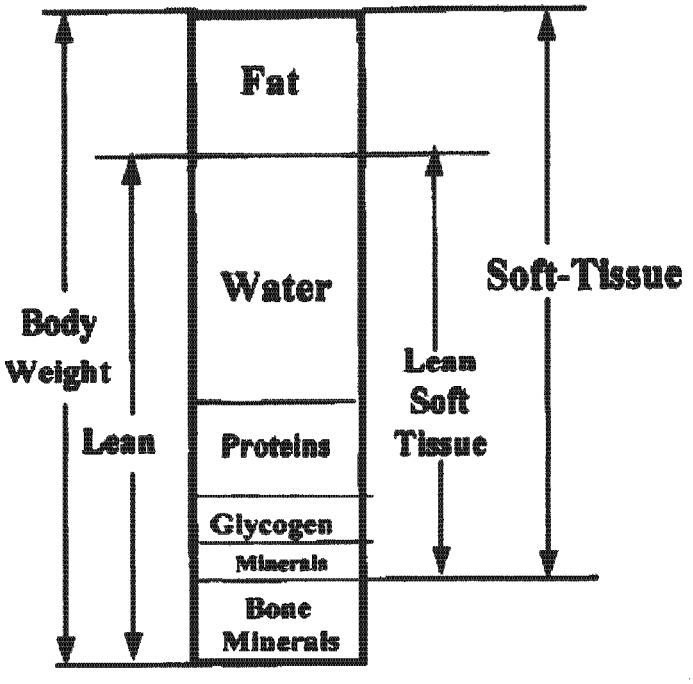

Figure 3.3 Illustration of the DEXA 2C model (Pietrobelli *et al* 1996)

In figure 3.3, fat is compositionally different from lean (fat free) body mass, as is bone minerals compositionally different from soft tissue. Since Lean soft tissue is different from fat and bone minerals, we can group these components together to determine the mass of each component using DEXA. A dual energy X-ray determines the real densities of two components simultaneously, hence the masses of the two components. It is now straightforward to derive the mass of an individual component of interest i.e. fat.

For each pixel of the image, DEXA will obtain a mass attenuation coefficient at high energy level and one at low energy level. The ratio of the low energy attenuation to the high energy attenuation is known as the "R value" (Mazess *et al* 1970, Preuss *et al* 1972, Peppler *et al* 1981, Gotfredsen *et al* 1986). The R value is used as it can identify the masses of the unknown components. (Pietrobelli *et al* 1996)

The R value can be interpreted in the following equation:

$$R = \frac{\ln\left(\frac{I}{I_0}\right)_L}{\ln\left(\frac{I}{I_0}\right)_H} \qquad (3.4)$$

Or

$$R = \frac{\ln(\mu_m)_L}{\ln(\mu_m)_H} \qquad (3.5)$$

Where:

L stands for Low energy beam

H stands for high energy beam

The R value measured by DEXA can be used to determine the composition of any of the two compartment models. In clinical trials; DEXA is often applied in 2 different types:

1. Fat vs. lean mass
2. Bone minerals vs. soft tissue

For this discussion the way in which the model works is discussed using Fat vs. Lean mass. We use fraction of the fat mass (FM_f) against fraction of the fat free mass (FFM_f).

$$R = (FM_f \times R_{FM}) + (FFM_f \times R_{FFM}) \tag{3.6}$$

Since

$$FM_f + FFM_f = 1 \tag{3.7}$$

By rearranging

$$FM_f = \frac{(R - R_{FM})}{(R - R_{FFM})} \tag{3.8}$$

and

$$FFM_f = \frac{(R - R_{FFM})}{(R - R_{FM})} \tag{3.9}$$

Where:

R = the measured value of heterogeneous absorber

FM_f = Fraction of the fat mass

FFM_f = Fraction of the Fat free mass

R_{FM} and R_{FFM} represent the R values respectively

3.5. Theoretical concerns and assumptions of the DEXA system

3.5.1 Theoretical R value VS Measured R value

In DEXA the body composition is determined from the *R* value of each of the components. Therefore it is important to know how the *R* value is determined.

R can be determined theoretically from chemical composition.
The theoretical *R* value for fat is about 1.21 which is determined from the *R* values of different triglycerides (Gurr and Harwood 1991).

The range of *R* values for different triglycerides is small mainly because the proportions of H C O (Hydrogen, Carbon and Oxygen) are stable for varying fatty acid chains. From the literature the *R* value is measured (~1.2) which correlates well with the theoretical value (Folch *et al* 1957, Heymsfield *et al* 1989).

Similarly, using Neutron activation analysis the theoretical R value for lean soft tissue is determined to be 1.369. In the literature, experiments show the *R* value to be 1.364 (Snyder *et al* 1975). The measured and theoretical values are very close for both Fat and lean soft tissues alike. This proves that DEXA stands on a strong theoretical basis.

3.5.2 Scan area with bone and non-bone present

During a DEXA Scan, a 2D subject image of the body is produced. Generally about 40-45 % of the pixels of the image contain bone. (Ellis 2000). The pixels which contain bone are excluded from the measurement. The residual area is measured using the above 2C model (refer to equation 3.8 &3.9) This means that DEXA measures about 55% of the body in two components (fat and lean tissue) and then needs to determine the fat and lean composition of the remaining 45% of the pixels that contain bone.

It is assumed that the composition of the soft tissue layer overlying bone has the same fat to lean ratio as that for non bone pixels, in the same scan vicinity (Kelly *et al* 1998, Pietrobelli *et al* 1996). Figure 3.4 indicates how the bone area is separated when scanning to reduce the number of components. When the dual energy X-ray beams passes through a portion of the body that does not contain bone, DEXA can analyze the area for soft tissue mass and bone mineral mass.

This means that nearly half of the body in a DEXA measurement is assumed. This concern has been tested and Michael *et al* (1998) and Pietrobelli *et al* (1998) have proved that this assumption does not produce significant errors on the measurement of body composition.

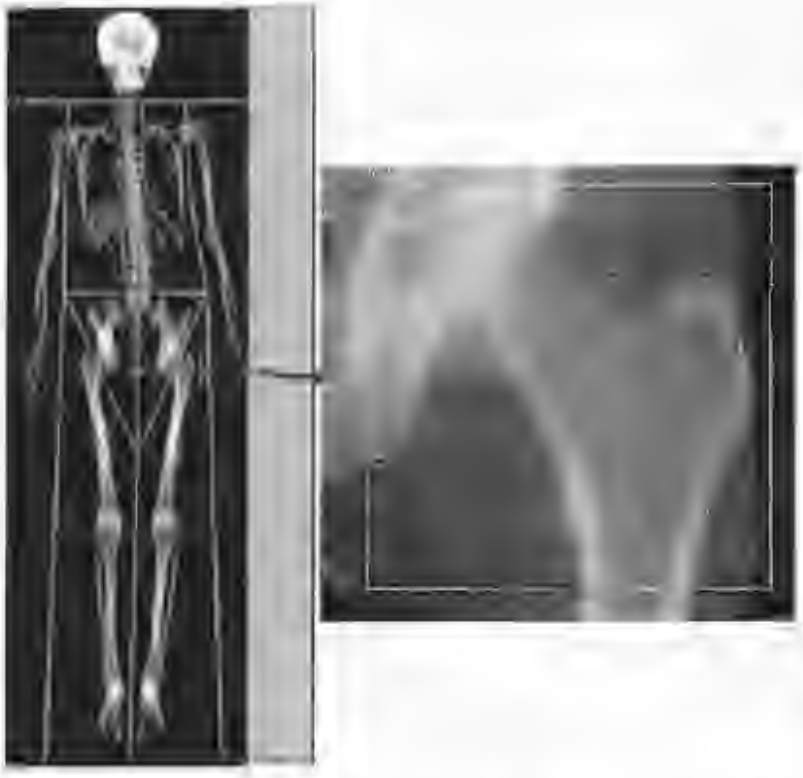

Figure 3.4 Whole body DEXA scan (left) and an area that contains bone (right) (www.gemedicalsystemseurope.com)

3.5.3. Hydration effects

When fluid levels in the tissue increase or decrease, there are quantitative and predicable changes in the tissue's R value. Studies also show that uncertainty in an individual's hydration could also lead to errors in the measurement (Pietrobelli *et al* 1996). Pietrobelli *et al* (1998) concluded that the change in R value is in fact very small if the fluid balance is altered by ~1Kg. Hence when DEXA is used as a gold standard, the hydration status of subjects must be carefully controlled.

3.6. Practical constraints of DEXA

The entire scan takes between 15 and 45 minutes. During scanning the subject must be absolutely still. It is not recommended for young people who find it difficult to keep still. Different versions of software also lead to different results (Vozarova *et al* 2001). Different manufacturers of the DEXA device also have different interpretations of the fat and lean tissue compartments.

In using DEXA for validation, the same system and software version must be used for all subjects so that the relationship between DEXA and the ADP system can be compared.

3.7. Conclusion

This chapter only covers the basic overview of the principles of the DEXA system. The detail of how the clinical system works is much more complex. DEXA provides an accurate whole assessment of body composition and shows consistent results.

It is concluded that despite the assumptions, DEXA is an adequate reference method for validating ADP results.

4. Principle of air displacement plethysmography and its theoretical concerns during in vivo studies

4.1. Introduction

This chapter is split into two parts. Firstly, the principle of Air Displacement Plethysmography (ADP) is described; thereafter the impacts of the complexities introduced during in vivo measurements are described. Each complexity is identified and solutions for each effect are proposed. Notice that this chapter only covers the best suggestion to determine body volume. Other concerns in terms of determining fat mass will be covered in chapter 5.

4.2. Principle of Air Displacement Plethysmography

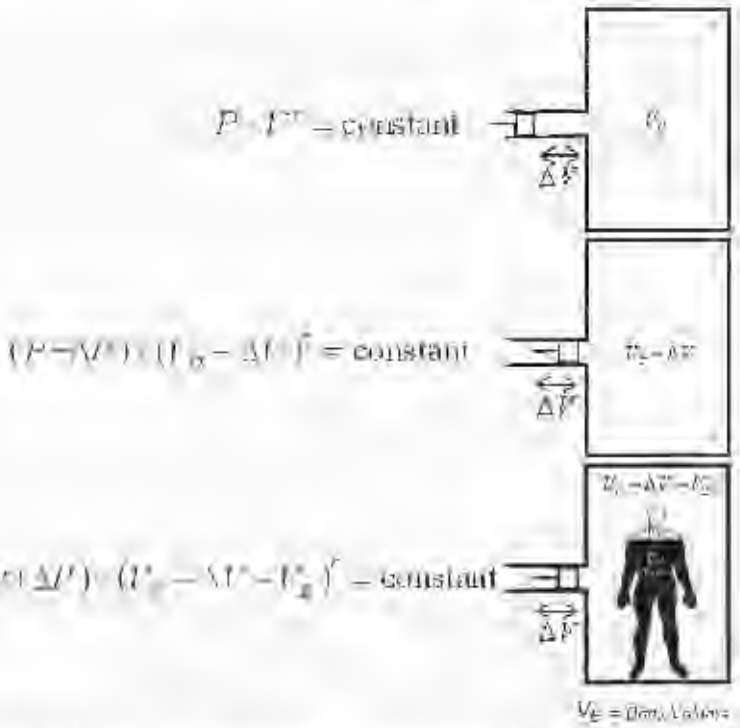

Figure 4.1 Theoretical representation of ADP analysis

The air displacement plethysmography concept is based on Boyle's law as mentioned before. Plethysmograph refers to a closed rigid chamber; in which the subject is placed during measurement. When compressing the air in the plethysmograph, the temperature within it will not be constant but energy will be conserved hence Poisson's Law will be applied under these conditions (this is known as the adiabatic condition).

$$P\gamma V^{\gamma} = \text{constant} \qquad (4.1)$$

Where;

P is the atmospheric pressure at the place of measurement.

V is the volume of the plethysmograph

γ is the ratio of the specific heat of the gas, normally equal to 1,4 for air (Daniels *et al* 1967)

(See first part of Figure 4.1)

From here, V is referred as the volume of the chamber (V_c).

v_b as the volume of the body (within the chamber or plethysmograph)

Within such a closed system; if the volume is reduced by a known amount of volume (ΔV), a corresponding increase in pressure (ΔP) will take place due to energy conservation law. Hence the equation can be rewritten as

$$(P+\Delta P)\cdot(V_c - \Delta V)^{\gamma} = \text{constant} \qquad (4.2)$$

(See the second part of figure 4.1)

Placing a subject with volume V_x into the plethysmograph; with the same volume ΔV displaced, the equation can be further rearranged to:

$$(P+\Delta P)\times(V_C-\Delta V-V_x)^{\gamma}=\text{constant} \qquad (4.3)$$

(See the third part of figure 4.1)

Because it is a closed system, from the energy conservation law, the energy inside this closed system will be conserved before and after the measurement hence the following equation can be obtained from (4.1) and (4.3):

$$P\times\left(V_C-V_B\right)^{\gamma}=(P+\Delta P)\times\left(V_C-\Delta V-V_B\right)^{\gamma} \qquad (4.4)$$

Where V_C-V_B is the volume of the remaining air in the plethysmograph when V_B is placed in the chamber

The equation has to be rearranged, in order to obtain V_B

$$\frac{P+\Delta P}{P}=\left[\frac{(V_C-V_B)}{(V_C-\Delta V-V_B)}\right]^{\gamma} \qquad (4.5)$$

With further rearranging; the equation can be present in the following form:

$$V_B = V_c + \Delta V \times \frac{\left(\frac{P+\Delta P}{P}\right)^{\frac{1}{\gamma}}}{1-\left(\frac{P+\Delta P}{P}\right)^{\frac{1}{\gamma}}} \qquad (4.6)$$

After canceling the common factors and expressing the formula in terms of V_B; the final equation can be obtained as follows:

$$V_B = V_c + \Delta V \times \frac{(P+\Delta P)^{\frac{1}{\gamma}}}{P^{\frac{1}{\gamma}} - (P+\Delta P)^{\frac{1}{\gamma}}} \qquad (4.7)$$

Where

V_B = Volume of the air displaced by the test subject

V_c = Volume of the air in the empty chamber

ΔV = change in volume of the chamber

ΔP = change in pressure in the test chamber

P = atmospheric pressure

γ = Ratio of specific heats, which equals 1.4 for air

See appendix A4 for the full derivation of the ADP theory

4.3. Essential components of a ADP system

A basic ADP system consists of a single measuring chamber which is essential by a change in volume (ΔV). The resulting pressure in the chamber can be determined using a differential pressure transducer. One side of the differential pressure transducer is placed in the measuring chamber while the other end is referenced to atmospheric pressure using a reference chamber (see figure 4.2)

Figure 4.2 Essential components of an ADP system

The differential pressure transducer measures ΔP; hence by knowing the absolute atmospheric pressure (P_{amb}), the volume of the subject (V_b) can be calculated.

Further design and analysis of the device is covered in the 5th chapter (Design of the device). Note that this theory is only applied during calibration of the device, (using inanimate objects) because there are more complexities involved for in vivo studies.

4.4. Complexities introduced by in vivo measurements for ADP

Although an inanimate object can be measured (by equation 4.7), there are some major issues existing during in vivo studies (which were identified in section 2.6.2). Temperature, humidity, respiration effects and the temperature in the chamber, are major issues that vary the outcome of the result.

4.4.1. Temperature effect

Temperature inside the chamber rises during human trials. This is caused by two major factors namely: breathing and body temperature. The temperature in the chamber will increase from the ambient temperature to a saturation point (close to body temperature). Breathing increases the temperature as cooler air is drawn into the lungs and warmed with each breath. It is important to understand and monitor the temperature inside the chamber to obtain accurate results. The following diagram illustrates the temperature behavior for in vivo studies:

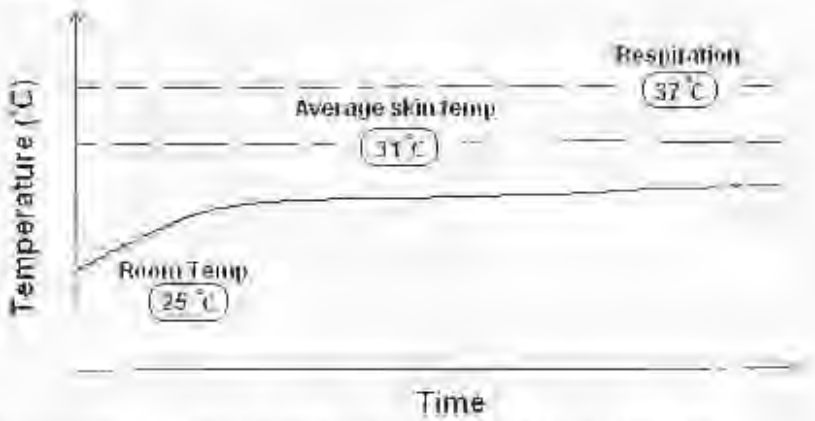

Figure 4.3 Temperature change in the chamber

In figure 4.3, average body skin temperature is ~31 °C and the body core temperature which is ~37 °C.

Temperature changes in the chamber can be seen as a form of energy. In a closed environment, the first law of thermodynamics (law of conservation of energy) is applied: which states that the energy of a system remains constant if the system is isolated from its surroundings as regards heat transfer and work. Human subjects can be regarded as heat generators. With the increase in temperature, the constant in equation 4.1 increases proportionally. In another words, with the same volume displacement the higher temperature will cause a larger change in pressure.

We can measure the changing temperature in the chamber, and then correct the constant in the equation from the temperature measurement.

Alternatively if more air is present, (the larger the plethysmograph) the slower the temperature of the chamber will rise. In this way we can treat the temperature effect as a part of a slow rising sinusoidal wave (i.e. the temperature is changing at low frequency). Therefore we can exclude this effect (temperature) by filtering its signal out.

4.4.2. Humidity effect

The test subject will be breathing into the chamber during the process; which will change the relative concentrations of O_2 , CO_2 and the relative humidity. This will affect the accuracy of the measurement as increasing the water vapor content causes a marginal increase in air density (Cronje 1992). This directly impacts on the volume of the chamber, as ratio of specific heats of the air (γ) changes with level of CO_2 increase and the amount of water vapor content.

According to the universal gas law, all gases, including the humidity will behave equally, as long as the air inside the plethysmograph remains unsaturated.

4.5. Adiabatic air vs. isothermal air

In the literature review, most of the ADP measurement procedures assumed an isothermal condition but failed to keep the chamber in the isothermal condition. A treatment for this is to assume adiabatic condition for the chamber and attempt to identify the isothermal factors and eliminate their effects (Effectively convert the isothermal effects into adiabatic readings). This can be done because air is 40% more compressible under isothermal conditions than it is under adiabatic conditions, (Dempster and Aitkens 1995) and this relation can be used to correct for the volume of the air which is under isothermal conditions.

When Air Displacement Plethysmography is applied during in vivo studies, some of the air will be exposed to a large surface (of the human body) at constant temperature. This air will exhibit isothermal conditions as it can exchange heat with the human body easily. The isothermal air is identified as:

- Thoracic gas (V_{th})
- Isothermal air around the skin
- Gastro intestinal tract gas (V_{GI})
- Air trapped by the clothing and hair

4.5.1. Thoracic gas volume (V_{th})

The thoracic gas volume (V_{tg}) is defined as the volume of air in the lung at the time of measurement at mid-tidal exhalation. The key assumption for this measurement is that the subject is breathing normally during the measurement (Dempster and Aitkens 1995).

The air in the lung is under isothermal condition and therefore its volume will be underestimated by 40% if adiabatic conditions are assumed. V_{tg} is estimated by the following equation:

$V_{TV} = FRC + 0.5\ V_T$ (4.8)

Where:

FRC is functional residual capacity

V_T is the tidal volume which can be measured during normal breathing using a spirometer.

FRC consists of residual volume (V_R) and expiratory reserve volume (ERV). FRC can be determined in two main ways, namely by measurement or by prediction.

In traditional pulmonary plethysmography; ERV can be measured at end-tidal exhalation (Dubois *et al* 1956) while V_R can be predicted by the following formulae. (Crapo *et al* 1982)

$V_R = 0.1970Ht + 0.1970A - 2.421$ (for Women) (4.9)

$V_R = 0.2160Ht + 0.0207A - 2.840$ (for Men) (4.10)

Notice that *Ht* is the subjects' height in centimeters and *A* is the age.

V_R can also be determined from the O_2 dilution N_2 wash out method (Forsyth and Shephard 1988)

Alternatively thoracic gas volume can be predicted by estimating FRC directly (Crapo *et al* 1982):

$$FRC = 0.0472Ht + 0.0090A - 5.920 \text{ (for Men and Women)} \qquad (4.11)$$

Many authors (Latin and Ruhling 1986, McCrory *et al* 1998, Forsyth *et al* 1988, Hackney *et al* 1985) have reported that there are no significant differences between measured V_{TG} and predicated V_{TG} however, there is research to the contrary (Wilmore 1969, Morrow *et al* 1986, Withers and Ball 1988) showing that the predicted method cannot be used to determined body density.

The dissident factions have notably all performed body volume measurements using the underwater weighing method where the estimation of lung volume is critical in the ADP method, however there is far less sensitivity to inaccuracies in the measurement of lung volume.

4.5.2. Isothermal air around the skin (V_{sa})

There is a volume of air above the surface of the skin that is isothermal. Isothermal air around the skin (V_{sa}) is referred to as a surface area artifact (SAA) in other studies (Dempster and Aitkens 1995, Field *et al* 2001).

V_{BSA} is proportional to body surface area (BSA). Taking an estimate of body surface area (BSA) by the formula derived from Dubois: (Dubois *et al* 1916)

$$\text{BSA } (cm^2) = 71.84 \times \text{Weight (kg)}^{0.425} \times Ht\ (cm)^{0.725} \qquad (4.12)$$

Currently there is no accepted range for V_{BSA} and no other established function for BSA. In this project, a first order value (K) is used to estimate the V_{BSA} through measurement (see equation 4.13).

$$V_{BSA} = K \times BSA \qquad (4.13)$$

Where K will be determined empirically

See section 6.6.2 for the suggested empirical method to determine K.

4.5.3. Gastro intestinal tract Gas Volume (V_{GIT})

The average volume of the Gas in the Gastro Intestinal Tract (V_{GIT}) is reported to be 115ml with a standard deviation (SD) $\pm$ 127ml and 116ml with SD $\pm$ 125ml for patients with lung disease (Bedell *et al* 1955).The absolute effect of GIT gas volume on the overall body volume is negligible due to the relatively low volume of air in the GIT.

4.5.4. Air trapped by the clothing and hair

It is worthwhile to mention that there may be other minor factors affecting body volume. An example is the effect of clothing and hair which can be handled by wearing a minimum of clothing and a swimming cap (to cover the hair). This can reduce a difficult to measure factor to a level which is not expected to have a sizeable impact on body volume. (Higgins *et al* 2001).

Once the GIT gas volume, Surface Area Artifact and Thoracic volume have been determined, the original body volume measurement can be adjusted as follows:

$$V_{Bcorr} = V_B + 40\% * (V_{GI} + V_{SAA} + V_{TH}) \quad [4.14]$$

Where V_{Bcorr} is the corrected body volume

4.6. Comparison between the solutions for each of the complicating factors

The temperature effect should be removed rather than corrected by continuous measurement. This is principally because accurate correction relies on the precise capture of the temperature and requires a sophisticated system.

Measurement of these variables will introduce errors and may make day to day results more difficult to interpret. By using the prediction method for V_{fat} and V_{bod}; constant results can be obtained in repeated measurements. This is in line with the aims of the project to provide a body composition measurement system that provides consistent results with relative accuracy.

In order to avoid the build up of humidity, the period of time between measurements should not be below one minute. This will also allow the temperature to return to room temperature. The exact time is determined empirically. The table below summarizes the main effects on volume and the treatment of them in this project:

Table 4.1

Effects on volume measurement and suggested solutions

Effects	Decision	Common Advantage
Temperature &humidity	Filter out with low pass filter	• Low cost • Fast
V_{fat} V_{body} V_{air}	Predicted with formulae	• Creating a constant offset rather than a variable

4.7. Effects on Volume Measurement

The common advantage of predicting these effects lowers the total cost of the project and also shortens the trial time for each subject. (This means the device can measure more subjects in the same period of time).

More importantly the same individual will have the same value for thoracic and gastrointestinal air volume between measurements. This approach introduces a constant offset, which improves the interpretation of results from day to day, as the only variable that will be changing is body fat, not the value of isothermal air for example. See section 6.6 for further discussion of this approach.

Note that the decision to change the volume of the chamber in a sinusoidal manner was made so that the signal can be differentiated from Temperature, Humidity and Respiration effects. The signals for Temperature, Humidity and Respiration occur at far lower frequencies than those for the changing pressure. Fourier analysis is used to filter out the complexities and their effects using a high pass filter. From now on, all the diagrams that represent changing pressure (ΔP) is shown in the sinusoidal waveform format.

4.8. Conclusion

The volume of an inanimate object can be determined using Poisson's law.

Complexities during the measurement of in vivo studies can be overcome by filtering out and by assuming adiabatic conditions. The isothermal effect can be compensated for by assuming that the isothermal volume is known. This is achieved by predicting the values of the isothermal factors.

5. Design of the Device

5.1. Introduction

The theory of ADP has been covered in the previous chapter. The previous chapter highlighted that in vivo measurement requires a high degree of precision. It is important to plan the design process to consider what might affect the precision of the measurement. There is two fold meaning here:

1. A systematic process can be followed to determine the most suitable parameter for each component of the device.

2. The assumption and the error that might come with the interpretation of its parameter can be identified and addressed.

With any body composition technology, it is important to establish its validity, reliability, and practicality. Garrow and Webster (1985) proposed that initial cost, training of the operator, maintenance and operating costs, precision, and accuracy are the five factors that should be considered when defining an ideal method for field studies.

Ellis (2001) added that the measured parameters should be able to be translated into useful biologically meaningful results.

As this is a health monitoring device rather than a life supporting device, the level of acceptance among its target audience also needs to be considered.

These factors serve as guidelines for this project. Based on these guidelines and the principle findings in chapter 2 and 4, this chapter is divided into the following divisions.

1. Goal setting for the measurement.

2. Theoretical interpretation; body fat % is derived as a function of other measurable parameters.

3. Practical interpretation; this determines instrument precision required for this project.

(See figure 5.1 for the theoretical and practical interpretation)

4. Introduction to the theoretical model; which illustrates the assumptions and errors in the whole estimation process.

5. Identifying the errors and optimizing design using the model.

6. Additional relevant design issues.

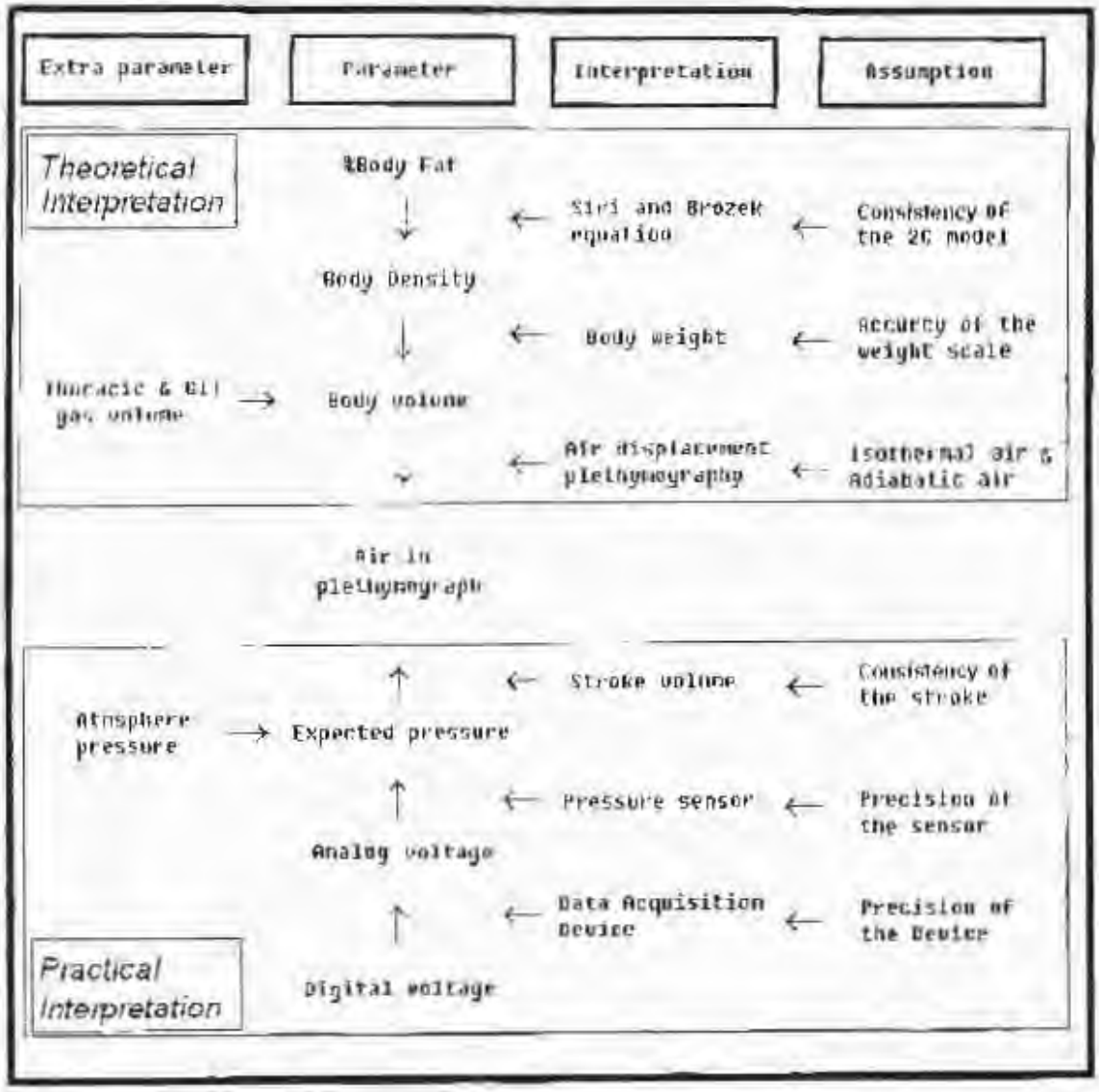

Figure 5.1 Relationship between the parameters

It is imperative for the design to accommodate the minimizing of errors in the practical interpretation. The design of the chamber is done in such a way to theoretically optimize the result.

5.2. Goal setting for the measurement of body fat

The design of the device cannot accommodate measurement of the whole range of body fat and height and weight. There is a range for each of these parameters for which the accuracy can be optimized. That is why I have set a limit on who we can measure and the degree of the accuracy we want to obtain. From the literature review, I feel that measuring within ±2% of body fat is a reasonable initial goal. Since the equation predicting lung volume is limited to individuals between 17 and 91 years old, this project will be restricted to that range. Following the principle finding of DEXA in section 3.7, test subjects were further limited to between 20 to 70 years.

The volume of the subject is directly related to the air displaced in the test chamber. This influences the accuracy; hence the volumes of the subjects are limited to be from 50 litres to 100 litres which translated to about 50 kg to 100 kg.

Table 5.1
Goal setting of body fat measurement

	Lower limit	Upper limit
Accuracy	±2% of body fat	
Age of the subjects	20	70
Weight of the subjects	50kg	100Kg

Shows the target groups and the accuracy

5.3. Theoretical interpretation

To measure body fat percentage we interpret body composition to consist of fat mass and fat free mass. The 2C model determines body fat by knowing the density of the human subject. By knowing the body weight and its volume, we have the Body Density (Mass / Volume). We are now able to interpret % body fat from body volume. Body volume is the output from the plethysmograph.

Determining the corrected body volume ($V_{b_{corr}}$) requires the measurement of height, lung tidal volume and personal information regarding the person's age and gender. This is for the theoretical determination of the total isothermal air (see section 4.4).

5.4. Practical interpretation

The theory of ADP measures body volume by essentially measuring pressure and the practical interpretation revolves mainly around the considerations in measuring the change in pressure that occurs in the plethysmograph (ΔP).

The change in pressure is determined from the difference between the peaks of the pressure sinusoidal wave, which is measured by the pressure sensor. The focus is in determining the amplitudes of the true peaks.

The instrument used to determine pressure is a transducer whose output is voltage.

The model is theoretically sound; however in practice many variables (including instrument error) are not perfect. The practical concerns are outlined below.

5.4.1. Problems if the measured pressure is too large

If the pressure is too big it is going to cause discomfort for the subjects. More importantly, it makes the true peak of the pressure impossible to determine (Figure 5.2) because of the accuracy of the pressure sensor. Therefore it is important to determine a dynamic range of the pressure expected in the chamber.

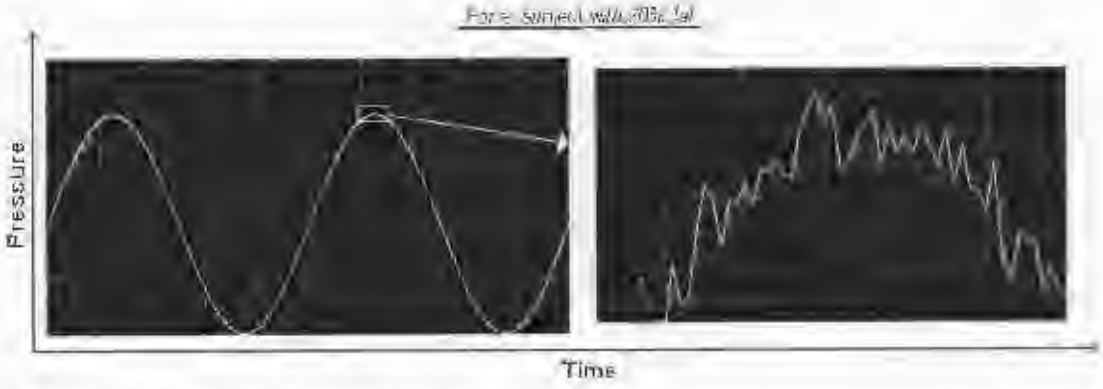

Figure 5.2 Typical wrong design1

(Source of error in the figure 5.2: instrument sensor error and noise)

5.4.2 If the measured pressure is too small

In this case, it is impossible to tell the difference between subjects as the pressure waves are too similar (figure 5.3). The pressure must be big enough to tell the difference between subjects.

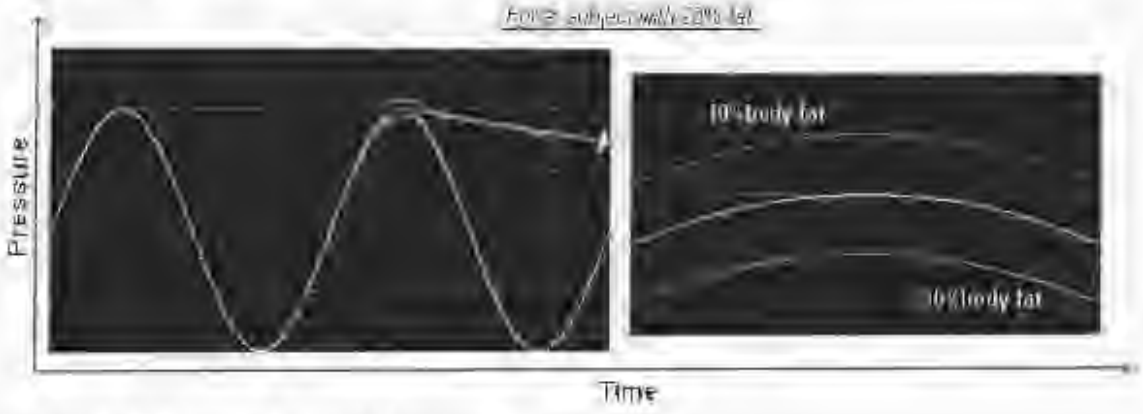

Figure 5.3 Typical wrong design2

5.4.3. Precision factor on pressure measurement

The four components that determine precision of the ADP device are

- Precision of the pressure sensor
- Precision of the Data acquisition (DAQ) device
- Size of the chamber
- Consistency of the stroke volume

(See figure 5.1)

All four factors interlink with each other. It is not possible to suggest the best solution for each of the parameters independently.

5.5. Optimized Plethysmograph and Stroke volume

The optimized relationship between the plethysmograph and stroke volume means: minimizing the size of the sinusoidal pressure when no test subject is present, at the same time; maximizing the dynamic range when the 100L test subject is present in the plethysmograph (see figure 5.4).

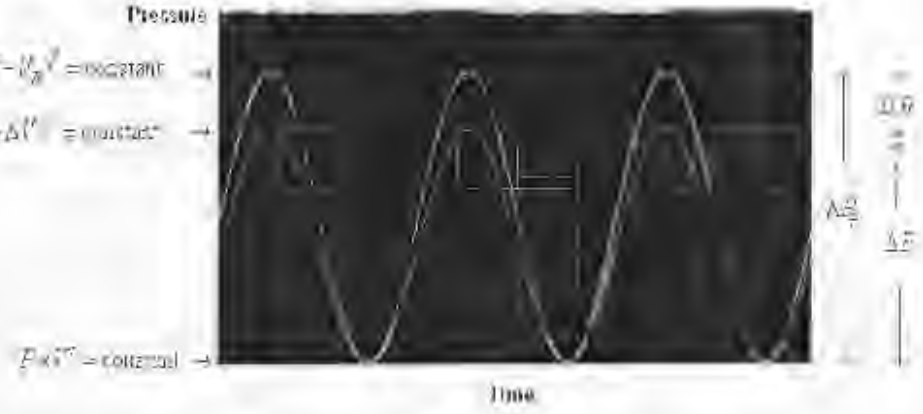

Figure 5.4 Optimized design of the ADP system

Where: The smaller sinusoidal wave refers to the measurement when the chamber is empty.

The bigger sinusoidal wave refers to the measurement when testing a 100 litre subject.

D.R. = dynamic range. This is the difference in reading between an empty chamber and a 100 litre subject.

Optimizing the relationship between the stroke volumes and volume of the plethysmograph can only be done to a limited extent because practically, these devices are only available in certain physical size.

The first step of the design is to identify the biggest limitation, which is a combination of the accuracy of the pressure sensor and the precision of the DAQ device

5,5,1. Largest limitation of the device

The most important limitation of this design is the precision of the pressure sensor and the DAQ device, because there is no way to compensate the random errors that both of these carry.

Honeywell DC series sensor is the most economic low pressure sensor (see datasheet in appendix C1) due to its accuracy, stability and availability. The smallest dynamic range of available sensors is 5 mBar with 2.25V offset and 2V output span. The accuracy of this sensor is ± 0.25% and the typical error is 3 % (This information is obtained directly from the data sheet).

NI PCI6013 from national instrument is the only affordable 16 bits DAQ card for this project. (See appendix C2 for the data sheet of this device) the absolute accuracy for this card is 41.2 μV at 5V full scale.

Table 5.2
Typical precision of the measurement instrument

Description	Unit Size	Accuracy	Description
Dynamic range of the pressure sensor	2.5mBar	0.25%	Of the size of the signal
Precision of the Data acquisition device	16bit	0,01%	With 5V full range

5.5.2 Size of the chamber

Size of the testing chamber should be between 350 and 550 litres due to the following reasons:

If it is bigger than 550 litres, it will be difficult to distinguish the difference between the subjects. (The difference between people will only be a small portion of the chamber.)

If the size of the chamber is smaller than 350 litres, then the isothermal air in the chamber will be proportionately too large. (See appendix B5 for the explanation). This will make our assumption of a predominately adiabatic condition wrong and discredit the results. In addition the air in the chamber would become saturated much faster (See section 4.4 2:).

The stroke volume is dependant on the size of the chamber and the largest expected pressure

5.6. Introduction to the theoretical model

There are three generations of model that have been developed over the course of this project. Each generation gives input to different stages of this project. The first generation model is in this chapter; the second generation is in the 6th chapter and the final generation of the model is in the 9th chapter. Note that the calculation of parameter values in these chapters is based on the theoretical model.

The final version of the model includes all three generations and is included in the CD. (See appendix B1 for instructions and appendix B2 for an explanation of how it was derived). Notice that design routine and development of the model is also included in appendix B2.

5.6.1. First generation of the model

The theoretical model is established based on the initial goal and the limitations mentioned in sections 5.2 and 5.5. This model is built using the Excel spreadsheet model. This allows the user to change any of the parameters to see the effect on the % BF. If a better instrument is obtained for future development, this model allows us to predict the improvement in measuring precision easily.

5.6.2. Analysis of the design

The optimized system in figure 5.4 has been derived by the theoretical model.

Theoretical optimized system:

Table 5.3
Results for the optimized single chamber model

	Optimized system
Size of the chamber	400Litre
Stroke volume	0.5
Expect pressure on 100L subjects	2.3684029mBar
Expected pressure on 50L subjects	2.029488mBar
Error in % body fat on 100litre subjects*	±8.12%
Error in % body fat on 50 litre subjects*	±3.48%

*Note that errors indicated here are only those generated from the instruments. See appendix B3 on how to obtain this result.

The level of the error is clearly unacceptable. This has been addressed carefully in successive chapters.

5.7. Dynamic dual chamber system

The Dynamic range can be increased by providing a sinusoidal pressure simultaneously into the reference chamber. The amplitude of this reference sinusoidal pressure should be the same as the pressure in the empty chamber. (See figure 5.5)

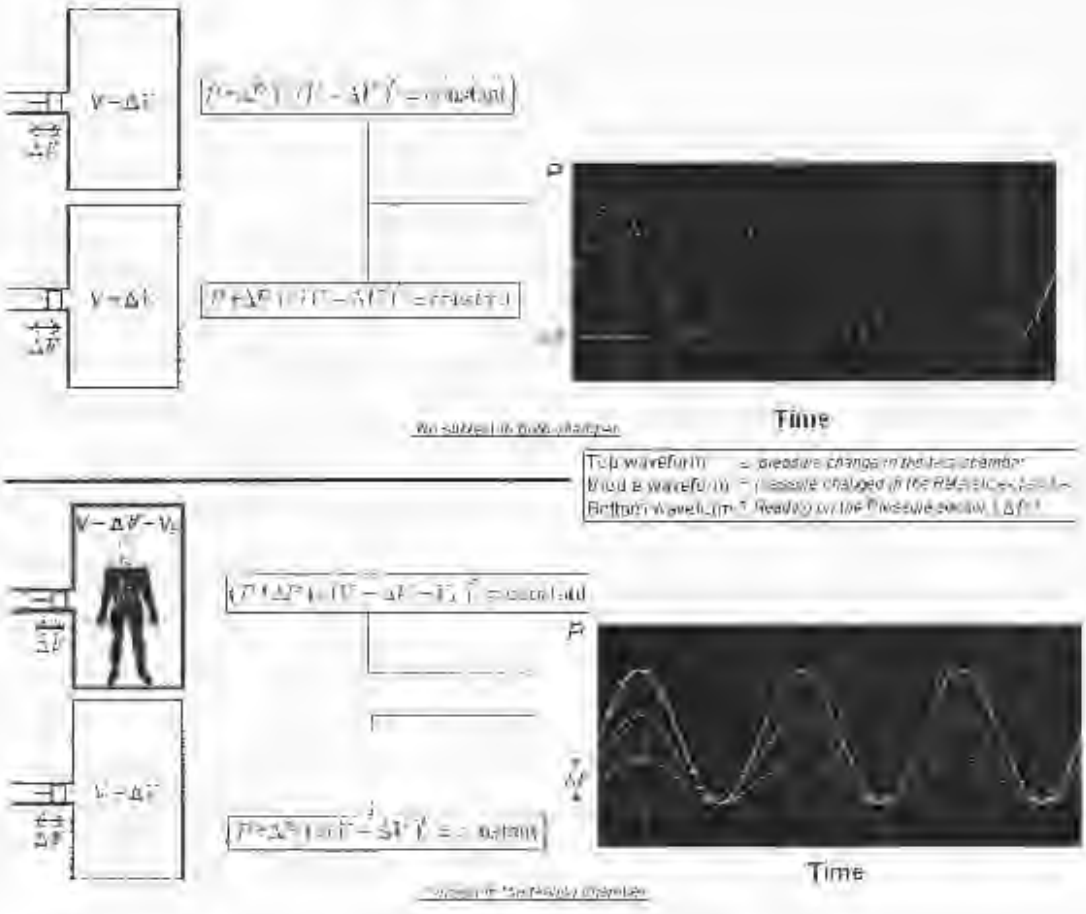

Figure 5.5 Concept of the dynamic dual chamber system

When no subject is present in the measuring chamber, the pressure amplitude in both chambers should be equal at all times. The reading on the differential should be zero. (See the top half of figure 5.5)

When a subject is present in the measuring chamber, the reading on the differential pressure sensor is equal to the difference between the two chambers. (See to the bottom half of figure 5.5)

5.7.1. Advantage of the dynamic dual chamber system

The two-chamber dynamic system successfully decreases the size of the expected pressure reading on the differential pressure sensor. This means the dynamic range can be increased to the desired level.

Hence the expected pressure in the test chamber can be increased without losing any accuracy.

5.7.2. Method of operation

A second chamber together with a second stroke volume is required for this purpose. The size of the second stroke is dependant on the ratio of the volume of the two chambers. The ratio between the size of the chamber and the stroke volume should be the same for the two systems.

Both stroke volumes should be linked so that the changing stroke can happen simultaneously

The reference chamber in section 4.3 is used as the second chamber.

5.7 3. Theoretical optimized dual chamber dynamic system

The new optimized system (table 5.4) has been derived by the theoretical model.

Table 5.4

Results for the optimized dynamic dual chamber model

	Optimized system
Size of both chambers	400Litre
Size of both Stroke volumes	1 litre
Expect pressure on 100L subjects	1.1901mBar
Expected pressure on 50L subjects	0.5097mBar
Error in % body fat on 100litre subjects*	±0.87%
Error in % body fat on 50 litre subjects*	±1.02%

*Note that this is only includes errors that might be generated from instruments. See appendix B4 on how to obtain this result.

The formula in section 4.7 can be rearranged, using the above design, to the following formula:

$$V_x = V_c + \Delta V \times \frac{\left(P + \Delta P_{\text{experienced pressure}}\right)^{\frac{1}{\gamma}} + \Delta P_{\text{reference chamber}}\right)^{\frac{1}{\gamma}}}{\left(P^{\frac{1}{\gamma}} - \Delta P_{\text{experienced pressure}}\right)^{\frac{1}{\gamma}} + \Delta P_{\text{reference chamber}}\right)^{\frac{1}{\gamma}}} \qquad (5.1)$$

Where $\Delta P_{\text{test chamber}} = \Delta P_{\text{experienced pressure}} - \Delta P_{\text{reference chamber}}$

5.8. Other relevant issues to this design

The basic structure of the chamber has been discussed above. There are other relevant issues to consider in the design of the device, such as: shape of the chamber, frequency of the changing stroke volume, Length of the trial period and air behavior in a multi-cycle environment.

5.8.1. Shape of the chamber

A round chamber allows the pressure to be distributed more evenly, compared to a rectangular shaped chamber. It can also be sealed better.

5.8.2. Frequency of the changing stroke volume

The frequency of the stroke volume should be smaller than 5 Hz, due to the rigidity of the chest wall (Peslin and Fredberg 1986) and larger than the breathing frequency (which is smaller than 0.5 Hz). Higher frequency also causes discomfort to the ear drum of the subject. The stroke frequency is determined to be between 1.5 and 3 Hz. It is important it notice that the wavelength (λ) should be large in comparison with the box dimensions at 5 Hz. For example at 5 Hz, $\lambda \approx 66$m (330/5), while at 1.6 Hz $\lambda \approx 206$m.

5.8.3. Length of the trial period

The length of the trial period is determined by the number of the samples needed as well as the amount of CO_2, humidity and heat generated by respiration in the test chamber.

The length of the trial period cannot be too long as the humidity

building will affect γ (section 4.4.2) and the assumption for adiabatic conditions will not hold. The number of samples in the trial period is directly related to stroke frequency. A sufficient number of observations are required to reduce random error of the instruments (A typical normal distribution should have more than 30 samples). These two factors are both taken into account for a trial period length of between 20 and 30 seconds.

5.8.4. More about isothermal and adiabatic air behavior in the chamber

In section 4.2, the principle of ADP is described in terms of one cycle of the stroke at a time. For statistical reasons, many samples will be taken which means multiple cycles. Ma (2001) describes how air behaves in the chamber using figure 5.6

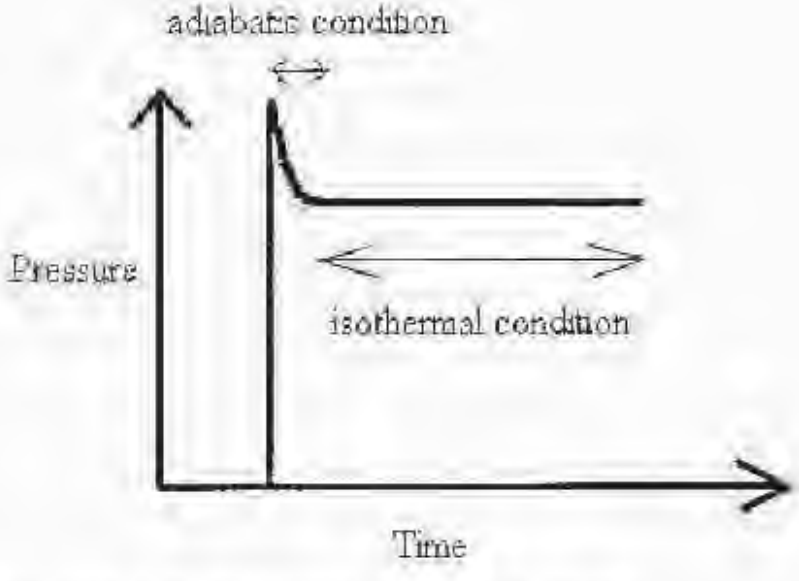

Figure 5.6 Air behavior in a closed system

In a multiple cycle environment, (See figure 5.7) when air gets

compressed inside a closed system, if not enough time is allowed for the air to get back to its isothermal stage the PV^{γ} constant rises. This effect will make it impossible to determine the differences between the peaks and troughs (e.g. in figure 5.7 the left side of any sinusoidal wave is never equal to its right hand side).

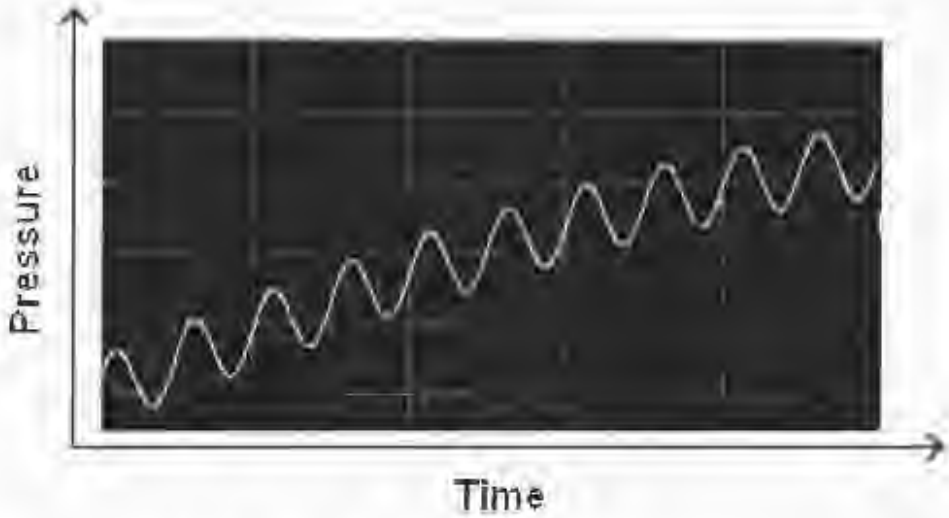

Figure 5.7 Air behavior during multi-cycle environment (diagram obtained from experiments)

The following two methods can be applied to address this issue; either filtering it out digitally or creating a known leakage to the chamber. The second method was adopted because the increasing of amplitude due to the slow gradient is much larger than the size of the pressure difference. This makes digital filtering impossible. See appendix B7 for more detail about the air leakage analysis.

In order to maintain the closed system assumption of the ADP theory

(in section 4.2) the leakage effect needs to be determined. See section 8.5.1 for how this is done.

Equation 5.1 is further developed to the following equation by including leakage effect on the changing pressure (ΔP_{change})

$$V_B^{\gamma} = V_c^{\gamma} + \Delta V^{\gamma} \frac{\left(P - \Delta P_{experienced\ pressure} - \Delta P_{reference\ chamber} + \Delta P_{leakage}\right)^{\frac{1}{\gamma}}}{\left(P^{\frac{1}{\gamma}} - \Delta P_{experienced\ pressure} + \Delta P_{test\ chamber} \Delta P_{leakage}\right)^{\frac{1}{\gamma}}} \qquad (5.2)$$

Where $\Delta P_{test\ chamber} = \Delta P_{experienced\ pressure} + \Delta P_{reference\ chamber} - \Delta P_{leakage}$

5.9. Design steps for the final design

The following component's parameters need to be determined:

1. Diameter of the two plungers
2. The two stroke volumes
3. The size of the two chambers

As all these factors are interlinked and it is important to establish the priority of which components to acquire first (e.g. the diameter of an available plunger will influence our choice of stroke volume) (See figure 5.8).The priority of the components is mainly decided by cost and availability.

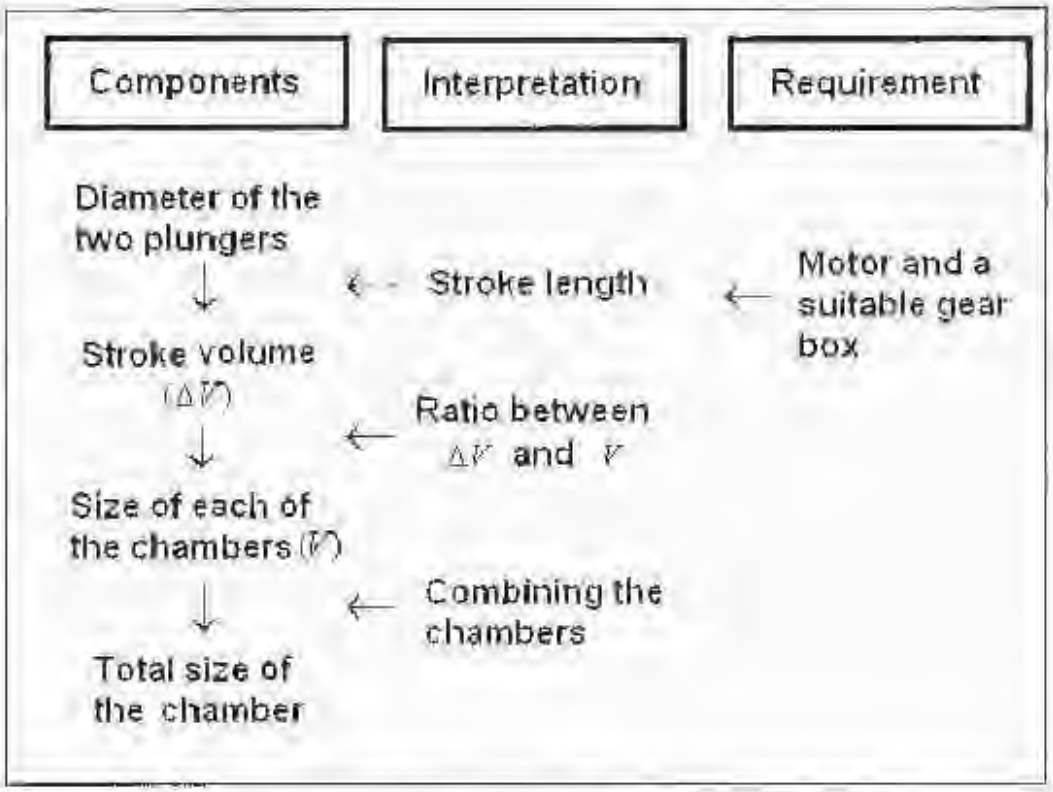

Figure 5.8 Flow chart showing the priority of obtaining each component

5.10. Materials for the prototype

The following materials were obtained in order of priority (as above). Due to budget constraint, two plungers were borrowed from Groote Schuur hospital RSA (One from the respiratory clinic and one from the respiratory ICU). The accuracy of these plungers is up to 0.01 mm in diameter. Their radii are 57.1 mm and 32.25mm respectively. The accuracy is necessary as if the radius is out by a small fraction, then the stroke volume becomes unknown. The length of the stroke is set to 60, 80, or 120mm to accommodate different sizes of the chambers (as yet unknown).

A DC shunt motor from Parvalex Pty. Ltd. (Bournemouth England) is used which allows us to set the frequency from 0 to 1.67HZ (100RPM) (see table B1 in appendix B1 for the spec of this motor). The motor drives the plunger by means of a scotch yoke type mechanism. The scotch yoke moves in a sinusoidal like pattern hence delivering a sinusoidal pressure waveform.

According to the design in section 5.7 and the size of the two stroke volumes, the size of the two chambers (test and reference) should be ~450 and 150 litres respectively. Hence the total size of the chamber should be ~600L. Two fiberglass baths have been donated from Libra Bathware Pty Ltd (see appendix D1). Both baths have approximate inner height 1860 mm, 960 mm width and 400 mm depth. The design is to put the two baths together and build a reference chamber inside the test chamber.

5.11. Conclusion

An initial goal for the design of this project has been set. Relationships between the parameters and employing the theory of ADP to determine the percentage of fat mass are illustrated. The practical limitations are identified and addressed using an excel model. An optimized system is suggested based on this excel model, and relevant issues regarding to the system have been discussed. Selections of building materials for this device are based on the conclusions of this chapter; which were constrained by both availability and cost. The physical size of each element is determined by the availability of the components.

6. Evaluation of the device using the theoretical model

6.1. Introduction

The main aim of this project is to investigate a low cost body composition analysis tool based on ADP analysis. This chapter is divided into the following steps to achieve this aim:

- Expand the theoretical model for the additional components
- Evaluate the device
- Provide a short note on the construction of the device

6.2. Second generation of the theoretical model

The second generation of the model is expanded from the first generation. A mathematical model has been created based on the physical parameters of the acquired components.

When one includes additional components the level of uncertainty is increased. This is why the theoretical model has been developed to consider the assumptions introduced with additional components.

The following has been added to this model:

- Components of the device
- Accuracy of the weight scale
- Assumption of isothermal air (which includes Thoracic air, GIT air and isothermal air around the skin)
- Determination of the surrounding atmospheric pressure

This evaluation is done using the model due to the following reasons:

1. The impact of each factor on the total accuracy in %BF can be estimated. A practical corollary of this is that the limited budget ($\leq USD1{,}000$) can be used wisely considering the importance of other factors.

2. The overall effect of the summation of factor errors on the total accuracy can be determined. This is important to decide whether the project is feasible under the current design.

3. If any of the components carry an unacceptable error, which affects the total accuracy, the design must be altered before construction of the device.

See relative information of the model in Section 5.6.1.

Some hidden factors may impact the whole system; such as the compatibility of the PC and the suitability of the motor. These are not included in the discussion as the present set up represents the best available equipment for this project.

6.3. Evaluation of the final design

6.3.1 Worst case scenario analysis

The error introduced by each assumption on the total accuracy (of percentage of body Fat), can be interpreted independently or in combination. Each assumption's error impacts the overall accuracy independently. The maximum error (worst case) for each assumption can be summed to see the worst case scenario on the total result.

The worst case scenario analysis is applied to the extreme case of our target subject. This happens to be the 50 litre person, hence "reference man". The physical attributes of the reference man is given in the following table:

Table 6.1
Information on the Reference man

	Information
Gender	Male
Age	35
Fat percentage	15%
Volume	50litres
mass	53.225KG
Lung volume	3.177L
Isothermal air around the skin	0.77L

Table 6.2 is compiled using the reference man which lists the assumptions, typical errors and how each error affects the overall accuracy. Notice these typical errors are only the initial step of estimations. Further adjustment should be made once the volume of the inanimate subjects is successfully determined.

Table 6.2

Estimation of the worst possible errors in body fat percentage from theoretical analysis

Element	Typical errors	Errors in term of %BF	Calculated worse case %BF for reference man
Weight	0.03 kg	±0.26%	14.8-15.3%
Isothermal air	10%	±1.65%	13.4-16.7%
Atmospheric pressure	0.05mBar	-0.182%	14.9-15.3%
Overall accuracy		±2.10%	13.02-17.23%

See appendix B6 for how these results are determined.

6.4. Discussion of significant factors that affect total accuracy

6.4.1. Weight

It is recommended to measure within 0.03kg. Any less precision will lead to a gross error in determining body composition

6.4.2. Isothermal air

The total volume of isothermal air is made up of the thoracic gas volume, Gastro Intestinal Tract gas volume and isothermal air around the skin. Handling these three items in turn:

Thoracic Gas Volume (V_{th})

The lung volume is determined using equations to predict the value. The equations are based on height and age (see formula 4.8 & 4.11). Reiterating section 4.5.2, the literature supports that lung volume prediction by these equations has little effect in determining %BF compared to lung volume obtained though measurements. The theoretical model shows that using the prediction method will not have a major impact on the total accuracy for differences between V_{th} and$V_{th_{pred}}$ is $\leq 10\%$.

For discussion, we must not exclude the possibility of extreme cases. The difference between V_{th} and $V_{th_{pred}}$ can be more that 10%, if say we use prediction to determine the volume of pediatric lungs or abnormal cases. I stress that the determination of isothermal air is necessarily approximate as there is no existing research that accurately specifies the calculation of isothermal air around the skin. The effect of less precise isothermal volume is less significant than say the lack of precision in atmospheric pressure as the volume of isothermal air in relation to the chamber is small. In order to check the effect of predicting lung volume, a first order test can be applied. The BMI should be calculated and compared with the calculated % body fat after a successful trial. If there is a discrepancy in this comparison the subject should undergo a lung function test. (See method of operation in 7.4.8)

Tidal volume (V_T) and V_{GT}

The typical size of Tidal lung volume is 500ml. This measurement is done using a spirometer. The typical resolution of the spirometer is 10ml. Typical V_{GT} is not more than 300ml (see section 4.5.3.).

Since V_{av} is determined by measuring mid tidal exhalation, the total effect of the tidal volume and the V_{GT} is small (~0.5 litres) compared to the size of air in the chamber (350 to 550 litres). According to the calculation by the theoretical model; the error is considered to be negligible.

Isothermal air around skin

In the literature, the typical amount of isothermal air around the skin is ~1litre (Fields 2002) for an average adult subject. There is no literature on their method of calculation apart from the figure being empirically determined.

In this project, a first order estimation of the isothermal air around the skin is attempted (see equation 4.13). This will be compared to different estimations in trial studies. The results will be cross referenced with the reference method (DEXA). (Method of operation is discussed in section 8.2.3). More specifically a large sample of subjects can be measured for body volume and body surface area and a regression performed to identify the random error which includes the effect of V_{skin}.

6.4.3. Practical interpretation

Here we have considered some of the most important factors that affect the result in the practical interpretation (table 5.4). This includes the instruments that determine the air in the plethysmograph such as the pressure sensor and the DAQ card.

The best solution (i.e. to improve accuracy) for these practical issues is to get better equipment. The model is used to show where better practical instruments are needed in order to obtain better results. In this project, the total cost on the materials and instruments is within budget (~USD 800).

In the process of finding a balance between cost and quality, assumptions have to be made, such as the motor is moving at constant speed. Every assumption carries potential error with it. Although there are so many sources of errors that impact the result; each of these errors are independent of one another. A short note is provided to address these significant factors that affect total accuracy.

6.5 Short note on construction of the device

The true volume of the chamber is difficult to measure since it is necessary to achieve a 1ml precision. It is not possible to determine the size of the chamber to the desired accuracy when constructing the chamber.

The size of the chamber is estimated as closely as possible, by filling it with water. When conducting practical experiments, inanimate objects of known volume should be used to calibrate the chamber. The model described in this chapter covers most of the errors that could occur.

There are still hidden factors that could impact on the measurement, such as the environment. These types of error can only be quantified empirically (See section 8.3 for the method of operation). The device should be constructed in such a way that each component is interlinked but independent. This facilitates future improvements. See appendix I for the implementation of these ideas.

6.6. Conclusion

The second generation of the theoretical model has been used to show that the lung volume can be estimated rather than measured in ADP analysis. The mass of the test subject and the atmospheric pressure must be known to high precision. The mode also shows that a combination of 10% error in lung volume, a 30g error in mass and a 0.05 mBar error on atmospheric pressure determination could also lead to > 2% error in determining %BF. This will happen even with an absolutely correct measurement in determine the amount of the air in the plethysmograph. Bearing the above discussion in mind, a prototype of the device was constructed and this is described in the following chapter.

7. Construction of the device

7.1. Introduction

Construction of the device was performed by implementing the concepts and design described in the last few chapters. The chapter is divided into the following sections to illustrate both the hardware and software development:

1. Basic components of the hardware
2. Orientation of the hardware
3. Introduction of the software
4. Concept of the software construction

Note that this chapter only covers the basic principle of the construction of this device. The detail of the construction of the hardware and the software are in appendix E.

7.2. Basic components of the hardware

This section is divided according to the theoretical and practical interpretation. The testing chamber, reference chamber, the dual piston mechanism with the stroke volume, differential pressure sensor and associated circuitry, barometer, data acquisition device (DAQ), computer, calibration tool, pressure release valves and leakage pipe are used to determine the amount of the air in the plethysmograph for practical interpretation.

Height meter, weight scale and spirometer are used to measure the factors necessary for the calculations in the theoretical interpretations. See figure 7.1 for a photo of the device. More photos and basic features of the elements are contained in appendix F1 and f1

Figure 7.1 The ADP Device

7.3. Organization of the hardware

The hardware construction is based on the short note in section 6.5. Each element is designed in such a way that it can be removed and replaced very quickly. The elements described in the theoretical interpretations are arranged in the same order as described in the testing steps. The practical interpretation is explained by following the energy transfer from one element to the next (see Figure 7.2).

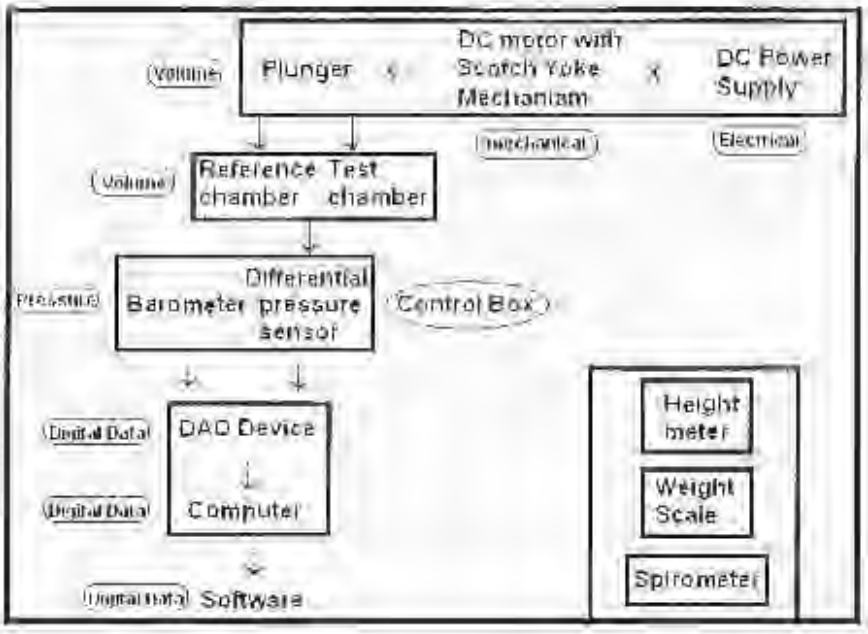

Figure 7.2 The block diagram representation of the hardware

A DC motor is used to drive a scotch yoke which in turn drives the pistons in a sinusoidal motion. This creates the sinusoidal changing volume in both of the chambers simultaneously. See Appendix H2 for the engineering drawing of the dual piston mechanism.

The pressure change in each of the chambers is proportional to the respective changing volumes. The plungers are connected to the chambers via circumferentially reinforced pipes. 5 mm diameter PVC pipe is used to connect the differential pressure transducer to each of the chambers. This allows the differential pressure sensor to detect the pressure difference between the two chambers. The differential pressure sensor and the barometer are located in the control box which in turn is located outside the chambers. See appendix E1 for the layout the control box.

A signal cable (SH6868-EP from national instrument) connects the signal from the control box to the DAQ device (see appendix C2 for the description of this cable). The DAQ device (NI 6013) is located in the computer; signals are collected and transferred to the digital signals by the DAQ device. The data is then sent to the software. The acquired data is ready for processing.

7.4 Introduction to the software

The software serves as a bridge (interface) between hardware and operators. A successful software design should be user friendly, easy to understand, and allow expandability for future development.

Three software packages namely: NI DAQ6.9.3, Measurement & Automation Explorer2.2, and Labview6i are used to perform the following task (figure 7.3.):

- To recognize the hardware (using NI DAQ 6.9.3),
- To allow the operator to communicate with the hardware (Using measurement & automation Explorer 2.2)
- To get the data and process it according to the conclusions from the last few chapters (Using Labview 6i)
- To analyse and evaluate of the results (using Labview6i)

See appendix E3 for the introduction and the historical review of these software packages.

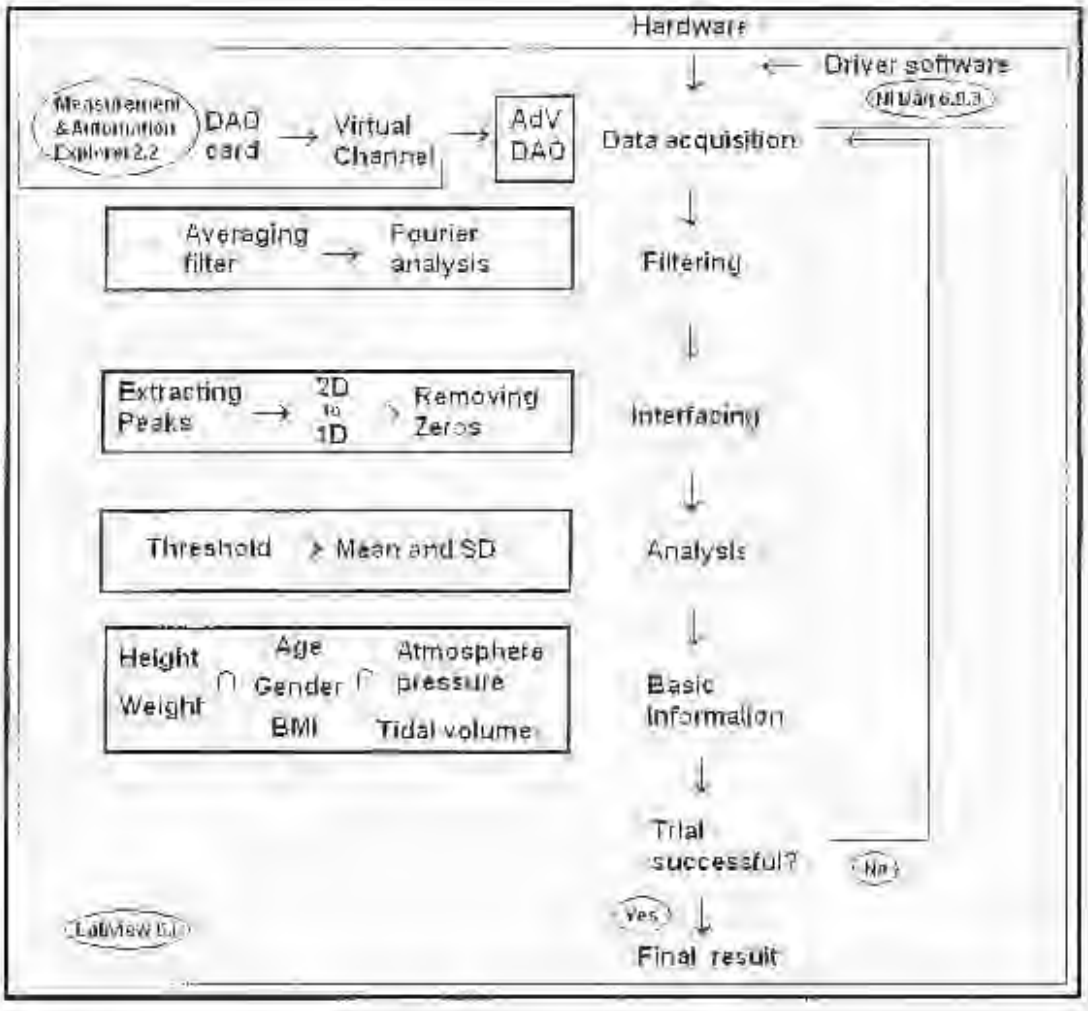

Figure 7.3 Flow chart of the software concept

7.4.1. Concept of the software

Data flow from one stage to the next is the main aim of this software. Only one task is completed in each of the stage at a time. These tasks are broken into smaller tasks which are performed by these three software packages. In this way the software can be improved easily. The software contains the following main tasks (figure 7.3):

- Data acquisition
- Filtering
- Interfacing
- Analysis
- Basic information
- Evaluation of the trial
- Final Result

7.4.2. Introduction to Labview

Labview programs are called virtual instruments (VIs). VIs are composed of two windows, namely Front panel and Block diagram. The front panels serves as the graphical user interface and contains the user input (also known as controls) and outputs (also known as indicators). They are displayed on the front panel in various forms required. See the arrangement on the front panel on page 208 for these controls and indicators.

VIs could be transferred into a Sub-VI which can be joined and placed into a higher order VI. This chapter only covers the basic principle of the first layer sub-VI; the second layers of the sub-VIs are covered from page 195 to 207 of appendix E3.

7.4.3. Data acquisition

Before the data can flow between the PC and the DAQ system, we must make sure that the pc can recognize the DAQ device (NI 6013). DAQ 6.9.3 creates the link between the DAQ card and the operating system (Microsoft, Window XP)

Once the PC detects the DAQ card, we must make sure the signal can be successfully transferred to the Labview program for further processing. The Measurement & Automation Explorer 2.2 is used to set up these virtual channels. Measurement & Automation Explorer2.2 also serves to convert the signal from voltage to pressure. i.e. from voltage to mBar.

After the data is captured successfully and transferred to Labview 6.1. A VI "ADV-DAQ" is used to set the sampling rate, duration of the trial and the desired sampling channels. The obtained from "ADV-DAQ" flows to the filtering section of the software. See table 7.1 for the default settings of the DAQ card.

Table 7.1
Default settings for the DAQ card

Controls	Physical amount and its unit
Sampling Rate	100,000Hz
Trial duration	20 seconds
Total sample	2,000,000
Sample channel	Differential pressure sensor

7.4.4. Filtering

Two VIs are included in this section namely "Averaging filter" and "Fourier analysis"

The data obtained is first sent to the "Averaging filter" for processing. Average filter divides the data stream into sets of 100 points and calculates the median of each set. This is done in order to minimize the random error created by the DAQ device. This procedure provides the desired sampling rate (1000 Hz). The signal is then processed further by using Fourier analysis to remove signals outside the frequency band of interest.

In the Fourier analysis, two mode of filter are available for selection: namely "Ideal filter" and "Butterworth band pass filter". Butterworth band filter is the default. Ideal filter mode is included for the possible further development proposed, as it is more suitable for an absolutely constant frequency input (e.g. precise electrical power driven loud speaker). Before analysis of the data, the filtered signal passes through an interfacing stage.

7.4.5. Interfacing

Three VIs are included in this task. Namely "Extracting Peaks", "2D to 1D" and "Remove Zeros". The peaks of the filtered waveform are firstly extracted by the "extracting peaks" VI, these peaks determine the changing pressure (ΔP). This result is in two dimensional (2D) matrix format. This data is rearranged into a one dimensional (1D) array by "2D to 1D" VI. The data then flows to the "Remove zero" VI. This removes any zero data due to distortions during the trial period or in the first and the last array.

This interfacing stage transforms the filtered data to a series of the changing pressures (ΔP). The size of this array ($size_{array}$) is used for feedback proposes (see section 7.4.8).

7.4.6. Analysis of the changing pressure (ΔP)

Two VIs are included in this process namely "Threshold" and "Mean and SD". Threshold VI excludes any ΔP that are out of the acceptable range. Some reasons why these erroneous ΔP's occur are:

- Movement of the subject in the chamber during the trial period
- Noise generated from the environment
- Accidentally opening and closing the door
- Shaking of the chamber

The size of the remaining data in the array ($size_{new}$) is used for feedback proposes (see section 7.4.8). The mean and the standard deviations of the changing pressure are calculated and fed into the Basic information VI.

7.4.7. Basic information

Two sets (measurements obtained from theoretical and practical interpretation) of data are entered into the basic information VI. ΔP is coming from "Mean and the SD" VI in the analysis section and the Height, weight, age, sex, tidal volume, atmospheric pressure value are entered manually. V_{tidal} and BMI are determined by these two sets of the data hence %BF of the subject.

7.4.8. Evaluation of the trial

This section is named "warning" in the software. Two type of the evaluation is applied here: firstly, $size_{old}$ and $size_{new}$ will be compared, If more than 25% of the ΔP values from the trial are outside of the threshold values, an error warning will be generated and the test will be reported. This type of error will occur if artifacts are generated during the trial. It is recommend the test to be repeated again. As an additional test, the calculated % BF is compared to BMI. If the result shows an unexpected disagreement for a particular test subject, it is recommended that the test be repeated and lung function be preformed. More detail is covered in the Warning section on page 205.

7.4.9. Final Result

If the trial passes two checks mentioned in the last section, the result is accepted. If the trial is reported to be unsuccessful, a new trial will need to be conducted.

7.5. Conclusion

The hardware and the software are constructed according the principle finding in the last few chapters. The whole package is constructed in a way that is user friendly and can be upgraded easily.

For both software and hardware, the components link to one another and are independent to allow the further development to be achieved from component point of view.

8. Test process and Results

8.1. Introduction

Previous chapters have outlined the theory of ADP and critical factors for obtaining accurate estimation for % body fat. A two chamber system has been designed and constructed based on these insights. As mentioned, the air in the chambers needs to be compressed in order to measure the resulting pressure change (ΔP). This chapter presents the results of chamber air compression using 4 different methods, of which the 4^{th} method was chosen in the final implementation of the device; namely a dynamic dual chamber system. The results using this system to measure the volume of inanimate objects are presented and discussed. The chapter is divided in to the following sections:

1. Method used in the testing procedure for the validation study
2. Investigation of three possible ADP designs
3. Dynamic dual chamber system
4. Identification of the errors in the practical interpretation
5. Evaluation of the design

8.2. Method of device validation

As previously stated, body composition analysis requires high precision. An error at any step of the testing procedure can have a large impact on the result. This means that studies have to be performed to identify sources of error, and these need to be minimized by suitable hardware and software design. Part of this is achieved through theoretical analysis (described in pervious chapters), however the final product need to be tested practically. Results of these tests are then used to redesign the device using the following chart:

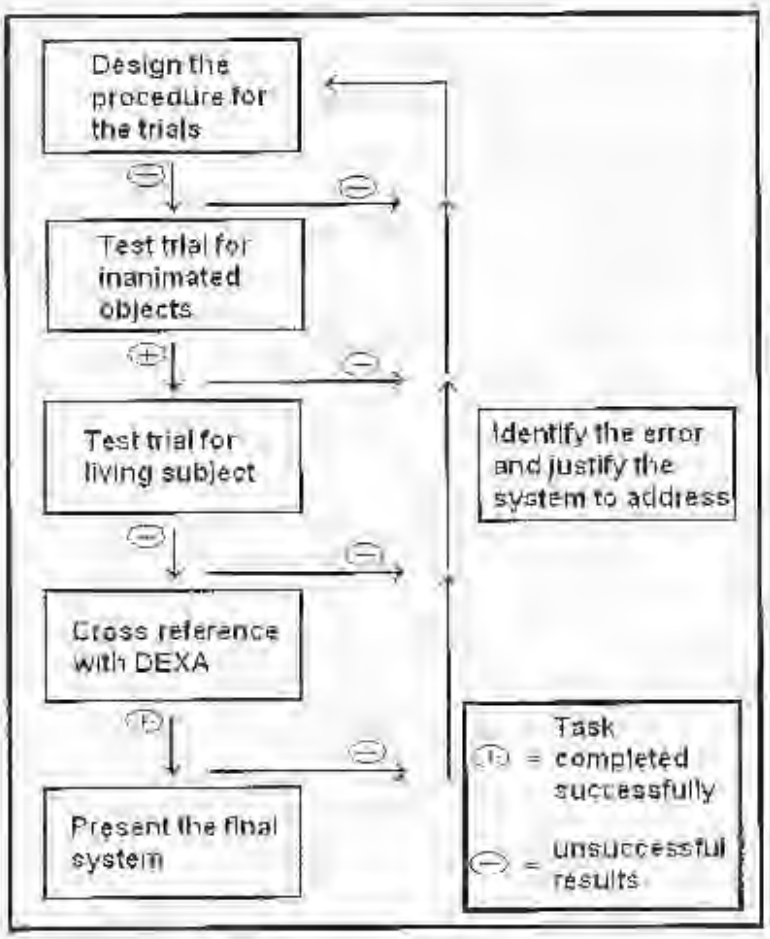

Figure 8.1 Flow chart of the device validation

In figure 8.1 the positive sign means that the result of the volume measurement is good enough and hence that we can move to the next step. A negative sign means that the result of the volume measurement is unacceptable or that there is disagreement between results. A poor result implies that some aspect of the set up has to be reviewed. These aspects could either be in the design stage or testing stage, either way the system must be adjusted to address this issue.

Trials can be divided into three main parts: those on inanimate objects (by using the calibration tool), human subjects and cross referencing with DEXA. See appendix F9 for the detail of operation of the ADP device.

8.2.1. Testing using inanimate objects

Styrofoam bricks, with known volumes were used to test the device; the bricks were added sequentially in multiple tests to achieve test volumes between 50 and 100 litres. In each test, the volume was compared to the true volume. A successful measurement means reaching the initial goal of this project at different points in time.

8.2.2 Testing using living subjects

Once the testing of inanimate subjects is completed, trials on human subjects can be performed. The measure of success is that different individual's results should be consistent and in agreement with the results from DEXA.

Test procedure for test subjects (see figure 8.2):

1. Trial subjects are required to sign their consent form (see appendix F2).
2. Trial subjects then do anthropometry measurements as well as fill in the personal information form (see appendix F3). This step provides the height, weight, sex and tidal volume of the test subject.
3. A calibration trial using a known volume inanimate object is done immediately prior to the measurement. This step happens at the same time while the test subject is busy filling their consent form and personal information form.
4. Inputting of the personal data to the software
5. Performing the trial according to the test procedure. See the detailed instructions in appendix F4 (for the test subject) and F10 (for the operator)
6. Results are presented in terms of % body fat, V_{body} (corrected body volume) and Body Mass Index (BMI)

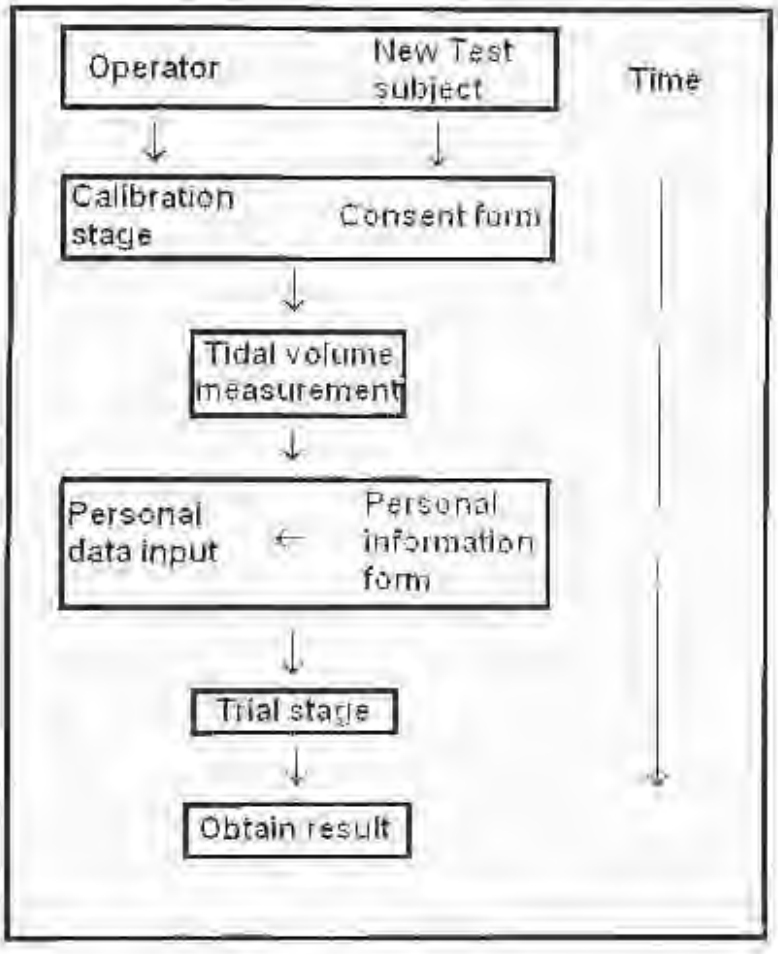

Figure 8.2 Flow chart of the test procedure

8.2.3. Cross referencing with DEXA

Once consistent results are achieved with body composition analysis using ADP, it can be compared with the reference method for this project, i.e. DEXA.

Using DEXA to determine the body composition will allow the assumptions of the ADP device to be refined. In particular, it is essential to estimate the volume of the isothermal air around the skin and so this will have to be determined empirically in a trial using DEXA.

A total number of not more than 10 subjects are appropriate for initial cross referencing. The subjects will not be permitted food or water between measurement of body composition with ADP and with DEXA, and these measurements will be performed as closely as possible in time.

The results of the two methods will then be compared. If the correlation between them agrees with the literature studies, the ADP device will be determined to have been successfully developed. On the other hand if unacceptable correlations are obtained; the assumptions such as isothermal air volume will be refined and the steps of the test procedure repeated until an acceptable result is achieved.

8.3. Investigation of three possible ADP designs

Three designs were investigated:

1. Using the lung diaphragm as the volume displacement generator.
2. Using a commercial ventilator as the volume displacement generator
3. Using a single chamber system with motor driven piston pump as the volume displacement generator

See Critical reasoning of these attempts in appendix F5 and details of these methods and related issues in appendix F5 to F8

8.3.1. Using the lung diaphragm as the volume displacement generator

In this design, the assumption is that the stroke volume (ΔV) can be caused and quantified by breathing and the resulting change in pressure (ΔP) measured. The body volume is calculated using the following equation:

$$V_{body} = V_t \quad P_{atm}\left(\frac{\Delta V_t}{\Delta P}\right) \tag{8.1}$$

Figure 8.3 shows the results obtained using this design. This graph is offset by the average value for 21 trials on the same subject, and only shows the variation of each separate trial (this also applies to figure 8.4 and 8.5). The differences in calculated body volume can be as large as approximately 20 litres from sample to sample.

Figure 8.3 Calculated body volume for 21 trials on the same subject using breathing as an air displacement generator

8.3.2. Using a commercial ventilator as volume displacement generator

The main assumption is that the ventilator delivers a constant stroke volume at a constant frequency. Two stroke volumes (0.75 litres and 1.5 litres) were used. Figure 8.4 shows the differences in calculated volume can be as large as 5 litres from the mean

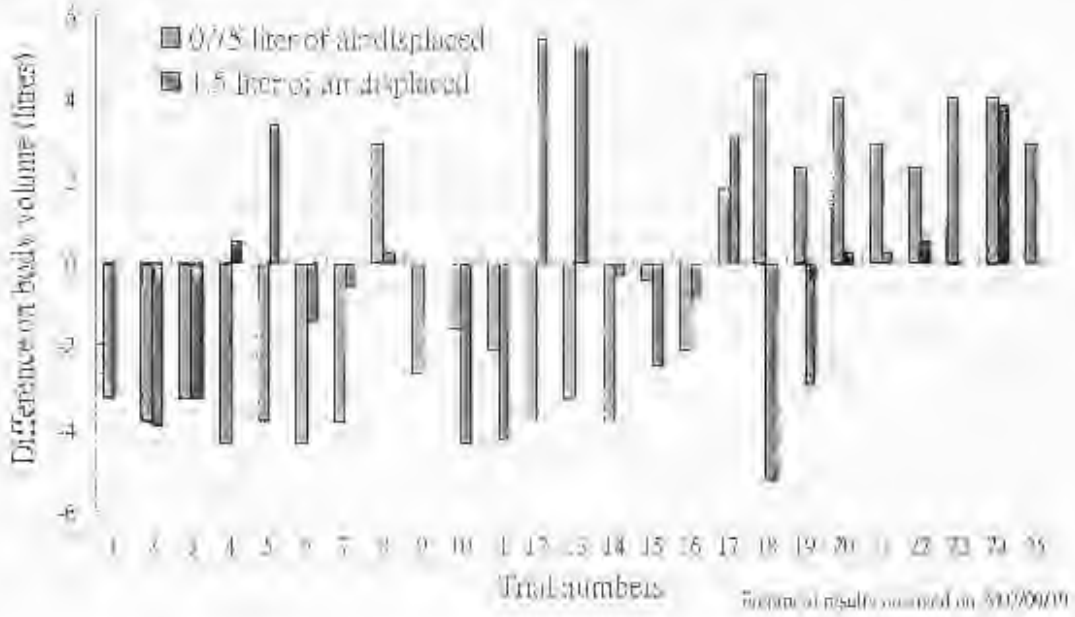

Figure 8.4 calculated body volume for 25 trials on the same object using a commercial ventilator as the air displacement generator

8.3.3. Single chamber system using a motor driven pump

The biggest advantage of using a motor driven piston type pump is that the pump delivers an absolutely constant volume displacement. This reduces the variation on body volume calculated from $\Delta P / \Delta V$, since ΔV is accurately known and absolutely constant. Figure 8.5 shows a maximum difference of 2.5 litres from the volume between 15 trials in a single subject using a motor driven piston pump to drive a single chamber.

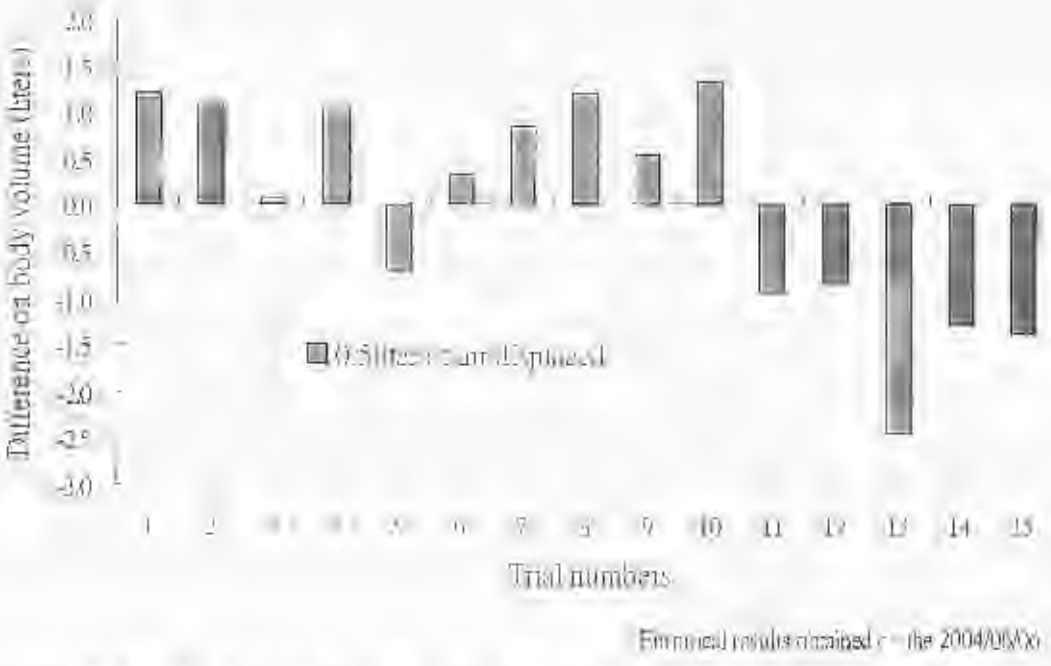

Empirical results obtained on the 2004/05/06

Figure 8.5 calculated body volume for 15 trials on the same subject using a single chamber driven by a motor driven pump

8.3.4. Discussion of these three designs

None of these three design is able to measure the body volume to the necessary level of accuracy (200ml) required for body composition analysis. The best design of the three is the motor driven piston pump as the stroke volume is known accurately and is constant. This reduces the error in calculating body volume considerably. See further discussion in Appendix F5

The empirical results serve to validate the theoretical model, as empirical studies for the single chamber analysis agree with the predicted results from the theoretical model in table 5.3 (where in the theoretical model 2%BF accuracy is interpreted as 200 ml variation in volume. Similarly 1 litre represents more or less 10% of BF).

8.4. Dual chamber dynamic system

This design uses two chambers, namely a test chamber and a reference chamber, each driven by a piston pump. The difference in pressure between the chambers is monitored. The idea here is that the pressure difference between the two chambers that is due to extraneous effects will be reduced while those due to the object being measured are enhanced.

8.4.1. Method of operation

The sizes of the test chamber and the reference chamber are determined using the single chamber method as described in the previous section. It is the most readily available method to determine the sizes of the chamber as well as the effect of the air leakage. By using the same method, constant variables[1] are generated (because the size of the two chambers does not change over time) using formula 5.2 which is used to determine body volume (V_b). See more discussion about these constant variables in section 8.5.

With the established chamber sizes, the volumes of the test objects were measured. The absolute difference between the true and the empirical values for the inanimate objects are determined and discussed. Based on these findings, the deviation between empirical values for the inanimate objects and the average value are used to calibrate the device. See the rectification process in appendix F9.

---

[1] Constant variable refers to the parameters that are regarded as constant over the duration of an experiment.

8.4.2 Results

After more than 5,000 samples of study, the pressure change in the test chamber in response to the known changing volume (ΔV), was consistent with a chamber size of ~588 litres, and reference chamber ~174 litres. These volumes are larger than those obtained by filling the chambers with water, e.g. filing the test chamber with water yield a volume of ~520 litres. The disagreement between the two results is due to controlled air leakage into the chamber. The leakage makes the experienced pressure seem smaller hence the chamber size looks greater. This result agrees with the theoretical test chamber (585.2 liters). See appendix B7 for the detail of the simulation.

More than 20,000 sets of data were obtained using the dynamic chamber system. Most of the data follows a similar pattern. Typical data were selected to represent the problems encountered during the development of this device.

The following result compares the difference between the measured volume and true volume of inanimate test objects. The average of 15 successful trials is used here to represent each point.

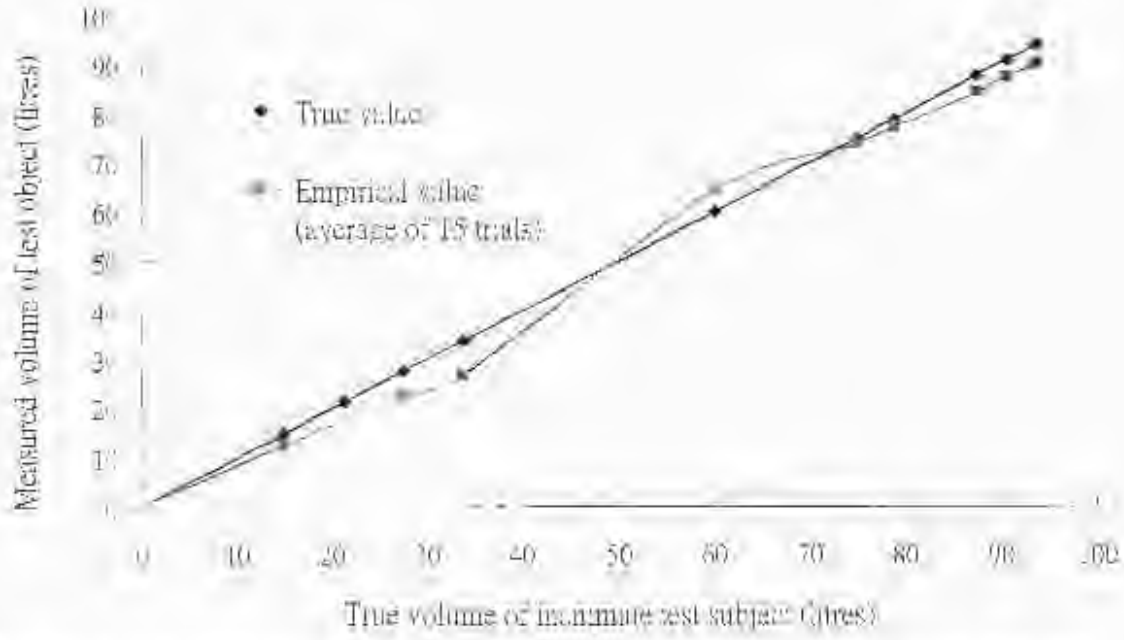

Figure 8.6 Comparison between the measured volume and true volume of inanimate test objects

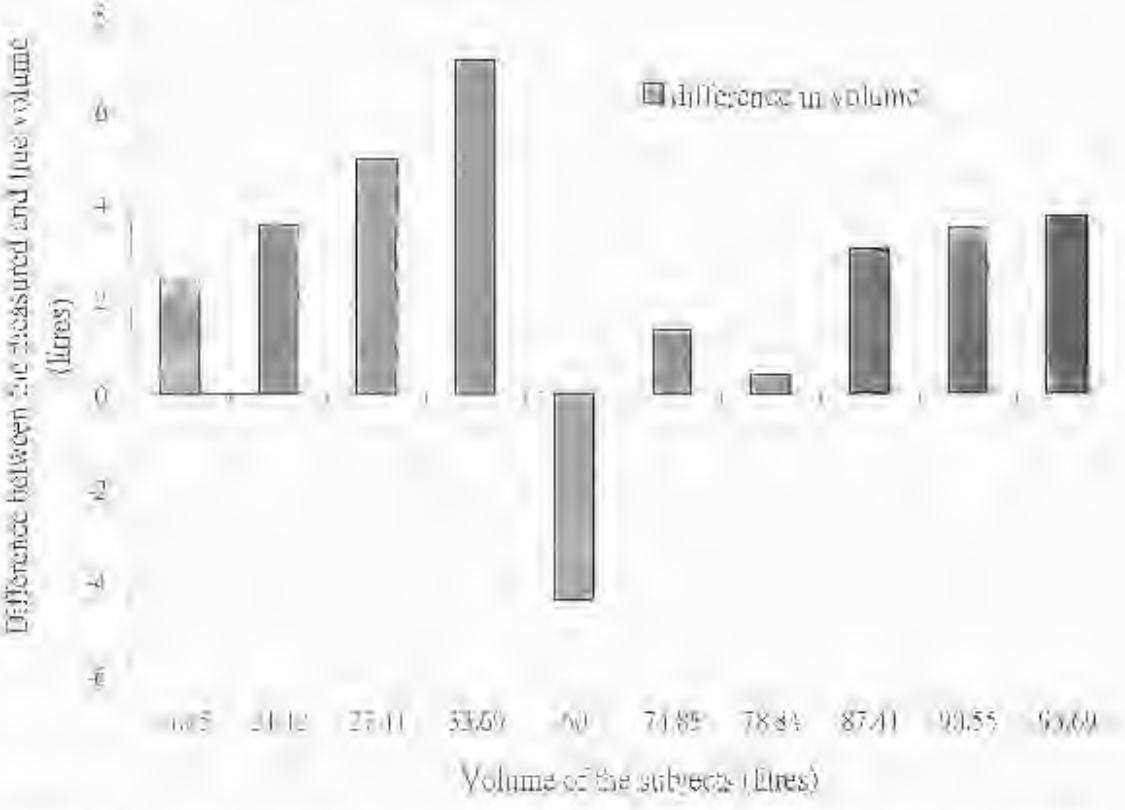

Figure 8.7 Differences between the true volumes and the empirical volumes for inanimate test objects

The relationship between the volumes of inanimate test objects to their corresponding experienced pressure has also been investigated. A second order curve has been fitted to these empirical results. These results are compared with two theoretical curves: One generated with no air leakage from the chamber and the second generated from the case of controlled air leakage from the chambers using 1.5 m long pipes of radius of 3mm (figure 8.8).

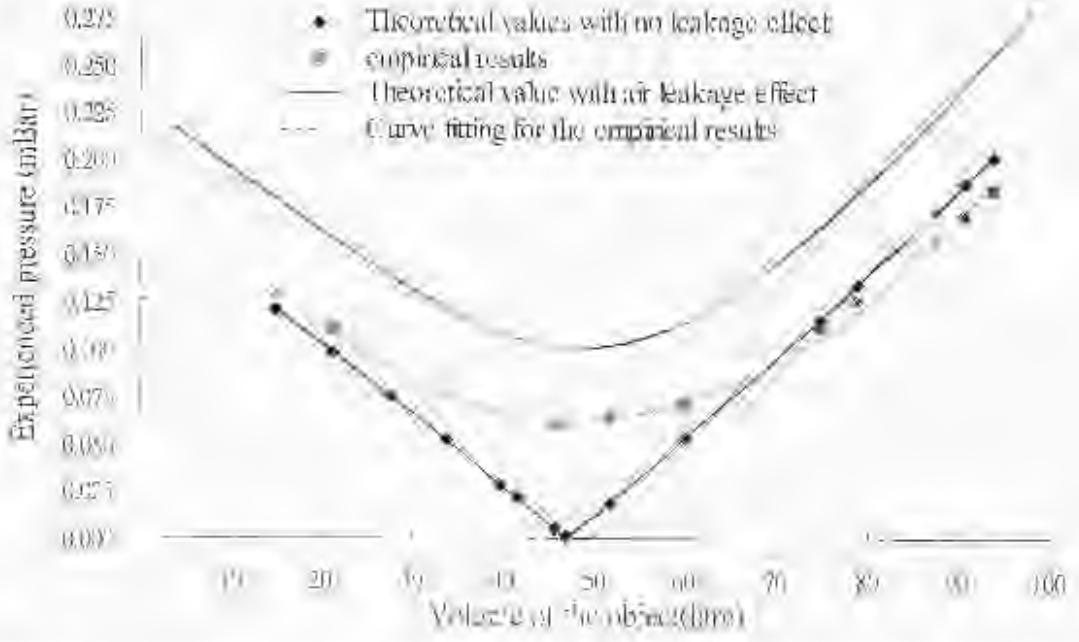

Figure 8.8 Measured and theoretical pressure difference for inanimate objects in a dual chamber system

8.4.3. Discussion of the results

The theoretical analysis (in figure 8.8) shows the pressure difference between the two chambers to be almost constant for the test objects between 10 and 60 litres. In this range it is difficult to determine a unique value of the volume since the experienced pressure curve in this range is almost flat. These measured results are very similar to the

theoretical result in this regard, reinforcing that this volume range should be avoided when performing volume. The empirical results do not closely match either of the theoretical values. There are two major reasons for this. Firstly, since pressure is almost the same for the two chambers the relative amplitude of the surrounding noise becomes more significant. Secondly the true volume of the test and reference chamber is roughly estimated in the air leakage analysis. Due to these observations, any further experiments for subjects between 40 and 60 litres are excluded at this stage. For this discussion, the results are grouped into two divisions: 0-40 litres and 60-100 litres. Result obtained from both groups are investigated and compared separately. This serves to help aid further development by determining whether to decrease the size of the test or reference chamber. This approach shows that for further development, the test chamber size should be reduced by at least 60 litres or alternatively the reference chamber by at least 20 liters to circumvent the problem. In figure 8.8, a constant offset is also observed between the empirical result and the theoretical value with the air leakage effect. This could result from the assumption concerning the constant variables. Individual trial results should be investigated to verify this presumption.

8.4.4. Individual trial results

Two groups of results are evaluated (see figure 8.9 & figure 8.10). 15 trials were performed with 4 objects of different volumes. The average value of the 15 successful trials is used as the zero and the spread is shown by the difference between each trial and the average value.

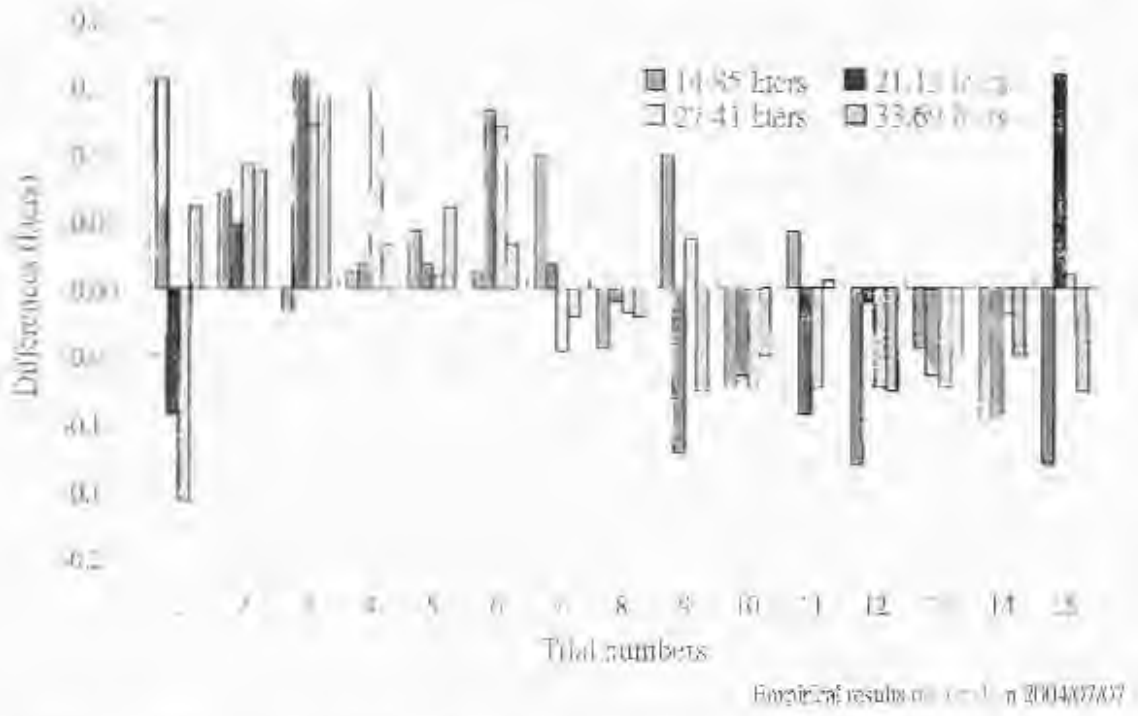

Figure 8.9 Empirical studies for the test objects form 0-40 litres

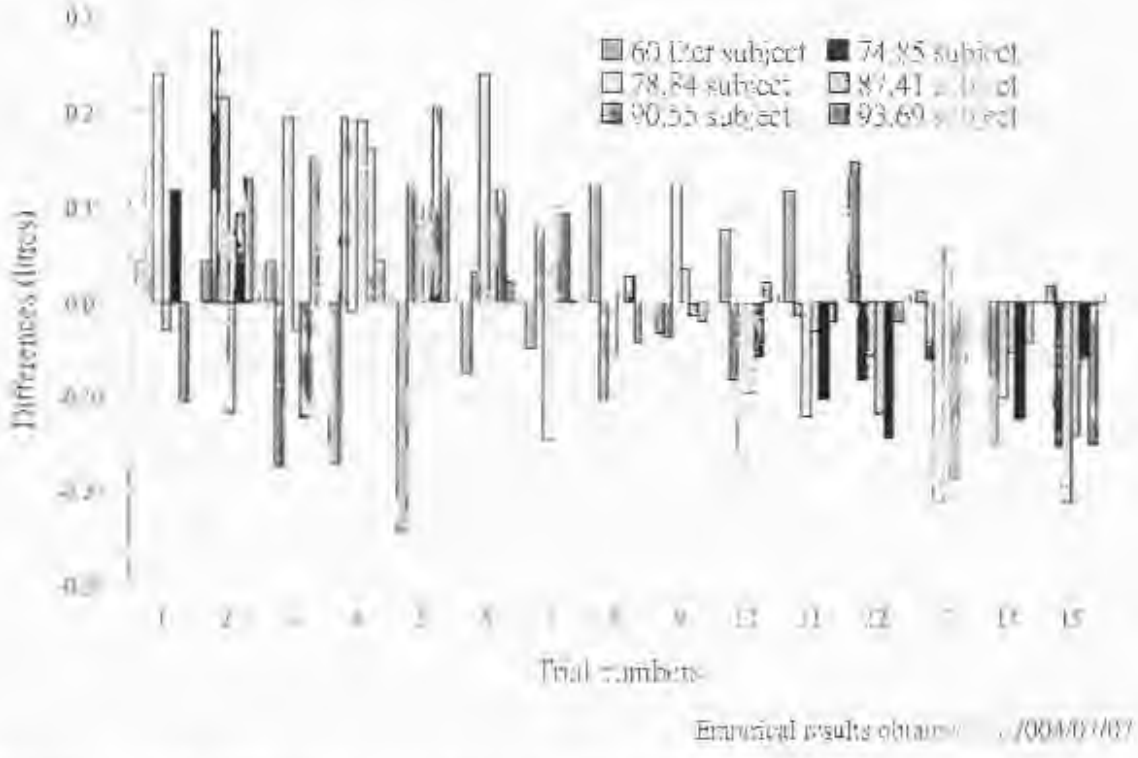

Figure 8.10 Empirical studies for test objects form 60-100 litres

The same 60 litre object was measured on three different days. Figure 8.11 shows the result of the three measurements. Similar to above, the average value of the all the results is used as the zero.

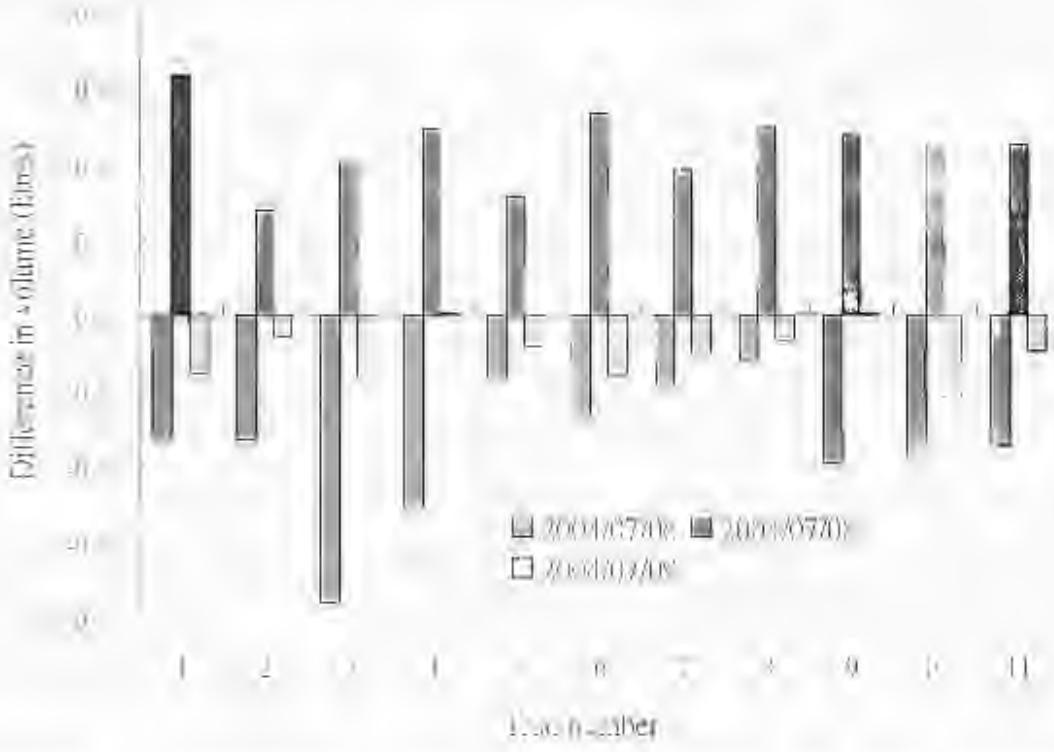

Figure 8.11 Comparison of the measured volumes for the 60 litre test object over three days.

8.4.5. Analysis of the individual results

In figure 8.9 & 8.10 individual trial results are found to be repeatable. This verifies the earlier presumes in section 8.4.3. Figure 8.11 shows consistent results on any given day. The similar trend but slight variation between the three different days could therefore be due to different atmospheric conditions. Although the variations are compensated for in the software, inaccuracies in the barometer can cause errors from day to day as identified in appendix E2.

Due to budget constraints of this project; it is not applicable to acquire a more precise barometer. To accomplish this issue, the absolute atmospheric pressure is assumed to remain constant for a short period of time (within one hour); hence the atmospheric pressure becomes another constant variable in the project.

8.5. Critical reasoning about the constant variables

The following variables are assumed constant in the calculations

- Size of the test chamber
- Size of the reference chamber
- Leakage air from the test chamber
- Leakage air from reference chamber
- Atmospheric pressure at the time of the trial
- Frequency of motor which drives the piston pump

Unless one can be certain about the absolute value of each of the components, a calibration stage is needed. It is unavoidable to make the assumptions that the above mentioned variables are constant during the measurement time. Subject to these assumptions; the ADP device can be calibrated by objects of known volume. For each known calibration volume, the relationship between the change volume due to the pump (ΔV) and differential pressure (ΔP) is measured. This relationship is constant, and allows us to determine an unknown volume from ΔP alone. See appendix F9 for the detailed calibration procedure. The calibration is performed separately for objects below 40 litres and above 60 liters (see figure 8.12 and 8.13).

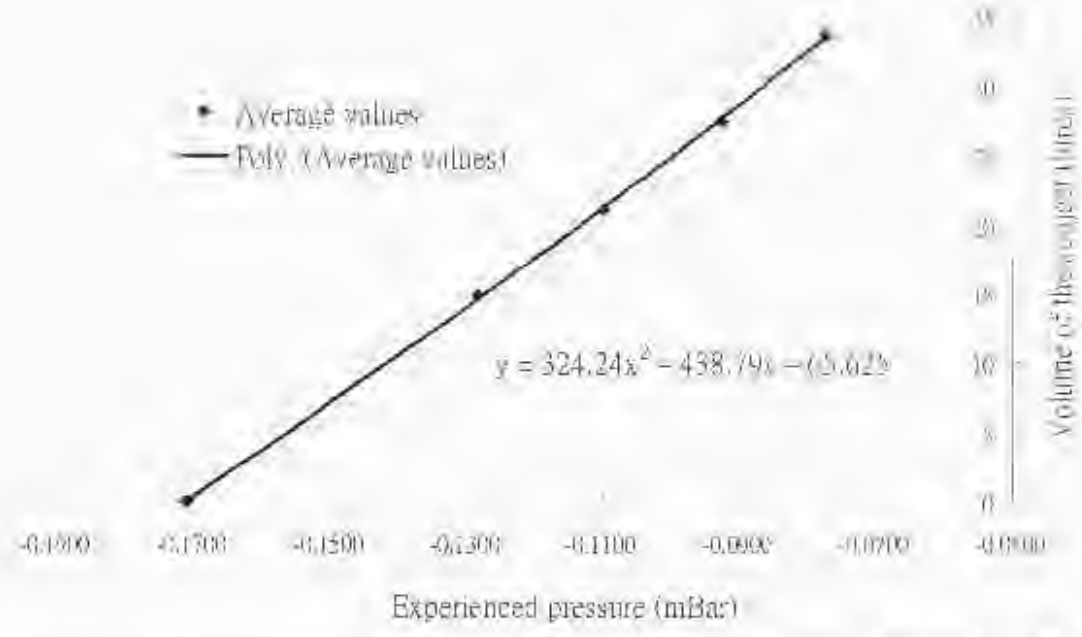

Figure 8.12 Relationship between pressure and the volume of calibration test objects between 0-40 litres placed in the chamber

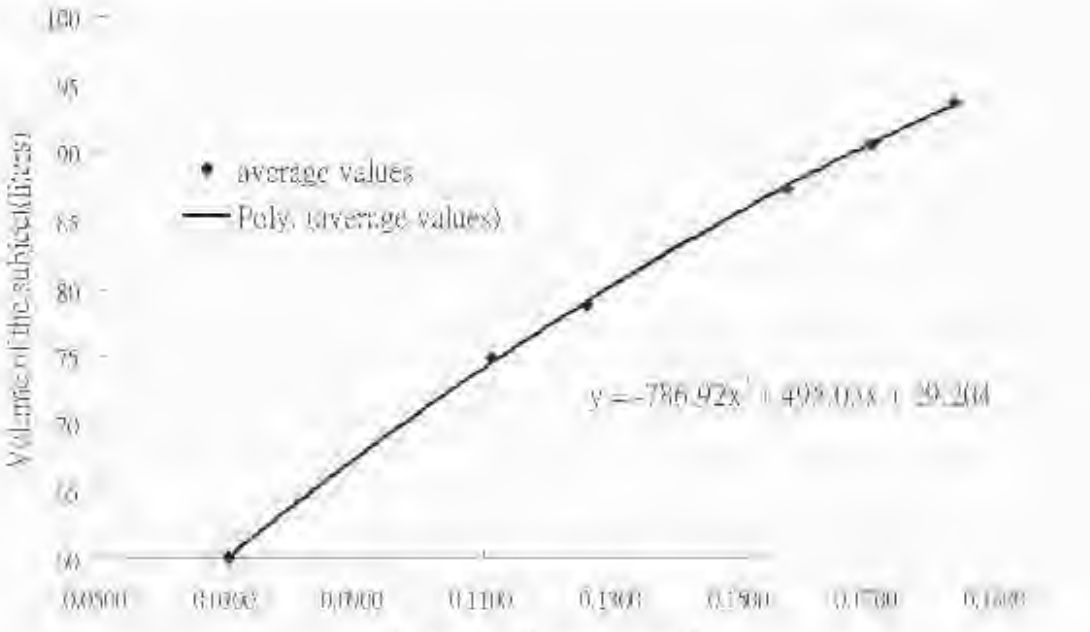

Figure 8.13 Relationship between pressure and the volume of calibration test objects between 60-100 litres placed in the chamber

A second order curve fitting was fitted to the empirical results. The coefficient of the equation is used to calculated the volume (V_g) from measured differential pressure (ΔP). The relationship allows us to calculate the volume of any test object from the (ΔP). Figure 8.14 shows the calculated volume of the test subjects, using the empirical equations.

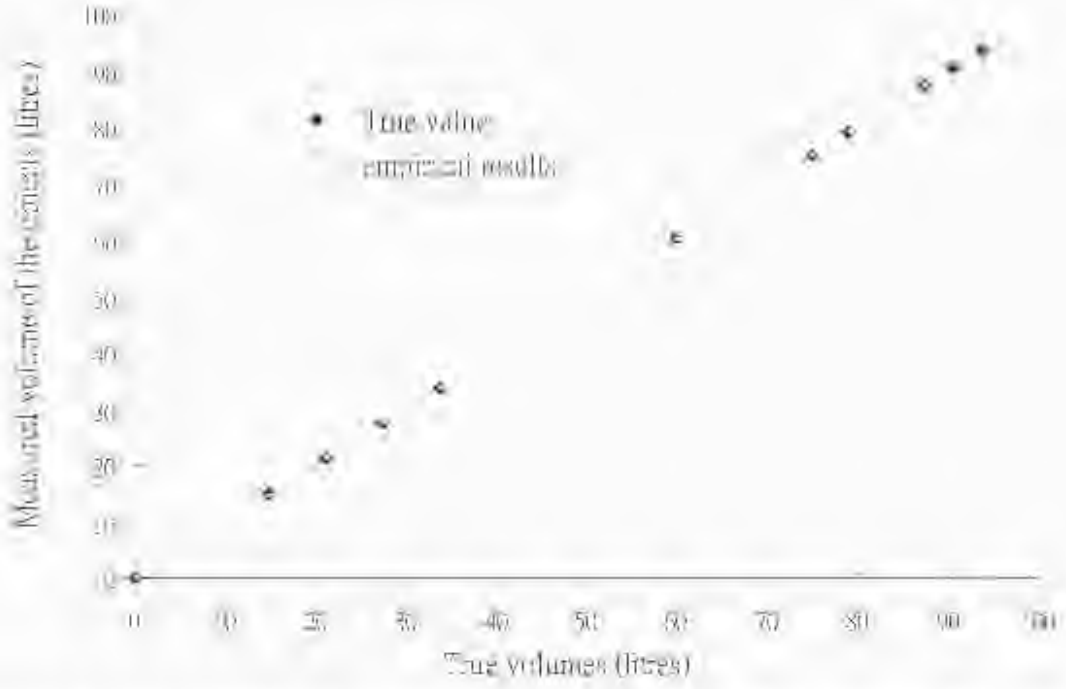

Figure 8.14 Comparison between the true and the empirical volumes after calibration

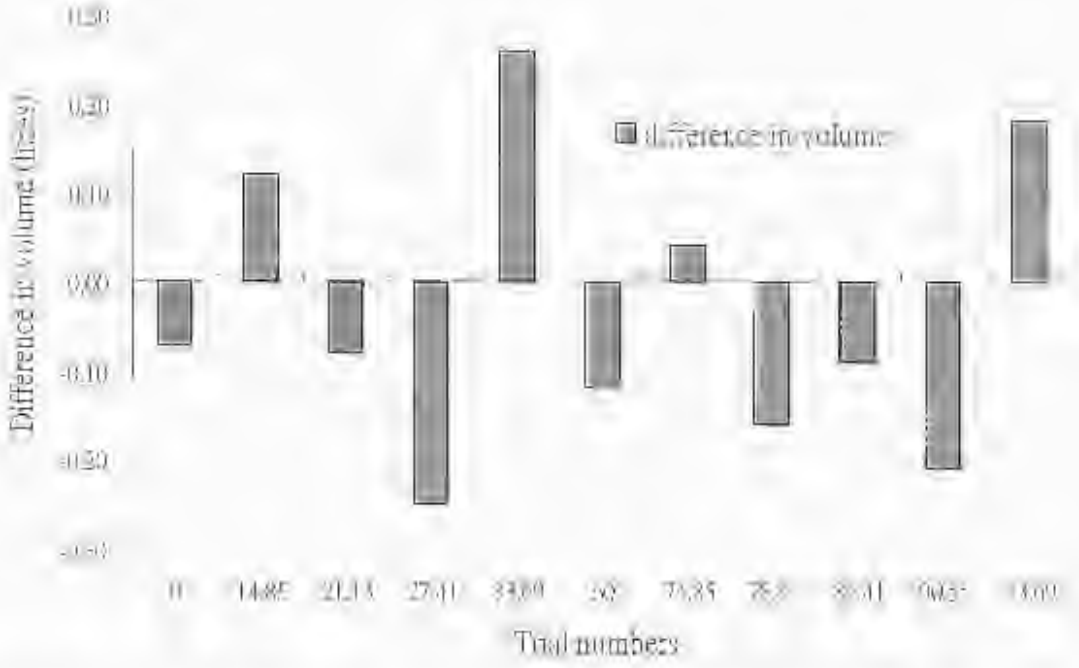

Figure 8.15 Difference between the true volume and the measured volume

8.6. Analysis of the calibrated results

In figure 8.15, the measured volumes closely match the true values after calibration of the system. However the results still contain unacceptably large errors (i.e not within 200ml).

One of the assumptions for this project is that the motor which drives the piston pumps is moving at a constant frequency (section 6.7). If the assumption is made that motor frequency is constant, then the calculated volume of the test object will contain an error if the motor frequency varies.

A linear relationship has been found between the speed of the motor and the calibrated volume of the test objects (figure 8.16). Description of this linear relationship would be: the higher the average motor speed, the larger the subject appears to be.

An explanation for this is that when the motor is revolving at a higher frequency, the AC leakage becomes relatively smaller in comparison to the stroke volume; (see the description of the AC leakage in appendix B7) leakage volume from the chamber is proportional to the amount of time over which the leakage occurs, so for a higher frequency, (period of cycle is shorter), there is a lower leakage from the chamber. When the AC leakage is small, the experienced pressure (ΔP) is large, due to this effect the size of the subject is over estimated vice versa for low frequency.

The result of an experimental study is shown on the following Figure 8.16. The relationship between the motor frequency and the calculated volume seems to be fairly linear. Variations in motor frequency therefore have a direct bearing on the calculated volume.

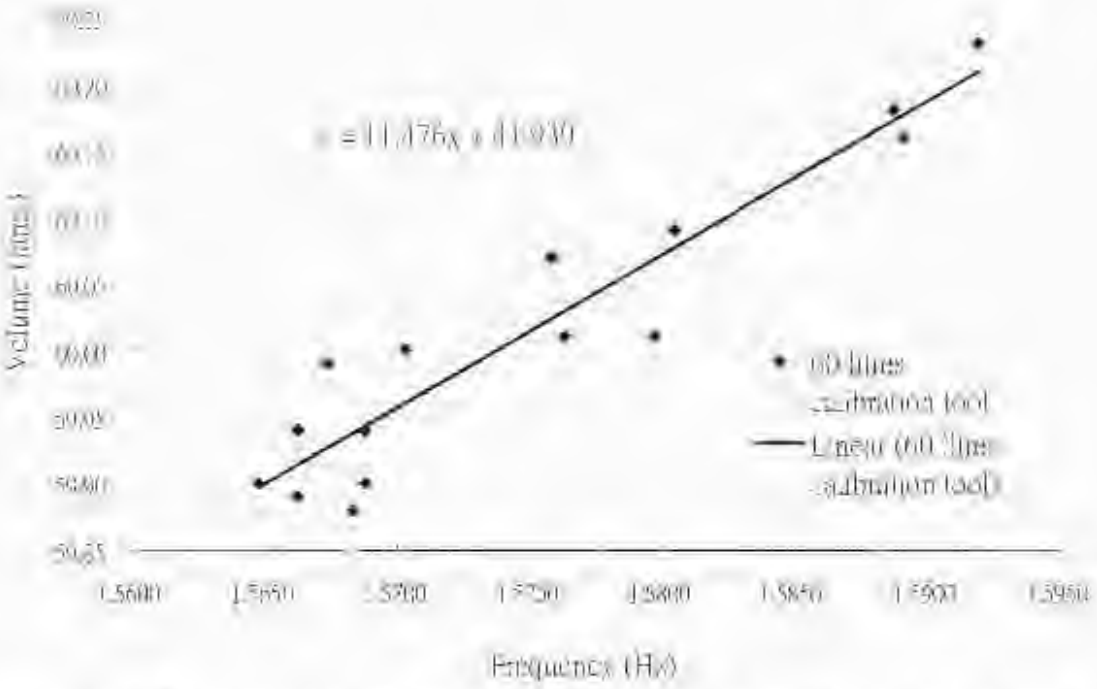

Figure 8.16 Relationship between calculated volumes (for a test object of true volume equal to 60 litres) with slight variation in the motor frequency

The fact is that figure 8.16 is not a perfectly linear relationship, could be caused by the following:

- The random error from the barometer
- The random error from the differential pressure sensor
- The random error of the DAQ card

These errors are always present and result in corresponding errors in body volume estimation. Because of these errors, it is inadvisable to correct the calculated volumes from motor frequency using the linear relationship determined earlier. The solution to this problem is to acquire an absolutely constant frequency stroke volume generator.

With the present set up. The size of an inanimate object can be determined within ± 300ml accuracy. (or 1% full scale) although this is precise in determining the remaining air in chamber, it is not good enough to provide a promising result for body composition analysis, where 200ml accuracy is required for a less than 2% error in body fat estimation. Although, with the present set up, the initial goal of 200ml accuracy has not been attained, the source of error has been identified and its effect quantified in determining the volume of the subjects. The next chapters give recommendations to overcome these problems, which if implemented, should result is an appropriate system for body composition analysis.

8.7. Conclusion

The procedure for measurement and the calibration steps are proposed in this chapter. By using a stable frequency motor to drive the air displacement into two chambers (reference and test chamber) and by measuring the pressure differential, good correlations have been obtained between the true volume and the calculated volume of inanimate test objects.

It is concluded that consistency of the motor frequency is the major key in ADP analysis for body composition analysis (beside the accuracy of the pressure sensor and the volume precision of the DAQ system). A further development system is suggested in the next chapter based on these conclusions.

9. Discussion and Recommendations

9.1. Introduction

This chapter is divided into two parts. discussion and recommendations of the ADP device and the 2C model. Recommendations for the device include suggestions to improve the present set up. A detailed plan and cost to implement this is also included.

Even if the measurement of the subject's body volume can be as precise as necessary, this would not circumvent the main limitation of this project, which is the assumption of a 2C model. In the second part of this chapter, the major factors that influence the assumption of a 2C model are discussed. The theoretical model has been extended to understand the impact of body composition assumptions in the 2C model. This model has also been extended to quantify the hydration effect in body composition analysis. The primary motivation is that hydration has a major impact on other body composition methods (BIA and DEXA).

9.2. Discussion on the ADP device

Various methods of body composition analysis have been described. ADP was chosen as the best available method. The theory of the ADP device was described in detail. A theoretical model based on all the parameters was used to calculate the optimal value for each parameter in the device. As one of the aims was for this device to be developed at low cost; great care was taken to optimize the performance within the budgeted constraints. Various method to compress the air in the chamber were attempted. These included using a standard ventilator, where the change in volume, and the frequency could be set on the front panel, as well as using the natural breathing rhythms of the subject to compress the gas in the chamber. Although these methods are attractive in term of ease of use and cost, none of them proved accurate enough for the purpose of body composition analysis. For the best accuracy, it is necessary to utilize a compression device with a constant stroke volume such as a piston. Even so, a single chamber device with the resultant change in pressure referenced to atmospheric pressure was not accurate enough. The final design was for a dual chamber system, each with its own air compression piston. The difference in pressure between the chambers is monitored; this set up optimized the change in pressure that occurs when an unknown volume is placed within the test chamber. A plethysmography device was carefully designed and constructed from the acquired materials.

This final design successfully achieves the aim in term of the cost. In terms of performance, the device was able to measure the volume of inanimate test objects to within ±0.3litre in 500 litres. Although this is remarkably high accuracy, it is not sufficient to produce a meaningful result in term of % BF fat.

The major sources of errors have been identified. In particular the consistency of the mechanism to change the chamber volume, the precision of the pressure sensor and the DAQ device are the key components which influence the precision of the ADP device. The solution to overcome these problems is included in further recommendations which include the plan as well as the budgeting for this.

9.3. Recommendations for the ADP Device

The main focus of this project was to measure the volume of air in the plethysmograph. The following two factors were identified In Chapter 5:

1. To generate a change of known volume at an absolute constant frequency in the chamber.
2. To pick up the resultant pressure signal that is generated accurately.

The following system (see figure 9.1) is suggested based on the shortcomings of the present device:

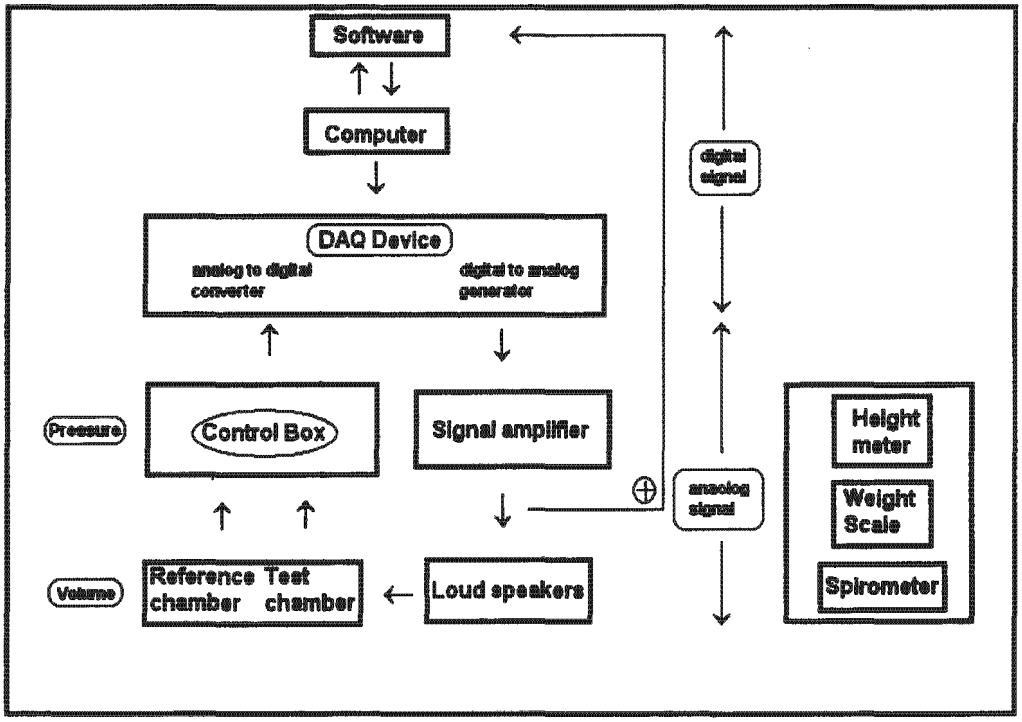

Figure 9.1 Suggested further development

The requirement for an improved pressure sensor and DAQ card can be developed where the device relies on two loud speakers that replace the pistons. The speakers will provide a clearer volume displacement - with lower noise.

9.3.1. Required elements and their cost

1. A dynamic signal acquisition and generation system (USD3,295)
2. A ultra low pressure sensor with 0-0.254 mBar full scale (USD520)
3. Two Speakers which are able to develop ~240ml and 76ml changing volume
4. A more precise atmospheric sensor should be obtained. See appendix G1 for the data sheet of the suggested device.

9.3.2. Basic description of the suggested device

The operator will use the software to set the amplitude at the desired frequency. This digital signal will be converted to an analogue signal by the digital to analog converter. This analogue signal then passes though a signal amplifier. This is an advantage as we will know the amplitude of the signal as well as its frequency. The signal will be used to drive the two loud speakers and at the same time this signal will be fed back to the Fourier transform analysis.

Instead of the present set up, the two loud speakers will create a volume change in the chambers. The output of the loud speaker must deliver the required change in volume regardless of the change in pressure in the chamber. The rest of the system will be the same.

9.3.3. Advantages of the suggested system

Advantages of the suggested system would be:

1. Higher accuracy of the overall system.
2. It is just one button control.
3. The frequency and the size of the signal is known and can be fed back to ensure consistency.
4. The motor does not need to be reset before the start of each trial.
5. An ideal filter can be applied. This is because the signal is generated at an absolutely constant frequency.

9.3.4. Additional concerns

A lot of noise is coming from the environment. In order to minimize this effect, a level of sound proofing should be constructed, as this provides an alternative way of blocking out all the other signals that interfere with the change in pressure signal and the absolute pressure readings.

9.3.5. Alternative suggested design

With the present design, an alternative approach would be to replace the DC motor by a precision stepper motor. This will ensure a precise constant volume output. The motor, its gear box, and controller cost roughly about ZAR15,000. See appendix G2 for the specs of the alternative suggested system.

Even if the volume of the test subject can be determined as precisely as necessary, this only solves part of the problem. The density of the FM and FFM mass is the other major issue that needs to be addressed. The following section discusses the inconsistency of the density of FFM.

9.4. Discussion on the 2C model

The biggest assumption for the two compartment model is that the density of the lean mass remains constant among individuals. This assumption relies mainly on two components in the body: The level of the bone marrow density and the muscle fibre density.

Due to the variability of these two components; many studies (Scholler1989, Burke *et al* 1986, Wang *et al* 1996, Lim 1963 ,Borkan *et al* 1983, Wedgwood 1963, Schutte *et al* 1984) show that the density of an individual changes with growth, sexual maturation, ageing, physical activity and a number of diseases. Hence there are fundamental errors in the assumptions of the 2C model. It is essential to understand how each of these factors could affect the 2C model assumptions.

9.4.1. Differences amongst racial groups

In general, African origin groups have a denser and heavier skeletal mass, (Merz *et al*1956, Seale 1959, Trotter and Hixon 1974, Schutte *et al* 1984, Ortiz *et al* 1992), hence the assumption that the density of lean tissue is equal to 1.1g/cc amongst all races is not correct. Bone mineral has three times the density of other lean body tissues. Hence there is fundamental error in the assumptions of the 2C model.

Schutte, 1984 proposed that lean body density for African origin groups be adjusted to 1.13g/cc. If this value is used instead of the value suggested by Brozek; percentage of body fat for the reference man (in table 6.1) would be 18.09 % instead of 15%.

9.4.2. Difference in age

Ageing people lose their bone mineral content as well as muscle. (Bunt *et al* 1990, Pollitzer *et al* 1989, Forbe *et al* 1987)

9.4.3. Gender difference

With people of the same age, the bone marrow content is dependent on the gender type. This phenomenon is especially true after menopause. Also the types of the muscle fibres are fundamentally different between the sexes (Withers *et al* 1998, Baumgartner *et al* 1991).

9.4.4. Overall evaluation

There are many sources of error in measuring body fat percentage. Many are avoidable; however these are certain fundamental limitations using ADP analysis. Even if the measurement is perfect, it does not solve the problem of the 2C model. Different 2C model prediction equations (Schoeller *et al* 1989, Ortiz *et al* 1992) have been suggested to accommodate different group of subjects but there is no agreed standard among all researchers. It is important to understand and quantify the influences of these factors as they directly impact the principle assumption of using ADP analysis to determine %body fat.

9.5. Final generation of the theoretical model

9.5.1. Two component (2C) model

The theoretical model has been expanded to illustrate the impact of incorrect density assumptions based on the available three assumptions of the 2C model. The effect of this error can be determined in the final generation of the theoretical model. See next section for the recommendation on the research direction.

9.5.2. Hydration effect

The hydration effect has been included in the theoretical model. If a known amount of water is added and the impact on our % BF measured, (based on the 2C model), the following were observed:

1. If a 50 litre subject is over-hydrated by 2 litres, body fat will be over estimated by ~1%.
2. The same effect will happen to the 100 litre person when the person is over hydrated by ~4 litres.

(See appendix B8 on how to obtain these results)

Based on the above discussion, the hydration effect is concluded to be negligible when the subject is within 2 litres of its hydration level.

9.5.3 Further recommendation on the research direction

Once we can measure the body volume to acceptable accuracy (at least to 100ml accuracy), then Random trial studies should be done on a large scale, among the samples, bone mineral content should be included in this analysis (from DEXA) and the differences between races and sex can also be recorded.

Once these results are obtained, statistical analysis can be applied to reveal any correlations among the factors. If factors are statistically significant, a more precise 2C model equation can be created. This model could contain factors such as age, gender type as well as the race type. This formula can be developed in the future and evaluated by other groups in ongoing research.

10. Conclusions

Determining the fat mass is an important tool for doctors in health assessment. The aim of this project is to design a low cost field method that can be used in the gym or shopping mall. Most of the common methods of body composition analysis are reviewed. Based on this review, ADP has the potential to achieve this aim. DEXA is used as a reference method for this project.

The theory of ADP was successfully implemented to determine the volume of air remaining in the plethysmograph to within 300 ml. Although this is not accurate enough to produce a meaningful result in term of % BF, the major sources of error were identified. The solution to overcome the problem is included in further recommendations.

Anticipating future development, the design has been chosen so that each component of the device can be independently replaced by a better component. A change to the hardware or software can be made in a short time period.

To conclude this project, I state that in all of the approaches to determine percentage body fat, limiting assumptions are present. The best solution of determining body fat mass should be a low cost approach, with reasonable assumptions, and which is easy and convenient to use.

References

1. Aristimuno GG, Foster TA, Voors AW, Srinivasan SR, Berenson GS (1984). Influence of persistent obesity in children on cardiovascular risk factors. *The Bogalusa Heart Study,* 69:895-904.
2. Baumgartner RN, Chumlea WC, Roche AF (1988). Bioelectric impedance phase angle and body composition. *Am J Clin Nutr,* 48:16-23
3. Baumgartner RN, Heymsfield SB, Lichtman S, Wang J, Pierson RN Jr (1991). Body composition in elderly people: Effect of criterion estimates on predictive equations. *Am J Clin Nutr,* 53:1345-1353.
4. Bedell GN, Marshall R, Dubois AB, Harris JH (1955). Measurement of the volume of gas in the gastro-intestinal tract. Volume in normal subjects and ambulatory. *Patients Am J Physiol*, 336-345.
5. Behnke AR, Feen BG, Welham WC (1942). The Specific gravity of healthy man. *J Am Med Assoc,* 118:495-498.
6. Berenson GS, McMahon CA, Voors AW (1980). Cardiovascular risk factor in children. *The early natural history of atherosclerosis and essential hypertension.* New York Oxford University.
7. Biaggi RR, Vollman MW, Nies MA, et al (1999). Comparison of air displacement plethysmography to bioelectric impedance and hydrostatic weighing for the assessment of body composition in healthy adults. *Am J Clin Nutr*, 69(5):898-903.

8. Bohnenkamp H, Schmah J (1931). The pure volume as well as specific ditch humans and the determination of this large. *Pflugers Arch Ges Physiol*, 228:100-124.
9. Borkan GA, Hults DE, Gerzof SG et al (1983). Age change in body composition by Computed Tomography (CT). *J Gerontology*, 38 (6):637-677.
10. Brozek JF, Anderson T, Keys A (1963). Densitometric analysis of body composition: revisions of some quantitative assumptions. *Ann NY Acad Sci*, 110: 113-140.
11. Brunton JA, Bayley HS, Atkinson SA (1993). Validation and application of dual energy X- ray absorptiometry to measure bone mass and body composition in small infants. *Am J Clin Nutr,* 58:839-845.
12. Burke LM, Gollan RA, Read RSD (1986). Seasonal changes in body composition in Australian rules footballers. *Brit J sport Med*, 20 (2):69-71.
13. Chumlea WC, Guo SS (1997). Bioelectrical impedance: A history, research issues, and recent consensus. In: *Emerging Technologies for nutrition Research*. Carlson-Newberry, RB Costello. Washington, DC: Nation Academic Press P.169-192.
14. Clark RP, Edholm OG (1985) *Man and his thermal Environment,* P57-58 Edward Arnold.
15. Collins MA, Millard-Stafford ML, Sparling PB, et al (1999). Evaluation of the BOD POD for assessing body fat in collegiate football players. *Med Sci Sports Exerc*, 31:1350 -1356.

16. Coulam CM, Erickson JJ (1981). Interactions of radiation with matter in the physical basics of medical imaging. FD Rollo and AE James. New York: Appleton- Century-Crofts P213-229.
17. Crapo RO, Morris AH, Clayton PD, Nixon CR (1982). Lung volumes in healthy nonsmoking adults. *Bull Europ Physiopathol Respir*, 18:419-425.
18. Cronje TF (1992). A plethysmographic device for determining human body volume and body density. University of Cape Town Msc dissertation.
19. Daniels F, Alberty RA (1967). *Physical chemistry*, New York: John Wiley and Son, Inc.
20. Dempster P, Aitkens SA (1995). A new air displacement method for the determination of human body composition. *Med Sci Sports Exerc*, 27:1692-1697.
21. Deurenberg P, Weststrate JA, Van der Kooy K (1989). Body composition changes assessed by bioelectrical impedance measurements. *Am J Clin Nutr*, 49:401-403.
22. Dewit O, Fuller NJ, Fewtrell MS, Ella M, Wells JCK (2000). Whole-body air displacement plethysmography compared to hydrodensitometry for body composition analysis. *Arch Dis Child*, 82:159-164.
23. Dubois AB, Botelho SY, Bedell GN, Marshall R, Comroe JH (1956). A rapid plethysmographic method for measuring thoracic gas volume: a comparison with nitrogen washout method for measuring functional residual capacity in normal subjects. *J Clin Invest*, 35:322-326.

24. Dubois D, Dubois EF (1916). A formula to estimate the approximate surface area if height and weight to be known. *Arch Intern Med*, 17:863-871.

25. Edelman IS, Olney JM, James AH Brooks L, Moore FD (1952). Body composition: studies in the human being by the dilution principle. *Science*, 115:447-454.

26. Ellis KJ (2000). Human body composition: In Vivo method. *Am Physiol Soc*, 80:649-679.

27. Ellis KJ, Shypailo RJ, Schanler RJ (1999). Measurement of body water by multi-frequency bioelectrical impedance spectroscopy in multiethnic pediatric population. *Am J Clin Nutr*, 70: 847-853.

28. Enderle J, Blanchard S, Bronzino J (2000). *Introduction to biomedical engineering*. P. 722-723 San Diego, California: Academic Press.

29. Evans WJ, Campbell WW (1993). Sarcopenia and age related changes in body composition and function capacity. *J Nutr*, 23:465-468.

30. Fairburn CG, Hay PJ, Welch SL (1993). Binge eating: and bulimia nervosa: distribution and determinants. In C.G. Fairburn & G.T. Wilson, *Binge eating*. P. 123-140. NY: Guilford.

31. Fields DA, Hunter GR, Goran M (2000). Validation of BOD POD with hydrostatic weighting: influence of body clothing. *Int J Obes*, 24:200-205

32. Fields DA, Goran MI, McCrory MA (2002). Body composition assessment via air displacement plethysmography in adults and children: a review. *Am J Clin Nutr*, 75(3):453-467.

33. Folch J, Lee M, Stanley GHS (1957). A simple method for the isolation and purification of total lipids for animal tissues. *J bio Chem*, 226:497-509.

34. Forsyth R, Plyley MJ, Shepard RJ (1988). Residual volume as a tool in body fat prediction. *Ann Nutr Metab,* 32:62-67.

35. Friis-Hansen B (1963). The body density of newborn infants. *Acta Paediatr*, 52:513-521.

36. Gotfredsen A, Jensen J, Borg J, Christiansen C. (1986). Measurement of lean body mass and total body fat using dual photon asorptiometry. *Metab Clin Exp*, 35: 88-93.

37. Garrow JS, Webster J (1985). Quetelet's index (W/H2) as a measure of fatness. *Int J Obes Relat Metab Disord*, 9:147-153.

38. Gnaedinger RH, Reineke EP, Pearson AM, et al (1963). Determination of body density by air displacement, helium dilution and underwater weighing. *Ann N Y Acad Sci*, 110:96-108.

39. Gundlach BL, Visscher GJ (1986). The plethysmometric measurement of total body volume. *Hum Bio,* 58:783-799.

40. Gurr, MI, Harwood JL (1991). *Lipid biochemistry: An Introduction* (4th Ed.) London: Chapman and Hall.

41. Hackney AC, Deutsch DT (1985). Accuracy of residual volume prediction – effects on body composition estimation in pulmonary dysfunction. *Can J Appl Sport Sci,* 10:88-93.

42. Haecker TL (1920). Minn. Univ. Agr Exptl Station Research Bull P193.

43. Heymsfield SB, Wang J, Kehayias J et al (1989). Chemical determination of human body density in vivo: relevance to hydrodensitometry. *Am J Clin Nutr*, 50: 1282-1289.

44. Higgins PB, Field DA, Hunter GR, Gower BA (2001). The effect of the scalp and facial hair on air displacement plethysmography estimates of percentage of body fat by the BODPOD. *J Obes Res*, 9:326-330.

45. Hubbell JH (1969). *Photon Cross sections, attenuation coefficients and energy absorption coefficients from 10keV to 100 GeV*. Washington, DC: US national Bureau of Standards P1-85.

46. Iwaoka H, Yokoyama T, Nakayama T, et al. (1998) Determination of percent body fat by newly developed sulfur hexafluoride dilution method and air displacement plethysmography. *J Nutr Sci Vitaminol* (Tokyo), 44: 561-568.

47. Jongbloed J, Noyons AKM (1938). The determination of the true volume and the specific weight of humans by means of Luftdruckveranderung. *Pflugers Arch Ges Physiol*, 240:197-201.

48. Kelly TL, Berger N, Richardson TL et al. (1998) DXA body composition: theory and practice. *Appl Radiation Isotopes*, 49:511-513.

49. Kohlrausch W (1930). Methodik zur quantitativen Bestimmung der korperstoffe in vivo. *Arbeits Physiol*, 2:23-45.

50. Kohrt WM (1998) Preliminary evidences that DEXA provide an accurate assessment of body composition. *J Appl Physiol*, 84(1):372-377.

51. Latin RW, Ruhling RO (1986). Total lung capacity, residual volume and predicted residual volume in a densitometric study of older man. *Brit J Sports Med*, 20(2):66-68.

52. Levenhagen DK, Borel MJ, Welch DC et al (1999). A comparison of air displacement plethysmography with three other techniques to determine body fat in healthy adults. *J Parenter Enteral Nutr*, 23: 293-299.

53. Life measurement INC. Concord, CA. http://www.bodpod.com (last accessed on 2004/7/26).

54. Lim TPK (1963) Critical evaluation of the pneumatic method for determining body volume: it history and technique Ann. *NY Acad Sci*, 110:72-79.

55. Lukaski HC (1987). Methods for the assessment of human body composition: Traditional and new. *Am J Clin Nutr*, 46:537-556.

56. Ma CHP (2001) A model investigation for air displacement plethysmography. University of Cape Town. BSc Dissertation P49.

57. Mazes RB, Cameron JR, Sorenson JA (1970). Determining body composition by radiation absorption spectrometry. *Nature*, 228:771-772.

58. McCrory MA, Gomez TD, Bernauer EM, Mole PA (1995). Evaluation of a new air displacement plethysmography for measuring human body composition. *Med Sci sports Exerc*, 27:1686-1691.

59. McCrory MA, Mole PA, Gomez TD, Deway KG, Bernauer EM (1998). Body composition by air displacement plethysmography by using predicted and measured thoracic gas volumes. *J Appl Physiol*, 84(4):1475-1479.

60. Merz AL, Trotter M, Peterson RR (1956). Estimation of skeleton weight in the living. *Am J Phys Anthropol,* 14:589-609.

61. Michael GJ, Henderson CJ (1998). Monte Carlo modeling of an extended DXA technique. *Physics Med Boil,* 43:2583-2596.

62. Michael GJ, Sim LH, Van Doorn T et al (1997). A Monte Carlo model for bone mineral measurement using dual energy x-ray absorptiometry. *Austr Physics Eng Sci Med,* 20(2):84-91.

63. Microchip Technology Inc. http://www.microchip.com (last accessed on 2004/7/27).

64. Microdyne Pty Ltd. http://www.microdyne.co.za (last accessed on 2004/7/27).

65. Millard-Stafford ML, Collins MA, Evans EM, Snow TK, Cureton KJ, Rosskopf LB (2001). Use of air displacement plethysmography for estimating body fat in a four component model. *Med Sci Sports Exerc,* 33(8):1311-1317.

66. Morrow JR, Jackson AS Jr, Bradley PW, Hartung GH (1986). Accuracy of measured and predicted residual lung volume on body density measurement. *Med Sci Sports Exerc,* 18: 647-652.

67. Motorola MPX100AP Pressure sensor and its circuit design. http://www.ece.osu.edu/~bibyk/ee720/AirPressure.pdf (last accessed on 2004/7/27).

68. Moulton CR, Trowbridge PF, Haigh LD, (1922). Studies in animal nutrition II. Changes in proportions of carcass and offal on different planes of nutrition. *Agr Exp Stn Res Bull,* P.54 University of Missouri.

69. Murlin JR, Hoobler BR. (1913). The energy metabolism of normal with special reference to the specific gravity of the child's body. *Proc Soc Exp Biol Med,* 11: 115-116.

70. National Institutes of Health (1996). Bioelectrical impedance analysis on body composition measurement: National Institutes of Health Technology Assessment Conference Statement. *Am J Clin Nutr,* 64 (Suppl): 524S- 532S.

71. National Instruments. http://www.ni.com/ (last accessed on 2004/7/27).

72. Noyons AK, Jongbloed (1935). More the determination of the true volume and the specific weight of humans and animal by Luftdruckveranderung. *Pflugers Arch Ges Physiol,* 235:588-596.

73. Noakes T (2001). *Lore of Running* 4th Ed. P. 125, 1191, 1156 Oxford University press.

74. Peppler W, Mazess RB (1981). Total body bone mineral and lean body mass by dual photon absorptiometry. Theory and measurement procedure. *Int J Calc Tiss,* 33:353-359.

75. Peslin R, Fredberg JJ (1986). Oscillation mechanics of the respiratory system. *Handbook of physiology,* Macklem PT, Mead J Ed. P.164 The Baltimore: William and Wilkins.

76. Petty DH, Iwanski R, Gao CX, et al (1984). The total body plethysmography for body volume determination. *IEEE Frontiers Eng Computing Health Care,* 6:316-319.

77. Pfaundler M (1916). Body mass studies in children. IV. Concerning body volume and body density. *Ztschr f Kinderheilk,* 14:123-37.

78. Pietrobelli A, Formica C, Wang Z, Heymsfield S (1996) Dual energy X-ray Absorptiometry body composition model: review of physical concepts. *Am J Physiol,* 271 E941-E951.

79. Pietrobelli A, Formica C, Wang Z, Heymsfield SB (1998). Dual energy X-ray Absorptiometry body composition: fat estimation errors due to variation in soft tissue hydration. *Am J Physiol,* 274: E808-E816.

80. Pitts GC (1963). Studies of gross body composition by direct dissection. *Ann NY Acad Sci*, 110: 11-19.

81. Popovic-Grle S, Pavicic F, Bicanic V, et al (1989). Correlation of the size of the residual volume measured by whole body plethysmography and the single breath helium dilution method. *Plucne Bolesti,* 41(1-2):78-82.

82. Preuss LE, Bolin FP (1972). The analysis of mammalian tissue into lipid and lipid free fractions using X and gamma radiation. *Int J Appl Rad*, 23: 9-12.

83. Prior BM, Cureton K, Modlesky C, Evans EM, Sloniger M, Saunders MA, Lewis R (1997). In vivo validation of whole body composition estimates form the dual energy X-ray absorptiometry. *Am J Physiol*, 83(2):623-30.

84. R.S. Components INC. online catalogue http://rswww.com (last accessed on 2004/7/27).

85. Rao PS, Gregg EC (1975). Attenuation of Monoenergetic gamma rays in tissues. *Am J Roentg*, 123:631-637.

86. Roubenoff R, Kehayias JJ, Dawson-Hughes Heymsfield SB (1993). Use of dual energy X-ray absorptiometry in body composition studies: not yet a goal standard. *Am J Clin Nutr*, 58: 589-591.

87. Schoeller DA (1989). Changes in total body water with age. *Am J Clin Nutr*, 50:1176-1181.

88. Schreiner PJ, Pitkaniemi J, Pekkanen J, Salomaa V (1995). Reliability of near-infrared Interactance body fat assessment relative to standard anthropometric techniques. *J Clin Epidemiology*, 48(11) 1361-1367.

89. Schutte JE, Townsend EJ, Hugg JH et al (1984). Density of lean body mass is greater in blacks than in whites. *J Appl Physiol*, 56:1647-1649.

90. Seale RU (1959). The weight of the dry fat- free skeleton lander. PA Huijing, G Degroot Ed. American white and Negroes. An- and Medicine in Swimming. Champaign, IL: Human Thropol. *Am J Phys*, 17:37–48.

91. Siri WE (1961). Body composition from fluid space and density: analysis of method. *Techniques for measuring body composition*. Brozek Henschel eds. P223-224 Washington DC: National Academy of Sciences, National Research Council.

92. Snyder WS, Cook MJ, Nasset ES et al (1975). Report of the task group on Reference man. *International Commission on Radiological Protection*, no. 23. Oxford, UK: Pergamon Press.

93. Svendsen OL, Haarbo J Hassager C, Christiansen C (1993). Accuracy of measurement of body composition by dual energy X-ray absorptiometry in vivo. *Am J Clin Nutr,* 57:605-608.

94. Taylor A, Scopes JW, Du Mont G, Taylor BA (1985). Development of an air displacement method for whole body volume measurement of infants. *J Biomed Eng*, 7:9-17.

95. Tothall P, Avenell A, Love J, Reid DM (1994). Comparisons between Hologic, lunar and Norland dual energy X-ray absorptiometers and other techniques for whole body soft tissues. *Eur J Clin Nutr*, 48 781- 794.

96. Trotter M, Hixon BB (1974). Sequential changes in weight, density, and percentage ash weight of human skeletons from an early fetal period through old age. *Anat Rec*, 179: 1-18.

97. Vozarova B, Wang, J, Weyer C, Tataranni PA (2000). Comparison of two software versions for assessment of body composition analysis by DXA. *Obesity research*, 9(3): 229-232.

98. Wagner DR, Heyward VH, Gibson AL (2000). Validation of air displacement plethysmography for assessing body composition. *Med Sci Sports Exerc*, 32:1339-1944.

99. Wang ZM, Gallagher D, Nelson ME, et al (1996). Total body Skeletal muscle mass: Evaluation of 24 –H urinary creatinine excretion by computerized axial tomography *Am J Clin Nut,* 63:863-869.

100. Wedgwood RJ (1963). Inconsistency of the lean body mass Ann. *NY Acad. Sci,* 110: 141-151.

101. Wells JCK, Douros I, Fuller NJ, Elia M, Dekker L (2000). Assessment of body volume using three-dimensional photonic scanning. *Ann N Y Acad Sci*, 904:247-254.

102. Weltman A, Katch V (1981). Comparison of hydrostatic weighing at residual volume and total lung capacity. *Med Sci Sports Exerc*, 13(3):210-213.

103. White, DR, Peaple LHJ, Crosby TJ (1980). Measured attenuation coefficients at low photon energies (9.88-59.32 KeV) for 44 material and tissues. *Radiat Res*, 84: 239-252.

104. Williams DP Going SB Lohman TG et al (1992). Body fatness and risk for elevated blood pressure, total cholesterol and serum lipoprotein ratios in children and adolescents. *Am J public health*, 82:358-263.

105. Wilmore JH (1969). The use of actual predicted and constant residual volumes in the assessment of body composition by underwater weighting. *Med Sci Sport,* 1:87-90.

106. Withers RT, Ball CT (1988). A comparison of effects of measured, predicted, estimated and constant residual volumes on the body density of female athletes. *Int J Sports Med*, 9(1):24-28.

107. Withers RT, LaForgia J, Pillans, Shipp NJ et al (1998). Comparisons of two-, three-, and four-compartment models of body composition analysis in men and women. *Am J Physiol Soc,* 85(1):238-245.

108. University of Vermont Department of Nutrition & food science http://nutrition.uvm.edu/bodycomp/ (last accessed on 2004/7/16.

Appendices

Appendix A Formula related

Appendix A1 Derivation of the two-component (2C) model:

The body is assumed to be composed of two compartments, fat and fat free. The total mass of the body is equal to the sum of the fat mass and the fat free mass.

$$\text{Density (D)} = \frac{\text{mass}}{\text{volume}}.$$

Densities of the "2 components":

$$\text{Density} = \frac{\text{fat mass + fat-free Mass}}{\text{volume}}$$

$$\text{Density} = \frac{\text{fat mass + fat-free Mass}}{\text{f volume + ffm volume}}$$

$$D = \frac{FM + FFM}{(FM/fd)+(FFM/ffd)}$$

Where:

FM = mass of the fat compartment

FFM = mass of the fat free compartment

fd = fat density (grams per cc)

ffd = density of fat-free mass (grams per cc)

body mass (BM) = fat mass + fat-free mass

$$\therefore D = \frac{FM + FFM}{(FM/fd) + (FFM/ffd)}$$

$$D = \frac{FM + (BM - FM)}{(FM/fd) + (FFM/ffd)}$$

$$D = \frac{FM + (BM - FM)}{(FM/fd)+((BM - FM)/ffd)}$$

$$D = \frac{BM}{(FM/fd)+((BM - FM)/ffd)}$$

$$\frac{BM}{D} = (FM/fd) + ((BM - FM)/ffd)$$

$$BM \times \frac{fd}{D} = \{(FM/fd) + [(BM-FM)/ffd] \times fd$$

$$BM \times \frac{fd}{D} = FM + BM \times \frac{fd}{ffd} - \frac{fd}{ffd} \times FM$$

Rearranging

$$BM \times (\frac{fd}{D} - \frac{fd}{ffd}) = FM - \frac{fd}{ffd} \times FM$$

$$BM \times (\frac{fd}{D} - \frac{fd}{ffd}) = FM \times (1 - \frac{fd}{ffd})$$

$$\frac{FM}{BM} = \frac{fd}{(1-(fd/ffd)) \times D} - \frac{fd/ffd}{1-(fd/ffd)}$$

$$\%BF = 100 \times \left(\frac{fd}{(1-(fd/ffd)) \times D} - \frac{fd/ffd}{1-(fd/ffd)} \right)$$

Siri assumed that fd= 0.9 and ffd =1.1 (gram/cc)

$$\therefore \%\ \text{Body fat} = \frac{495}{\text{Body density}} - 450$$

Brozek assumed that fd=0.9007 and ffd=1.1(gram/cc)

$$\therefore \%\ \text{Body fat} = \frac{497.1}{\text{Body density}} - 451.9$$

For African origin groups, Schutte assumed that fd=0.9007 and ffd=1.113 (gram/cc)

$$\therefore \%\ \text{Body fat} = \frac{437.4}{\text{Body density}} - 392.8$$

Appendix A2 - World health Organization's (WHO) interpretation for Body mass index (BMI)

Body Mass Index (BMI) = Weight (kg) / Height ^{2} (m)

For Males

	Classification
0≤BMI<17.5	Anorexic
7.5≤BMI< 19.1	Underweight
19.1≤BMI < 25.8	Normal range
25.8≤BMI< 27.3	Marginally overweight
27.3≤BMI< 32.3	Overweight
BMI≥32.3	Very overweight or obese

For Female

	Classification
0≤BMI<17.5	Anorexic
7.5≤BMI< 20.7	Underweight
20.7≤BMI < 26.4	Normal range
26.4≤BMI< 27.8	Marginally overweight
27.8≤BMI< 31.1	Overweight
BMI≥31.1	Very overweight or obese

Appendix A3 - Archimedes' Principle

The object's loss of weight in water is equal to the weight of the displaced volume of water.

Since density = mass/volume, knowing the density of water, the volume of water displaced can be calculated. The crown* could then be weighed underwater to find the difference between its weight in the air and in the water. This is equal to the volume of water displaced by the crown (dm^3), since density of water is $1kg/dm^3$.

*In the first century BC the Roman architect Vitruvius related a story of how Archimedes uncovered a fraud in the manufacture of a golden crown commissioned by Hiero II, the king of Syracuse. The crown (*corona* in Latin) was suspected to have some of the gold replaced by an equal weight of silver, Hiero asked Archimedes to determine whether the wreath was pure gold. Archimedes' solution to the problem was to see the displacement of water by placing the crown into a bath filled with water.

Appendix A4 - Full derivation of the ADP theory

In a closed system such as the plethysmograph

$$P \times V^{\gamma} = \text{constant} \quad (1)$$

When the volume of a closed system is decreased by a volume ΔV, the pressure goes up by ΔP:

$$(P+\Delta P) \times (V - \Delta V)^{\gamma} = \text{constant} \quad (2)$$

Due to the energy conservation law, the constant should remain the same though out the trial period.

By equating (1) and (2)

$$(P+\Delta P) \times (V - \Delta V)^{\gamma} = P \times V^{\gamma} \quad (3)$$

Rearranging we get the following equation:

$$\frac{P+\Delta P}{P} = \left[\frac{V}{(V - \Delta V_B)}\right]^{\gamma} \quad (4)$$

Giving

$$\left(\frac{P+\Delta P}{P}\right)^{\frac{1}{\gamma}} = \frac{V}{(V_c - \Delta V_B)} \quad (5)$$

$$V = (V - \Delta V) \times \left(\frac{P+\Delta P}{P}\right)^{\frac{1}{\gamma}} \quad (6)$$

$$V \times \left(1 - \left(\frac{P+\Delta P}{P}\right)^{\frac{1}{\gamma}}\right) = -\Delta V \left(\frac{P+\Delta P}{P}\right)^{\frac{1}{\gamma}} \quad (7)$$

Since $V_c = V + V_B$ the equation can be express in term of V_B

$$V_B = V_c + \frac{\Delta V \times \left(\frac{P+\Delta P}{P}\right)^{\frac{1}{\gamma}}}{1 - \left(\frac{P+\Delta P}{P}\right)^{\frac{1}{\gamma}}} \quad (8)$$

Hence

$$V_B = V_c + \Delta V \times \frac{(P+\Delta P)^{\frac{1}{\gamma}}}{P^{\frac{1}{\gamma}} - (P+\Delta P)^{\frac{1}{\gamma}}} \quad (9)$$

Where

V_B = Volume of the air displaced by the test subject

V_c = Volume of the air in the empty system

V = Volume of the air left in the close system which equal to $V_c - V_B$

ΔV =the change volume of the chamber

= the corresponding changing pressure in the test chamber

= the atmospheric pressure of the present place

γ = ratio specific heat =1.4

Appendix B: Theoretical model

Appendix B1 Instructions for using the theoretical model

Introduction

This theoretic model is derived from figure 5.1 (Relationship between the parameters) as the assumptions and their interpretations are included into the model. The model is in an excel spreadsheet format and consists of the following 6 sheets:

1. Precision & analysis
2. Weight
3. Isothermal gas
4. Practical 1
5. Practical 2
6. Results

Each of the parameters that influence the result is modeled independently.

Instructions for using this model

All the variables are included in the results sheet. By changing any of the variables; the impact on the "regional" parameter as well as the "global" accuracy can be seen. Here "regional" parameter refers to the parameter itself, "global" accuracy refers to the result. (% Body fat)

For each parameter there is a corresponding error. In the sheet "Practical 1" the Data acquisition card (DAQ), atmospheric pressure and pressure sensor errors can be manipulated in order to determine how accurately they need to be known in order to achieve a given degree of accuracy for the estimation of the body fat. See table B1 for list of errors and its corresponding sheet and errors.

Table B1
Information of the errors

Sheet	Errors	Corresponding cell
Precision & analysis	fat free mass error	J3
Weight	typical scale error	B11
Isothermal air	isothermal air error	B10
Practical 1	atmospheric pressure, sensor, DAQ device error	D6,B10,B11

The model mentioned in chapter 5 targets subjects between 50 and 100 litres. Analysis is done for the target subjects. Since extreme case errors occur at 50 litres and 100 litres, the total accuracy and the minimum and maximum reading for the %BF for these two cases are provided in the result sheet.

Total accuracy is shown in terms of percentage, where 100% would be an accurate measurement. (Refer to result sheet from cell F13 to F18)

The readings are shown in terms of body fat; where minimum reading is the lowest possible reading in body fat and vice versa. (Refer to results sheet from cell F20 to F22)

See the corresponding page for the effect of the error on regional parameters, as well as how the errors are derived. On the right end of the sheet, a color code and unit key is included for the parameters.

Information relates to appendix B3, B4, B6 and B8

Table format is used in these listed appendices, Follow the instructions indicated below to obtain the result for these appendices.

1. Open the indicated sheet
2. Follow numeric order of the operations by changing the corresponding cell
3. See the reason of the operation for the explanation of the operation
4. Obtain the results in the relative table in the test

Close the program without saving

Appendix B2 Investigation using the theoretical model

The formulas in this model are based on the formulas covered in the relevant chapters in the text.

Precision & 2C analysis

This is the first developed section in the whole model; it contains the Precision analysis and the 2C model analysis. These analyses are allocated to the same page because they share the same variables.

2C model analysis

This section compares the differences between Siri, Brozek and Schutte' equations as the different assumptions used by these investigators result in different values for the calculated %BF. This is because of the different assumptions in terms of FD and FFD. Fat free mass error can be added into the model (from Result page cell B11). It enables the user to see how the 2C model assumption effects the interpretation of the %BF.

Precision analysis

The mode of body fat for healthy males is 15% (Noakes T 2001). The model defaults to this value. In order to reach the initial goal (±2% accuracy); the system should be able to obtain values of between 13% (cell C5) to 17% (cell c4) body fat percentage for the average healthy male.

The next step is to understand how 2% BF can be interpreted in terms of body volume. This is done for all the three formulas (Siri, Brozek, and Schutte). See the derivation of the 2C model formula in appendix A1. As this is an independent study, the mass scale error is ignored for this moment.

In order to estimate body fat percentage to within 2% accuracy, we need to obtain an accuracy of 0.2 liters for body volume (see Cell C9, Cell C14 Cell C19). This result (which appears in cell C14) is done by assuming the subject is 50litre while using Siri equation.

The required volume precision is determined to be 0.2 liters as the increment in volume prediction is incremented. This concept is applied through the whole model as this is highest precision required in volume measurement.

Weight

This sheet is colored in purple; as are the other weight related figures. This page allows the user to calculate the precision needed in terms of weight measurement. In the other words, it allows the user to show the relationship between an error in the measured weight and its impact on body composition analysis. A scale error can be added in this page (cell B11) as well as the result page (cell C11).

Isothermal air

This sheet is colored in orange; as are the other isothermal air related issues. Isothermal air includes V_{TG} , V_{GIT} and the air around the skin surface V_{Skin}. A total isothermal air error can be created in this page (cell B10) as well as in the results page (cell D11).A total error is calculated due to the following reasons:

- If V_{TG} and V_{GIT} combined in less that 1 litre, the corresponding errors can be neglected.
- The volume of the isothermal air on the skin V_{Skin} error is not reported in the literature, and so is determined empirically.

Practical parameters

Stroke volume, chamber volume, sensor accuracy, DAQ card accuracy, and atmospheric pressure are the five parameters covered in this sheet. Errors can be included in each of the parameters to be investigated during the calculation of body fat percentage. In which Cell E3 allows the user to generate errors in measuring the atmospheric pressure. Cell E7 and E11 are figures that were directly obtained from the datasheets in appendix C1 and C2.

Practical one

The user is able to change the stroke length (cell F2, F3 and F4) or the radius of the plungers (cell F5 and F6). This enables the user to determine the stroke volume of the two chambers separately.

Practical two

This sheet shows the predicted error in volume (column D and E) and in %BF (column G and H).

Hydration effects

Hydration effects are covered in the results sheet. The assumption of this section is that the density of the water is equal to $1\,g/cm^3$. When the subject drinks 1 litre of water, the sheet is programmed to add one litre to the subject's volume as well as one kg to the subject's weight. The new density is then calculated and this new density is used to determine the new % BF (see 28^{th} to 35^{th} row from column A to E)

Results

This page contains all the parameters (from cell I3 to I17) in the design. On this page the user is able to investigate the impact of any of the parameters on the calculated percentage body fat (see cell J3 to J17)

Appendix B3 Single chamber system Model

Open the "practical 1" sheet

Table B2

Instructions to determine the accuracy of the single chamber system

Experiment	Operation	Corresponding cell	Reason of the operation
Determine the behavior of single chamber	1. Change the test chamber size to 400L	Cell B2	The optimized chamber size
	2. Change to stroke volume1 to 0.5L	Cell B4	Since we are evaluating the effect of the single chamber system so no volume is displaced in the reference chamber.
	3. Change the stroke volume 2 to 0 L	Cell B5	
4. See expected pressure on 50 litre subject		Cell E15	Results in table5.3
5. See expected pressure on 100 litre subject		Cell E265	Results in table5.3
Open sheet "results"			
Determine the behavior of single chamber	6. Change Fat free error to zero	CellB11	This is done because we are considering the effect on the practical interpretation independently
	7. Change the scale error to zero	CellC11	
	8. Change the isothermal air errors zero	CellD11	
9. Error in % body fat on 50litre subjects		(cellF22-cellF21)/2	Results in table5.3
10. Error in % body fat on 100litre subjects		(cellF25-cellF24)/2	Results in table5.3

Appendix B4 Dual chamber dynamic system model

Open the "practical 1" sheet

Table B3

Instructions to determine the accuracy of the dual dynamic system

Experiment	Operation	Corresponding cell	Reason of the operation
Determine the behavior of dual chamber	1. Change the test chamber size to 400L	Cell B2	The optimized chamber size
	2. Change the reference chamber size to 400L	cell B3	
	3. Change the stroke volume1 to 1L	Cell B4	Ideally the condition of the two chamber should be the same at starting point
	4. Change the stroke volume 2 to 1L	Cell B5	
5. See the expected pressure on 50 litre subject		Cell E15	Results in table5.4
6. See the expected pressure on 100 litre subject		Cell E265	Results in table5.4
Open "results" sheet			
Determine the behavior of single chamber	7. Change the fat free error to zero	CellB11	Since we consider the practical interpretations independently
	8. Change the scale error to zero	CellC11	
	9. Change the isothermal air errors zero	CellD11	
10. See error in % body fat on 50litre subjects		(cellF22-cellF21)/2	Results in table5.4
11. See error in % body fat on 100litre subjects		(cellF25-cellF24)/2	Results in table5.4

Appendix B5 Determining the minimum size of the test chamber

Volume occupied by the subject

The initial goal for this project was to measure subjects of not more than 100 litres. For further development as well as from the design point of view; subjects of 150 litres should also be accommodated.

Maximum volume of the isothermal air in the chamber

The isothermal air in the lung could be as large as 4 litres and the isothermal air around the body could be as much as 1.5 litres.

Gaseous exchange in the lung is happening all the time. Assuming that the tidal volume of the subject is not more than 600 ml. (average tidal volume is 500ml) and that the subject takes no more than 20 breaths during the course of the measurement. Ten litres of warmed humidified air is fed into the chamber. This has the effect of increasing the density of the air in the chamber as well as the temperature. In addition during respiration, about 5ml of O_2 are inhaled for each 4ml of CO_2 exhaled for each 100ml of blood, so the effect is that the volume of the chamber is decreased slightly.

Apart from the breathing effect, the body temperature effect and the respiration effect also causes the *PV* constant to vary. The rate at which it changes depends on metabolic rate, which varies from individual to individual.

Due to its small size, V_{GIT} is not taken into consideration. Hence the total isothermal air could be as much as 10litre in the test chamber.

Minimising the errors due to isothermal air in the chamber

The total isothermal air should not be more than 10% of the total chamber size at any time or the validity of the result can be compromised. This means that the minimum volume of air should be 150 litres at all times.

Given that 150 litres of space should be reserved for the subject, the minimum size of the chamber should be approximately 350 litres.

Appendix B6 Worst case scenario analysis results

Open the "result" sheet.

Table B4

Instruction to determine the effects of scale errors in measuring mass on %BF using the model

Experiment	Operation	Corresponding cell	Reason of the operation
Determine the effects of errors in measuring mass on %BF using the model	1. Set Atmospheric pressure error ,DAQ card error and the differential pressure sensor errors to zero	E3, E7 & E11	Since these are the practical constraints of the ADP analysis
	2. Set 2C model error and the isothermal air error to zero	B11 & D11	since this is an independent study for weight parameter
3. See error in term of %BF expected for weight parameter		J21	Results in table 6.2
4. See how the reference man looks		F21	Results in table 6.2

Open the "result" sheet.

Table B5

Determination the impact of errors in estimating the volume of isothermal air on %BF

Experiment	Operation	Corresponding cell	Reason of the operation
Determine the impact of errors in estimating the volume of isothermal air on %BF	1. Set Atmospheric pressure error ,DAQ card error and the differential pressure sensor errors to zero	E3, E7 & E11	Since these are the practical constraints on ADP analysis
	2. Set 2C model error and the weight scale error to zero	B11 & C11	since this is an independent study for isothermal air parameter
3. See error in term of %BF for isothermal air parameter		J21	Results in table 6.2
4. See how the reference man looks		F21	Results in table 6.2

Open the "result" sheet.

Table B6

Instruction to determine the effect of errors in measuring atmospheric pressure on %BF

Experiment	Operation	Corresponding cell	Reason of the operation
Determine the effect of errors in measuring atmospheric pressure on %BF	1. Set DAQ card error and the differential pressure sensor errors to zero	E7 & E11	Since these are the practical constraints on ADP analysis
	2. Set 2C model error, the weight scale error the isothermal air error to zero	B11,C11 & D11	since this is an independent study for atmospheric pressure parameter
3. See the result of error in %BF for atmospheric pressure error		J21	Results in table 6.2
4. See how the reference man looks		F21	Results in table 6.2

Open the "result" sheet.

Table B7

Instructions to determine the over all impact of these three errors to %BF

Experiment	Operation	Corresponding cell	Reason of the operation
Determine the impact of these three errors on %BF	1. Set weight scale error to 0.03kg, Atmospheric error to 0.05mBar Isothermal air error to 10%	C11,D11 & E3	Since these are the basic assumption of using ADP analysis to determine %BF
	2. Set 2C model error to zero	B11	
	3. Set 2C model error the weight scale error to the isothermal air error to zero DAQ card error and the differential pressure sensor errors to zero	B11,C11 & D11	since this is an independent study for atmospheric pressure parameter
4. See the result of error in %BF for atmospheric pressure error		J21	Results in table 6.2
5. See how the reference man looks		F21 &F22	Results in table 6.2

Appendix B7 Air leakage Analysis

The effect of a controlled air leakage from the chambers

The *PV* constant increases as described in chapter 5 due to the multi-cycle displacement of the air. Experiments show that the pressure reading builds up in a very rapid fashion, since the size of this effect is much larger than the experienced signal in the chamber (known from experience). This effect has to be extracted before converting to digital signal. The best way to eliminate this effect is to create an air leakage in the chamber.

Electrical model representation of the device

The device can be presented by an electrical model (see figure B1)

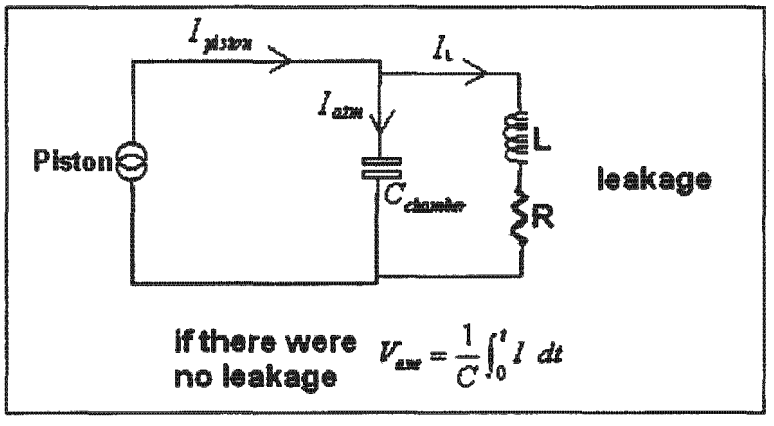

Figure B1. Electrical representation of the device

In this electrical model, if the resistor (*R*) is small, the DC current (I_{atm}) will flow through the resistor (*R*) causing a slight variance $\Delta I_{atm} \times R$. The AC current at the motor moving frequency (1.6HZ) will experience impedance (*Z*), where $Z = j\omega L + R$ which can be neglected if *L* is large or

compensated for. $C_{chamber}$ represents the volume of the chamber. These elements can be expressed by the following equations

$$Z_{total} = \frac{1}{j\omega C} // (j\omega L + R)$$

$$\Delta P = I_{piston} \times Z$$

$$C_{chamber} = \frac{V}{P_{atm} \times K}$$

$$AC_{leakage} = \frac{\Delta P}{R + j\omega l}$$

$$DC_{leakage} = \frac{\Delta P}{R}$$

Where

$$\omega = 2\pi f$$

$$R = \frac{8\mu l}{\pi \times r^4}$$

$$L = \frac{\rho \times l}{\pi \times r^2}$$

In the equation,

V is the volume of the chamber,

P_{atm} is the atmospheric pressure,

K is the absolute temperature,

μ is the viscosity of the air,

r is the radius of the pipe,

l is the length of the pipe,

ρ is the air density,

f is the speed of the motor.

A low value for R will reduce the pressure build up in the chamber to an acceptable level, a trade off being that a small but non-negligible AC flow from the chamber. This can be calculated and compensated.

Determining the leakage effects

In the last section the theoretical interpretation showed that the leakage can be treated as a constant variable subject to the motor moving at a constant frequency. After computing these equations into a program (see air leakage analysis.xls in the CD), leakage effect is determined and introduced to both of the chambers via plastic tubes. These plastic pipes are 1.5 meters in length and 0.6 mm in diameter.

Quantifying the leakage effect

The leakage effect can be quantified by the equations in the last section. The advantage of compensating for this AC flow (leakage) from the chamber is that the chamber size will be able to be determined more accurately. However the disadvantage of this is that the motor speed must be absolutely constant at all times. Otherwise frequency (f) can not be determined and this leads to AC leakage that cannot be determined. The motor used in the project does not rotate at a constant rate at all times. Although the variation in rotational speed is low, it causes errors in calculating the percentage body fat.

Calibrating the leakage

In calibration (which is discussed in appendix F9), it is assumed that the DC motor is moving at a constant frequency. From this assumption the leakage effect can be determined by applying the parameters and the variables to the equations. Table B8 contains the variables and the parameters applied to determine the leakage effect.

Table B8

Parameter and variable that determine the leakage effect

Parameters & variables	Value	unit
Motor frequency	1.6	Hz
Diameter	6	mm
Density of air	1.2	Kg/m^3
Viscosity of air	1.76×10^5	Ns/m^2
Length	1.5	meter
Atmospheric pressure	1013	mBar
Test chamber	520	Litre
Reference chamber	156	Litre

Based on these parameters and variables, the chamber volume is determine to be 585.2 litres (using leakage effect analysis.m in the CD) The relationship between the pressure difference and volume of the inanimate objects is plotted in Figure8.8.

Assuming that the dc motor moves at constant frequency, the leakage effect can be determined and treated as a constant variable[1]. It was decided to calibrate the device in order to take this constant variable, as well as the other constant variables, into account (see section 8.6). Compared to quantifying the leakage alone, calibration of the device makes fewer assumptions. The error results (in volume) generated from the inconsistency of the motor speed is accommodated by the software (see Threshold section in Appendix E3).

[1] It refers to the variable that occurs constantly. Eg. Pressure sensor noise.

Appendix B8 Determining the hydration effect in ADP analysis

Open the "result" page.

Table B9
Instruction to determine the hydration effect in ADP analysis

Experiment	Operation	Corresponding cell	Reason of the operation
Determine the hydration effects on ADP analysis	1. Change the hydration effect to 2 litre	A29	Since these are the basic assumption of using ADP analysis to determine %BF
	2. See the corresponding %BF on 50 litre subjects	E32	Result in 10.3.1
	3. See the corresponding %BF on 50 litre subjects	E35	
Determine the hydration effects on ADP analysis	1. Change the hydration effect to 4 litre	A29	Since these are the basic assumption of using ADP analysis to determine %BF
	2. See the corresponding %BF on 50 litre subjects	E32	Result in 10.3.1
	3. See the corresponding %BF on 50 litre subjects	E35	

Appendix C Device data sheet

Appendix C1 Data sheet for Honeywell DC series pressure sensor

DC SERIES

PRESSURE TRANSDUCER

DC 001 N B C4 000

Basic Multifunction DAQ
16-Bit, 200 kS/s, 16 Analog Inputs

Overview and Applications

Features

Driver Software

Ordering Information

Recommended Configuration

Basic Multifunction DAQ
16-Bit, 200 kS/s, 16 Analog Inputs

Services and Support/Training

Related Products

Multifunction DAQ Overview

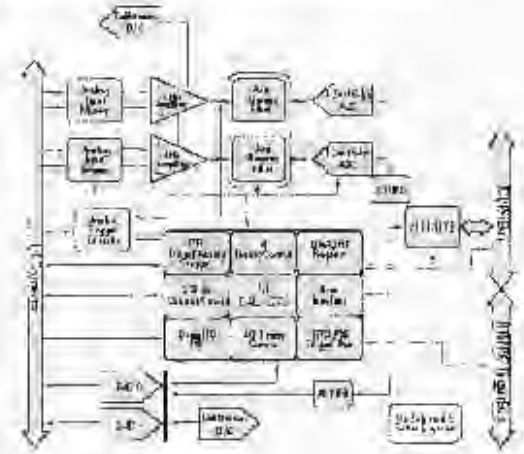

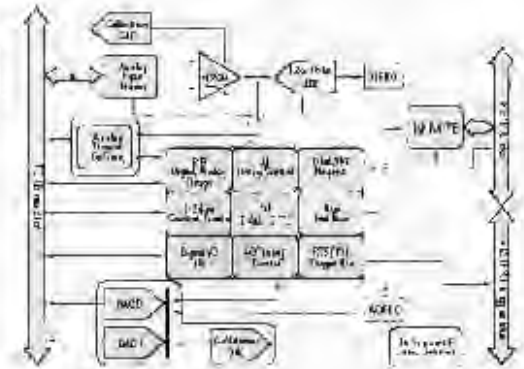

Multifunction DAQ Cable and Accessory Selection Guides

NI Cable Design Advantages

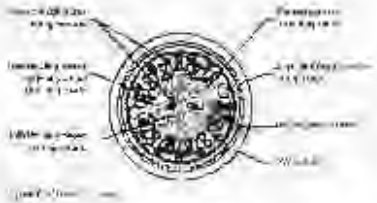

MOTOROLA

MPX100 SERIES

100 kPa Uncompensated Silicon Pressure Sensors

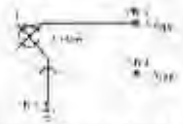

MPX100 SERIES

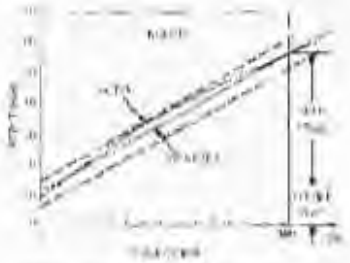

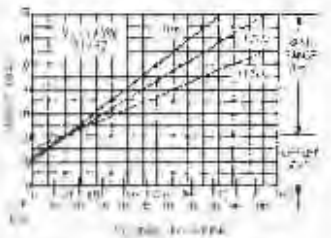

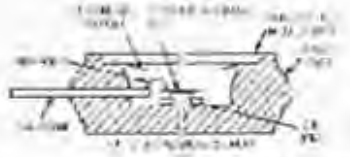

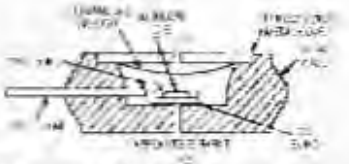

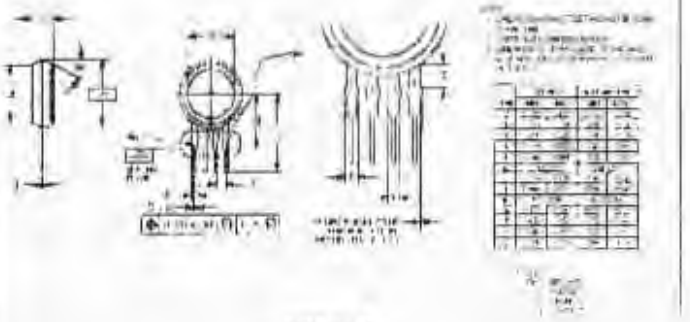

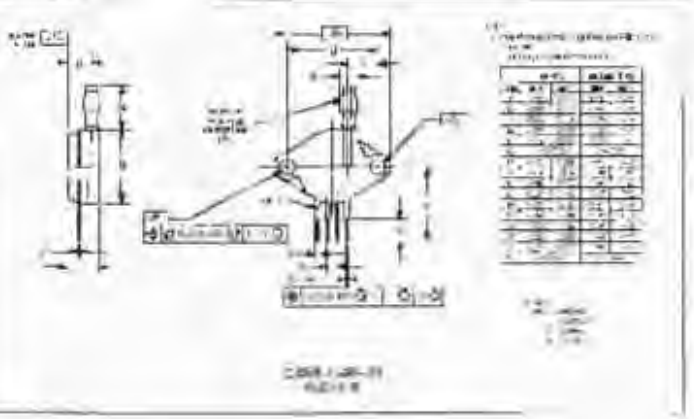

National Semiconductor

August 2000

LMC660

CMOS Quad Operational Amplifier

General Description

Features

Applications

Connection Diagram

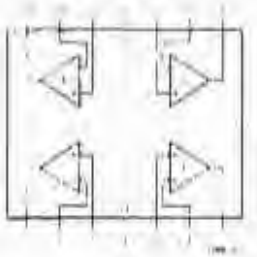

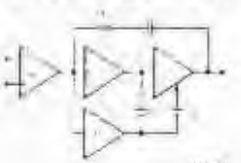

MICROCHIP

MCP6001/2/4

1 MHz Bandwidth Low Power Op Amp

Features

Applications

Available Tools

Typical Application

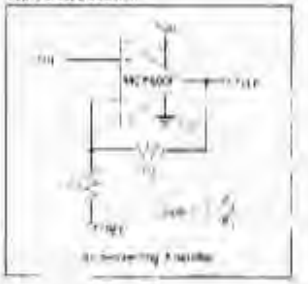

Description

Package Types

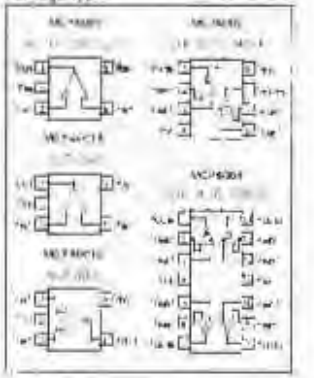

Appendix D letters

Appendix D1 Letter to Libra Bathware

UNIVERSITY OF CAPE TOWN

Department of Human Biology

[illegible]
University of Cape Town
Observatory Cape [illegible]
South Africa
[illegible]
[illegible]

Libra Bathroomware

Re: Request for donation of a bath

To whom it may concern

I am a Master of Science student in the department of Biomedical Engineering at the faculty of Health Science, University of Cape Town. I am currently performing medical research that requires the measurement of body composition. This measurement will need a sealed chamber into which a human subject can be placed. An idea, which I am investigating, is the use of two baths to construct the chamber.

The [illegible] is a bath which is suitable for such a construction. The modifications to the baths can be performed at the [illegible] workshop at the Faculty of Health Science. Mr [illegible] has kindly suggested that I may be in a position to obtain two baths for this research. This would be very much appreciated. Already his assistance and technical advice has been of immense help to me.

Thank you for helping in terms of medical research.

Yours sincerely

Peter Ma[illegible]

Appendix D2 letter to borrow the ventilator

UNIVERSITY OF CAPE TOWN

Department of Human Biology

Faculty of Health Sciences
University of Cape Town
Observatory, Cape 7925
South Africa
[illegible]
[illegible]

To: Respiratory ICU [illegible] 19/08/200[illegible]

<u>Request for a ventilator to perform medical research</u>

Dear Sir

I am a Masters student in the Bio-medical Engineering division of the department of Human Biology, University of Cape Town. I am currently doing research on measuring body composition via air displacement plethysmography, which is applying Boyle's law to determine the volume of the testing subject, to determine the ratio between the lean and the fat mass of the testing subject.

A closed chamber (plethysmograph) and a reference chamber together with other measurement transducers have been constructed. In order to run the experiment practically, it is required to change a known amount of gas volume at a required rate. At the moment, a 3-litre plunger has been used manually. However due to the operator error effect, it does not reach the desired accuracy.

Dr. J. Joubert has kindly suggested that it might be possible to borrow an old ventilator from your department. That will help me to solve the major problem in my research as a ventilator would be able to generate a constant volume change at the required frequency.

Thank you for your help.

Yours truly,

Peter Ma
Senior Master Student in Biomedical Engineering

Appendix E Construction related information

Appendix E1 Basic features of the hardware

The basic features, design, construction and orientation of the device are described below. As mentioned in chapter 7, it is important to ensure the safety, convenience and the expandability of the device. The features of each of the components of the system is described thereafter the orientation of the system.

Figure E1. Set up of the test and reference chamber

The detailed engineering drawing of the whole device is included in Appendix H1, more photos are included in Appendix I.

Test chamber

The test chamber (figure E1) has been designed to provide a comfortable airtight environment for the human subject during trials. Libra Bathware has donated two identical bath tub made from fiberglass. Both bath tubs have approximate inner heights of 1860 mm, width of 960 mm and depths of 400 mm. One of the bath tubs function as a base in which the subject sits while the other acts as a door and also contains a reference chamber.

Fiberglass and resin has been applied on the outside surface of both parts of the chamber for reinforcement.

The testing chamber has been designed to stand upright with a 5 degree slope rearwards, so that the weight of the door helps to lean on to the chamber and stay closed all the time. The slight rearward lean also adds to the subjects comfort while sitting inside the chamber.

Both baths come with two wooden blocks; holes have been made in these blocks in order to connect the steel frames (50 - 50mm tubes with 5mm thickness) which support the bath. Two additional wooden blocks have been placed on the base of the chamber to increase stability. The steel frames have been designed to be adjustable and can be reassembled. A fibreglass seat has been built inside the chamber, which has been supported by an extra steel frame under the seat for support.

A layer of seal rubber has been glued to both the "base" and the "door" part of the chambers (figure E1) in order to ensure an airtight seal. Two adjustable hinges (see figure I4 in appendix I) have been designed to ensure that the seal is evenly compressed. An acrylic window was inserted into the door so that the test subject and operator can see one another.

Two electromagnets are used to close the chamber and compress the rubber seal. Each magnet draws 0.5A current and provides 300ON of force. Two safety switches, one inside the chamber and one outside the chamber allow the operator or the test subject to open the door at any stage. This safety feature ensures the subjects can not get trapped in the chamber. The electromagnets will only hold the door shut once there is contact between the plates. A clamp together with a ball bearing (see figure I5 in appendix I) have been designed to close the door firmly, after which the magnets hold it shut. This design allows the clamp to fall back to its original position after bringing these electromagnets and plates together so that the subjects inside the chamber will not be trapped (see figure I5 in appendix I). The base of the chamber is furnished with wooden blocks and carpets.

Reference chamber

The reference chamber (figure E1) is located on the door part of the chamber inside the testing chamber. A 10mm thick reinforced acrylic wall ensures its rigidity. Having the reference chamber inside the testing chamber reduces the size of the test chamber and provides the closest

proximity to the test chamber (environment will be the same for both). Four additional rectangular acrylic blocks were added inside the reference chamber for reinforcement. The chamber is sealed with resin and fiberglass tape.

Piston mechanism

The piston mechanism (figure E2) is made out of a DC motor, scotch yoke mechanism and a plunger. Detail engineering drawings of the system is attached in appendix H2.

Figure E2. The dual piston mechanism and its power supply

A geared DC motor (See table E1 for the spec of the motor) is supplied with a constant DC voltage (figure E2). Input voltage is directly proportional to the rotational frequency of the motor. Adjusting the input voltage allows us to run the motor at the desired frequency. Running the motor at a constant frequency ensures that the pressure readings can be processed by digital filters. An assumption is that breathing will not affect the motor speed.

Table E1

Specifications of the motor

Spec of the motor	Information
Supplier	Parvalux Pty Ltd Bournemouth England
Type	DC shunt motor
Torque	47lbs. ins (5.315N/m)
Max Voltage	35
Max speed	100 rpm

The cam has three holes of different radii which facilitate three different stoke volumes. Two plungers were connected to the connecting rod. The other side of the stroke chamber is connected to the test chamber.

The Scotch yoke mechanism has been chosen because it allows the motor to drive the plunger in a sinusoidal like pattern. This will deliver a sinusoidal pressure waveform. This mechanism consists of casement, yoke, rod, disc, connecting pin between the yoke and the disc, connecting pin between the motor and the disc and supporting block for the rod.

Some considerations for each of the components:

- Base: It needs to be wide enough and long enough for the piston and the motor (including all components) to fit. The length of the base will be the length of the plunger added to the length of the scotch yoke. The base was constructed from a 12mm thick reinforced acrylic.

- The yoke: The inside surface was carefully milled and the smooth inner surface is ensured. This allows the pin to rotate inside the yoke freely. The yoke was constructed from stainless steel.
- The rod: The crux is to ensure that the rod is 100% inline with the piston.
- Disc: Three different radii represent 3 different stroke volumes. a connecting pin, connects the yoke and the disc.

Differential pressure sensor and its circuit

A Honeywell DC model ultra low differential pressure sensor is used in this project. It has been designed to maximize sensitivity at low pressure levels. This device gives a voltage output that is directly proportional to the difference in pressure between the two air inlets.

This sensor is internally calibrated and temperature compensated. The design provides an accurate and stable output over a 0°C to 50°C temperature range. This low-pressure circuit provices 0.5 to 4.5 V output for -5 to 5mBar pressure input. The sensor is powered by a 12 V battery, which is regulated to 5V and filtered to ensure noise free supply. See the data sheet in the appendix C1 for further details of this pressure sensor.

Experiments showed a 20 mV sinusoidal output from the pressure transducer. This noise is filtered out using a fourth order Butterworth low pass filter with a cut off frequency of 10Hz. The following diagram shows the response of the filter.

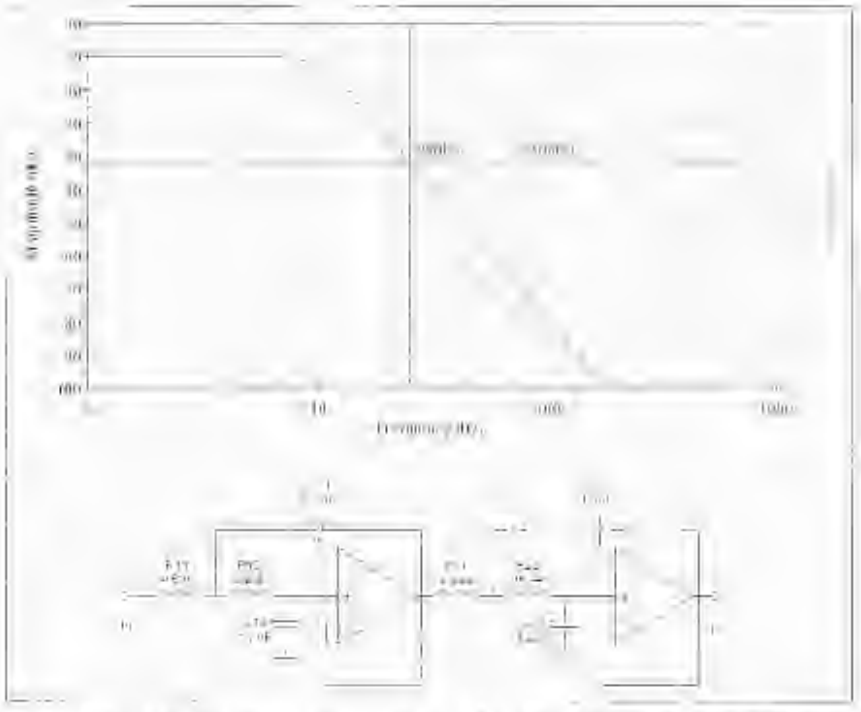

Figure E3. Frequency response of a fourth order Butterworth low pass filter (top) and its circuit representation (bottom)

This filter is constructed with a Microchip device, MCP6002 (See Appendix C4 for the datasheet of the device)

Analogue to digital converter (ADC) & Data acquisition (DAQ)

PCI6013 from National Instruments was used to sample and convert the analogue signals into digital signals. This device features 16 signal input channel at 200,000 samples per second, its 16 bits resolution enable us to detect changes of as little as 15uV (which is $1/2^{16}$). A connector block with 68 screw terminals and shielded I/O cables served as a termination accessory to connect the signal to the PC.

See appendix C2 for the data sheet of this device.

Computer

A PC with Intel Pentium III 450MHz CPU and 258MB Random Access Memory (RAM) is used. (See appendix E3 for the detail of the software)

Calibration tool

A Block of Styrofoam with 300× 400× 500 mm (60 litres) is used as a reference tool. The low cost, light weight and low compressibility were considerations when choosing the block. An accurate calibration must be preformed using this block before each trial.

Six additional cylinders made from Styrofoam were also used. These Styrofoam cylinders are 200mm in diameter and 100mm in height, giving each a volume of 3.14 litres.

Spirometer

A spirometer (from C F Palmer Pty Ltd) is used to measure the tidal volume of the subject. The measurement is used to predict the thoracic gas volume.

The spirometer is also used in the study where the lung is used as a diaphragm to displace the air. The resolution of the spirometer is 10ml in volume.

Control Box

Figure E4. Control Box

A metal box with dimensions 220 × 210 × 110mm is used as a Faraday cage in order to isolate the circuitry from strong electrical and magnetic field. The control box is mounted outside the testing chamber for safety and easy access. Two holes with 5mm diameter on the side of the box allow the pipes from the test and the reference chamber to come into the control box.

The Box contains one 12V sealed rechargeable battery, the Honeywell differential pressure sensor and its circuit, the barometer, a connector block, shielded I/O, cables and two pipes which connect the differential transducer to the test chamber and the reference chamber respectively.

Appendix E2 Development of a method to measure atmospheric pressure

Background

Air surrounding the earth is heated by the sun and cooled by the radiation into space. This cause the change in the air density and hence in the air pressure over geographic regions. Air pressure in the chamber alter the corresponding air pressure of the enclosed gas, therefore it is essential to measure atmospheric pressure accurately.

The available methods for measuring atmospheric pressure for this project

1. Measurement with mercury columns
2. Prediction using "calibration tools"
3. Prediction from the UCT weather station.
4. Direct measurement using an aneroid barometer

Determining the atmospheric pressure using mercury column

The mercury column is the most accurate method in determining atmospheric pressure. This is how atmospheric pressure is defined. (Subject to knowing the relative temperature of the mercury)

Method: use a closed tube filled with the mercury and then inverted into a reservoir or cistern of liquid. The liquid will fall, a vacuum will be formed on the top of the mercury column.

Advantage: precise

Disadvantage: inconvenient, availability

Figure 55: Mercury column Barometer

The atmospheric pressure can be calculated using the following equation:

$Pa = \Omega m \times Hm \times G$

Where

Pa is the atmospheric pressure,

Ωm is the density of the Mercury,

Hm is the height of the mercury and

G is the gravitor force.

Predicting the atmospheric pressure with "calibration tools"

The idea is to put two known calibration volumes into the chamber and to measure the resulting $\frac{\Delta V}{\Delta P}$ relationships. We have two unknown variables (the size of the chamber and the present atmospheric pressure) and two equations. The equations can then be solved simultaneously for chamber size and the atmospheric pressure.

By performing three measurements, the result of the first two trials will give us two equations to solve for the size of the chamber as well as for the atmospheric pressure. A third trial can be performed to validate the previous trials. Two calibration stages can be performed before the trial. This is assuming that the environmental factors remain constant during the calibration period. See the theoretic model in "Patm using calibration tool" VI in the CD

Problems using this method

The theoretical model shows that in order to reach the desired accuracy in atmospheric pressure measurement (0.05mBar), we need to successfully predict 10^{-4} mBar accuracy in experienced pressure (ΔP).

This is impossible. It is not considered to be a practical solution for day to day use of the plethysmograph. For future development, this method remains a potential validation method for the precision of barometer devices

Prediction from UCT weather station

UCT Department of Environmental Studies measures atmospheric pressure continuously. There are weather stations all over the Western Cape monitoring weather changes. The information from the weather station can be obtained from the following web address (http://www.csag.uct.ac.za/myweather/) (Last access 2004/07/19)

As they have one of the most accurate devices in terms of measuring atmospheric pressure, a portable weather station has been borrowed and set up in the flow studies laboratory near the ADP device. The results were recorded for two weeks (sampling was taken every 30 seconds).

Results

There was no obvious relationship between the UCT readings and the Lab readings. There was insufficient precision. This could be due to the following reason:

- Different air density between the indoor and outdoor;
- The two places are not close enough to have the same readings.

Hence this is not a suitable method for this project.

Aneroid Barometer

Motorola MPX100AP (see appendix C3 Data sheet of this device) is a sensor which measures pressure from 0-1000mBar. This device is based on an Aneroid barometer.

Principle of the Aneroid Barometer

As in figure E6, the Aneroid barometer consists of a sealed chamber. When the atmospheric pressure changes, air in the chamber will increase or decrease in volume. This effect mechanically moves the flexible membrane and hence, the pointer.

This method has the advantage that it is practical and easily available, but the disadvantage is that it has limited accuracy.

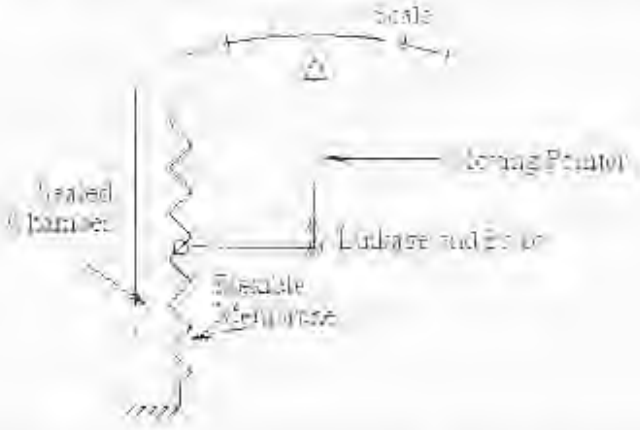

Figure E6. Basic principle of the aneroid barometer

Determine the interface for this pressure barometer

The atmospheric pressure is related to the altitude and temperature. Typical atmospheric pressure equals 1013mBar at sea level. Location of the ADP device is 83m above sea level (data obtained from satellite signals).

The World's highest recorded atmospheric pressure at sea level is1083.3 mBar and lowest recorded atmospheric pressure at sea level: 876.4mBar From this information, the dynamic range of the atmospheric pressure is determined to be from 950 to 1050 mBar. The corresponding voltage output range is determined from 1.5 V to 3.5 Volts (see figure E4).

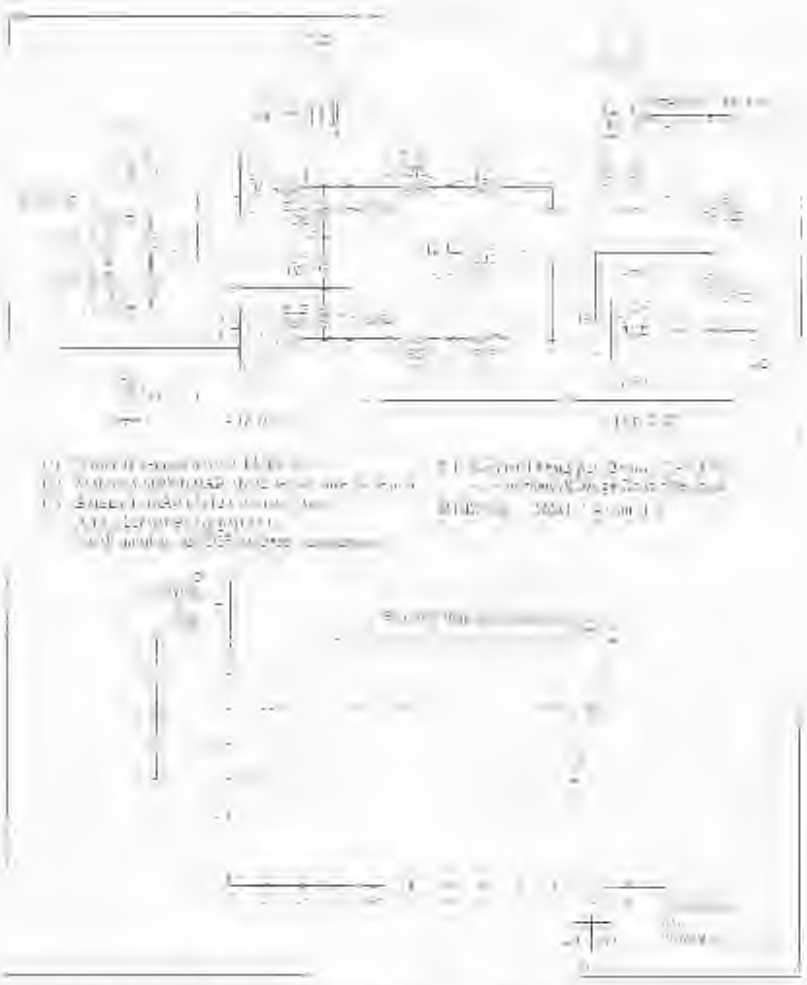

Figure E7. Representation of the relationship between voltages to pressure (bottom) and circuit diagram for the pressure sensor (top)

This sensor is located in the control box and its output is digitized via a channel on the DAQ device. See appendix C4 for the data sheet of the LMC660CN

Conclusion

Four potential methods to determine the Atmospheric pressure were compared. Each of the methods has advantages and disadvantages. The Motorola pressure transducer was selected as the most appropriate for this project.

Appendix E3 Software Design

This section covers the detailed functionality of the Measurement & Automation Explorer2.2 and Labview6i. Each sub-section of the two programs cover the algorithm developed from the design of the device as well as the current settings and the reason behind it. Appendix E11 give step by step instructions to operate this software.

Measurement & Automation Explorer 2.2

Device configuration

Measurement & Automation Explorer2.2 from National Instruments Inc. is used to configure the DAQ card. The PCI 6013 card and its instrument driver was installed successfully. This device has been seen under "Devices and Interfaces" icon. The following properties are set in order for the software to identify the card.

- Device number: Number "1" is assign to PCI 6013card
- Polarity of the Card has been set to -10V to +10V and differential mode has been selected in order to reduce the common mode ratio rejection ratio (CMRR).

Configuration of the data type

Virtual channels under "Data Neighborhood" provide a gateway for the signals to flow between the DAQ card and Labview6.i. Two virtual channels, named "Pressure" and "Temperature" have been created according to the nature of its signal type.

After setting up the Device and creating the virtual channel, the analogue signal can be converted into a digital signal ready for analysis

Labview6i

History and the concept of "Labview6i"

Labview programs are called virtual instruments (VIs). VIs are composed of two windows, namely Front panel and Block diagram. The front panel serves as the graphical user interface which contains the user input; also known as controls, and outputs; also known as indicators. They are displayed on the front panel in various forms required. VIs can be transferred into a Sub-VI which can be joined and placed (integrated) into a higher order VI. (This is already covered in chapter7 but clarifies the additional information in this section)

The block diagram window is where the source code is developed. All of the controls and the indicators from the front panel have an associated terminal that represents them on the block diagram. Operations are generated by wiring up the terminals to functions. Most of the operations and analysis on the data have been processed in this manner. (See figure E7 for an example of block diagram in Labview6.i)

Labview is technically a data flow programming language. This means that the data flows from a data source (e.g. a DAQ device) through the program. See figure E5 for the concept of data flow diagram

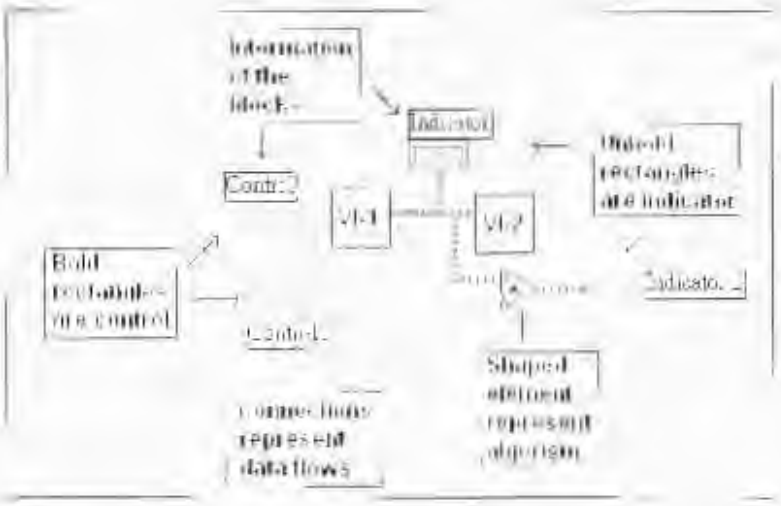

Figure E8: Diagram illustrating the block diagram concept of Labview6i

The actual diagrammatic sketch of the sub VI is included in the beginning of each section. The jargon used in the surrounding paragraphs can be put into context by the diagram. This is only the first level of the sub-VIs, but is similar in form to other levels of the sub-VIs. The details of the diagram are quite lengthy and have not been included. The main reason for the diagram is for the reader to be aware of the sub VI's and their location, especially for the reader who is going to continuing on the development of this project. It is sufficient to know that each block in the diagram has its own diagrammatic sketch or formula.

Overview of the dataflow

Data is flowing in from two sources. The first set of data is the personal information data details. The second set of data is captured from the DAQ card in voltages. It contains information of the volume of the subject as well as other components. This set of data flows though the following sub VIs, ADV DAQ, Filtering, Interfacing, Analysis, Warning and Final

result. Once a trial has been obtained and verified as successful, (see Evaluation of the trial on page 205 for how a successful trial is classified), the data will flow into a "basic info" sub-VI together with the personal information. The analysis of body fat percentage will be calculated accordingly.

Data acquisition

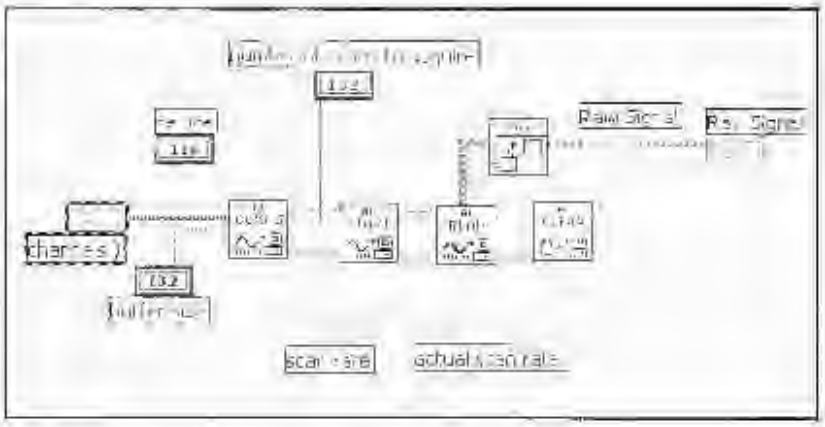

Figure E9. Block diagram of ADV-DAQ

Data acquisition operates under the "ADV-DAQ" VI. Four of the sub-VIs are included under this VI, namely AI-Config, AI-Start, AI-Read and AI-Clear.

"AI config" is used as a collecting point for the data, i.e. to take in the readings from the pressure and temperature channel from the PCI6024. Buffer size has also been set to 30000 in order to allow the program to run smoothly. For each of the trials "AI Config" generates a task ID as well as an error cluster. All the sub-VIs in "ADV-DAQ" carried the same task ID to ensure its identity.

"AI- Start" sets the scan rate to be 100,000 per second. Trial duration appeared as a control and the total number of samples obtained is equal to the sampling (i.e. Total sample multiplied by the Sample rate). Actual scan rate is shown as an indicator. This is used to compare with the scan rate to ensure that no error occurs during the sampling process.

"AI-Read" sets the time limit for the trial, as well as giving a graph indicator for the waveform captured from the card. It is named "raw signal". Output is presented in a 2D array form (containing the raw data and its corresponding time). The task ID will be carried into "AI clear" VI and it clears the buffer area in the PC memory so that the software is ready for the next set of data.

See "the arrangement of the front panel" in page 208 for these controls and indicators.

Filtering

This section is made out of three Sub-VIs named: Average filter, Butterworth band pass filter and ideal filter. Filtering is one of the most important parts in the whole software design. It differentiates the wanted signal from the unwanted signals. By looking at the signal in the frequency domain, two major peaks as well as some smaller peaks can be identified.

The two major peaks are a resulted of breathing and the volume displacement generated from the motor. The smaller peaks are a combined effects of noise, room temperature fluctuation and humidity generated from the subject. The small peaks could also be due to instrumentation errors. VIs in this sections were built to identify the difference between the signals and to extract the wanted signal (i.e. experienced pressure from the air displacement generator).

Average filter

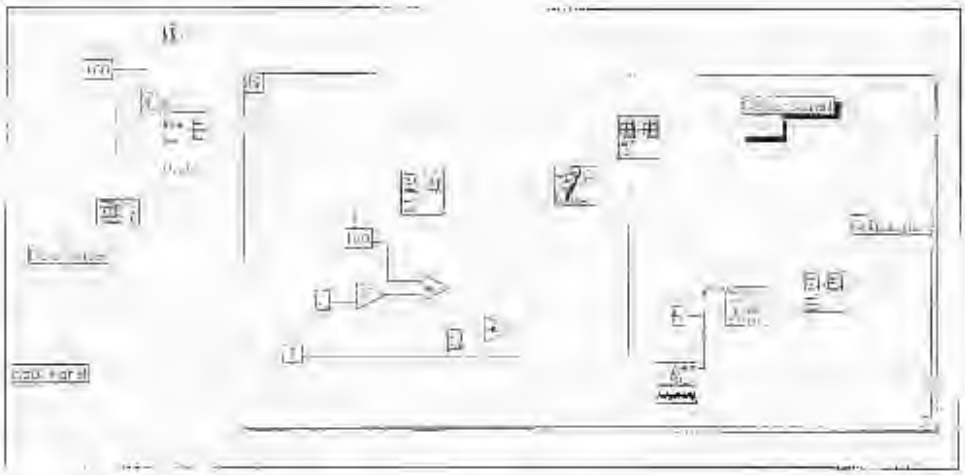

Figure E10. Block diagram of Average filter

Average filter takes the input signal from "ADV-DAQ". For each 100 points we take the median and use this point to represent the value of these 100 points. This is done in order to reduce the random error of the DAQ device. The desired sampling signal is at 1000 Hz (to satisfy the Nyquist criterion). This procedure does not take out the important information (sample rate =100,000 and divided by 100 is equal to 1000 Hz).

In this project after the average filter, the signal is then sent to a Butterworth band pass filter. An ideal filter is also included in the software design for further development. This will be used if further funding can be granted to build a constant volume generator.

Butterworth band pass filter

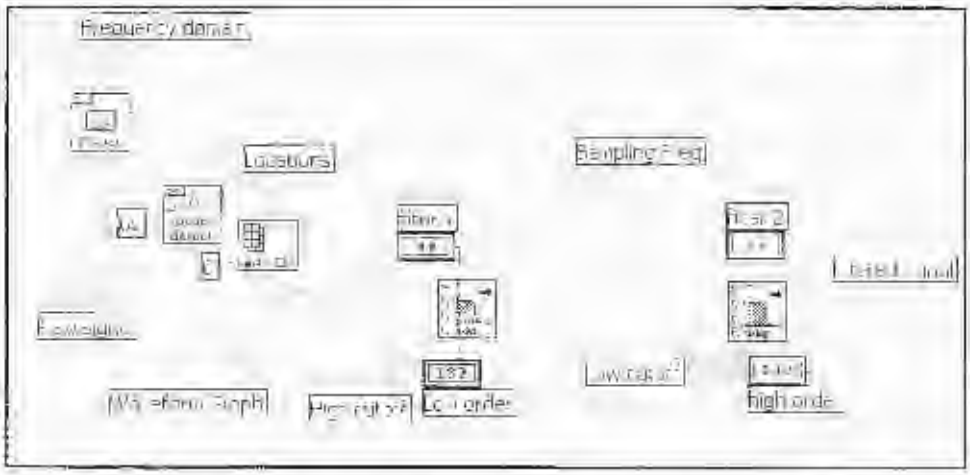

Figure E.1 Block diagram of Butterworth band pass filter

This Butterworth filter is made from the combination of a Butterworth low pass filter and a Butterworth high pass filter. As our present motor is a DC motor, it is not running at an exact frequency at all times. To include all the frequencies that are in the required range, a Butterworth filter is the most appropriate for this application. The pass band is set to be from 1Hz to 3Hz and this cuts off the noise and the signal above 3Hz, since the motor is running between 1.5 and 2Hz.

Ideal filter

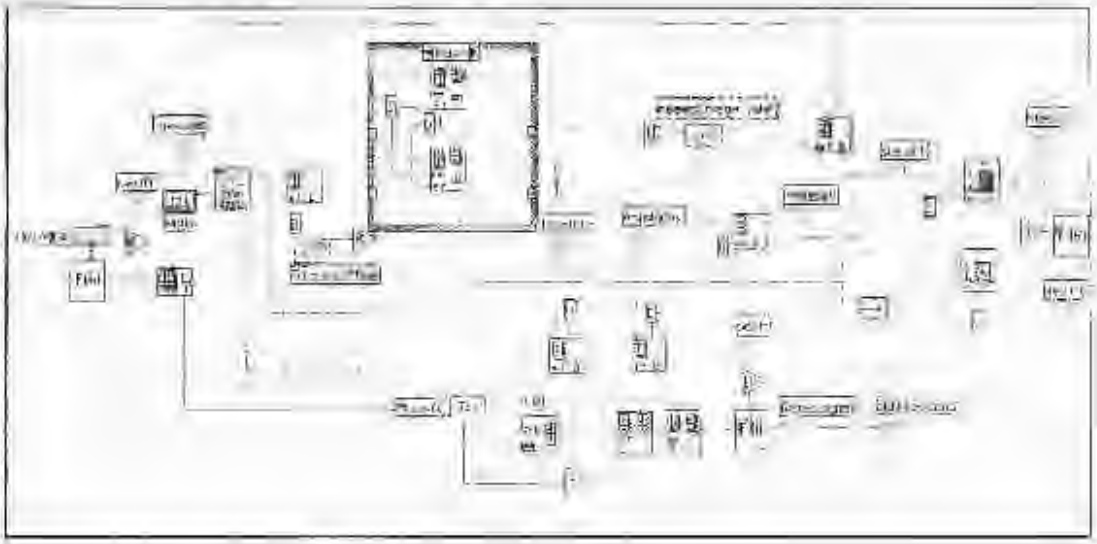

Figure E12. Block diagram of ideal filter

In future developments, a pure sinusoidal displacement in volume waveform signal should be generated. When data flows to the idea filter, the signal will be Fourier transformed (FT). By transforming the signal to the frequency domain, the absolute frequency that the volume generator is moving at can be determined, hence excluding all the other signals. Then an inverse Fourier transform (IFT) is applied to this signal. A pure sinusoidal signal is then presented as the filtered signals. The outcome of the filtered signal is presented on the front panel in graphic form

Interfacing

It is important to convert the signal to a series of numbers (subsequently referred to as an array). These arrays contain the changing pressure (ΔP). Three Vis display are included in this section namely: Finding Peaks, 2D to 1D and Erase the zeros.

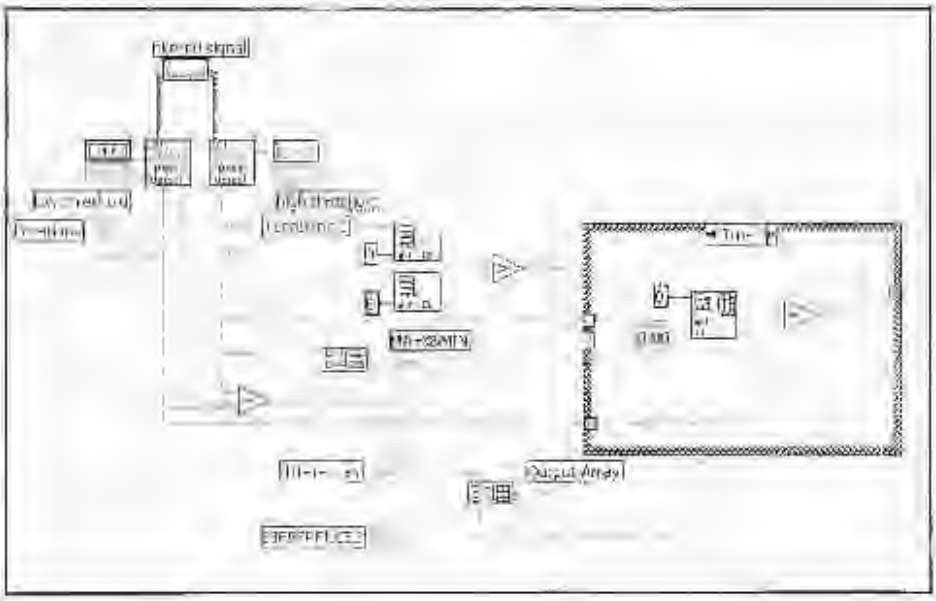

Figure E13. Block diagram of Finding peaks

The filtered signal will be filtered by the "Finding peaks" VI. It will be fed into two of the peak detectors. One is for picking up the all the maximum pressure values and the other is to pick up the minimum pressure values. The peak has been defined as a value which is bigger than the 100 samples ahead and 100 samples behind it, as this allows the program not to mistakenly determining the noise in between.

Thresholds (in the amplitude) have been set for both the maximum and minimum peaks to ensure that only the correct values are returned, acting as another layer to block noise or distortion. Both minimum and maximum peaks are sent into two separate arrays

After determining the peaks in the pressure waveform, the software is programmed to calculate the difference between the n^{th} maximum peaks and the n^{th} minimum peak. Then the software compares the peak location of the first maximum and minimum peaks. If the first minimum peak is detected before the first maximum peak, the software will work out the difference between n^{th} maximum and the $(n+1)^{th}$ minimum, if the first maximum peak occurs before the first minimum peak, it calculates the different between first n^{th} minimum and the $(n+1)^{th}$ maximum. This step is to ensure that both sides of the curve (the increasing and the decreasing part of the sinusoidal pressure signal) are included

2D to 1D

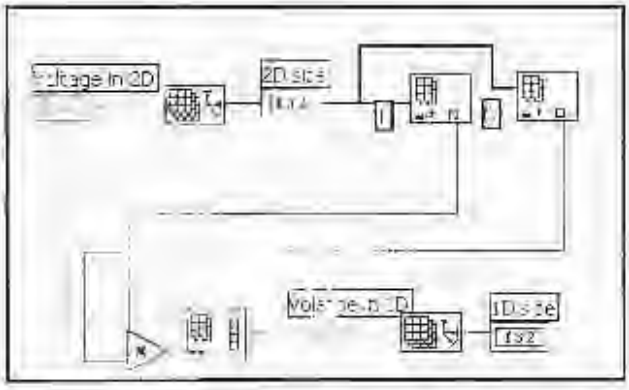

Figure E14. Block diagram of 2D to1D

Output of the difference between peaks is presented in a 2D array form. In order to operate on the entire signal, it is essential to transform the signal into a 1D array. This is to append each row of the array one after another. A 1D array was created according to the size of the 2D array. This 2D array is then reshaped in to an 1D array. The size of this 1D array is displayed in the front panel as initial size.

Remove zeros

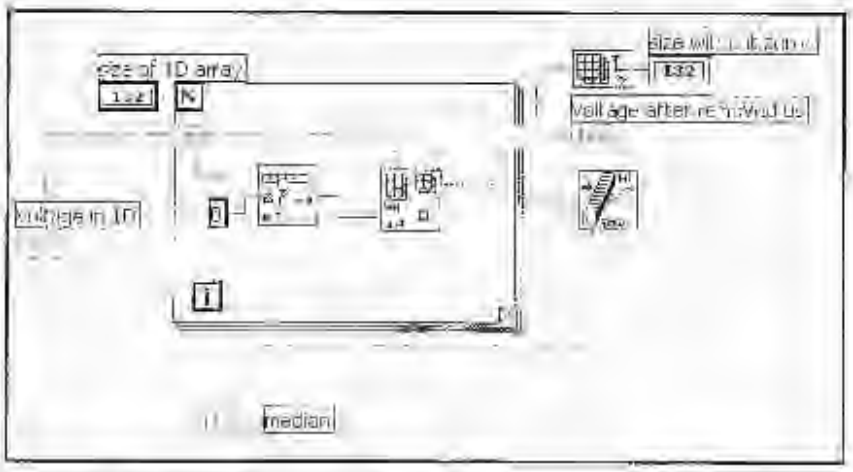

Figure E15. Block diagram of Remove Zeros

During the trials as well as interfacing the data, some of the signal might appear to be zeros. This step is to remove all the zero data so that it does not affect the mean of the differential signals. Any zeros will be removed, after which the median number of the data is identified.

Analysis

Threshold

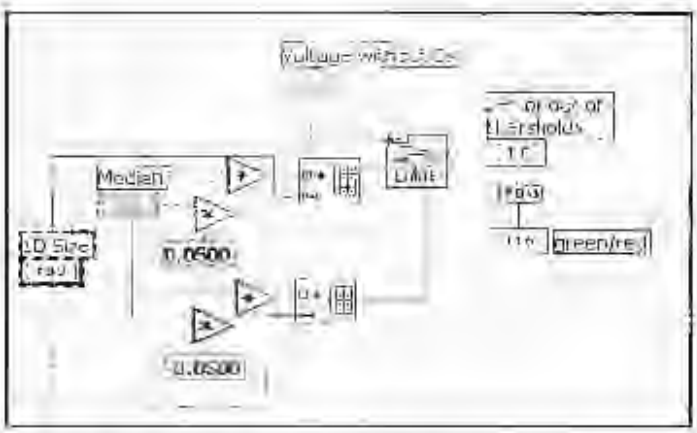

Figure E16. Block diagram of Threshold

Two sub-VIs are included in this section, namely: Thresholds, Means & SD. The threshold is required because of the following two main reasons.

1. When applying a filter to almost any data, the first few and the last few numbers do not always produce a smooth output, due to its non-continuous nature.
2. During the measurement in the trial, any environmental factor or distortion of the motor could vary the measurement in any single sinusoidal measure. This creates an overall measurement error.

A threshold is set in order to include only the data that is within 5% of the median. (We use the median number because the differential pressures are random variables) The median number is used here instead of the mean, because mean is not a true reflection of the true range of data when there is some unwanted data in the array. Median number will give a better reflection of what is the true range of the data. This threshold is acting as another level of filter that excludes these error data out of the array.

Mean & SD

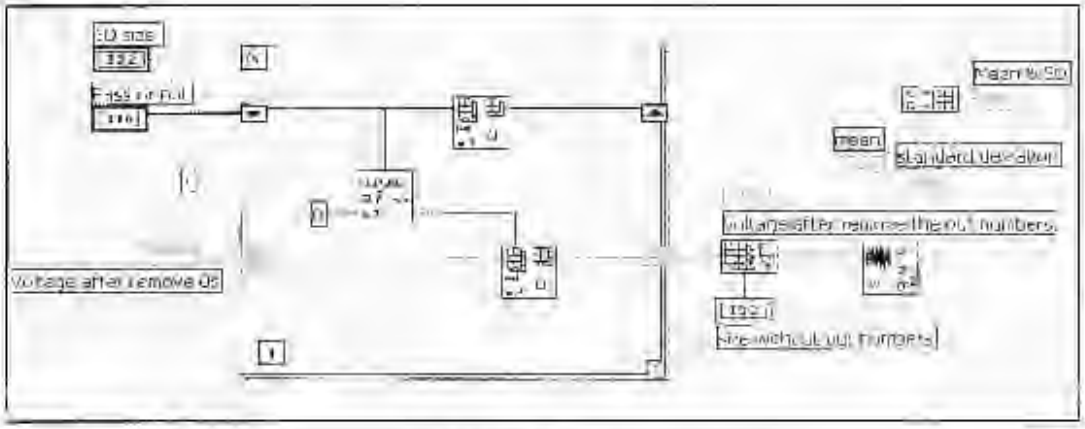

Figure E17. Block diagram of Mean & SD

After excluding those unwanted signals (experienced pressure difference) which are not in the threshold that we set, the mean and standard deviation of the data will be calculated. The number of the data that is left in the array are shown in the front panal (named final size).

Warning

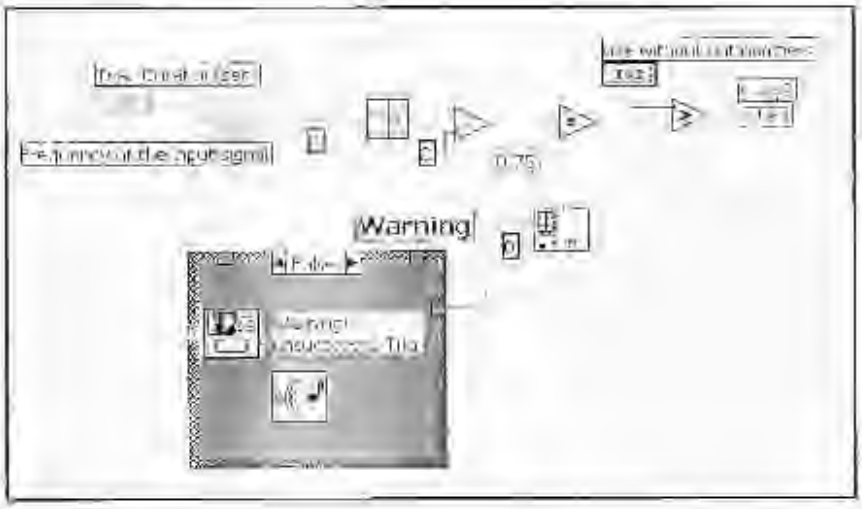

Figure E18. Block diagram of Warning

The purpose of this VI is to give a feedback to examine whether the trial is successful or not. A reference value is obtained by multiplying the trial time (s) to the frequency of the experienced pressure (ΔP). Doubling this reference number should give an indication of the original data that should be in the array (because of the increasing and the decreasing part). Due to processing of the data and excluding the distortion from filtering, a corrected reference number can be worked out by the reference number minus 2 and then multiplied by 0.75. Final data size will be compared to this corrected reference.

If the final size of the array in mean & SD sub-VI final size is smaller than this predicated reference size, this means that there is too much variation during the trial. This VI will indicate "Warning! Unsuccessful trial!" to the user and stop the program. If there are enough samples in the desired range, this sub VI will direct the data to "Basic Info." The trial will be indicated to be successful. The BMI value is then required to be compared with the calculated %BF by the operator. The outcome of this first order comparison determines whether a lung function test is necessary or not.

/Atmospheric pressure

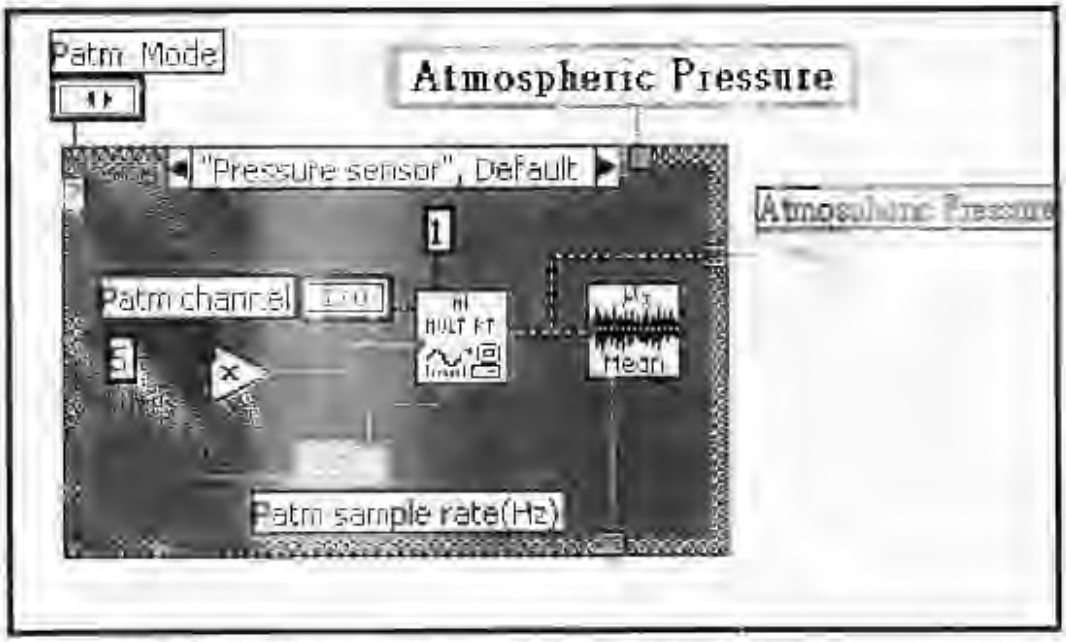

Figure E19. Block diagram of Atmospheric pressure

The software is set by default to acquire the atmospheric pressure from MPX100AP, the pressure sensor is determined to be the reading obtained from the pressure sensor at the time that the chamber door is closed and when the trial just started.

For the purpose of further development, we also allow the user to manually input the atmospheric pressure. The pressure input mode can also be changed in the front panel.

Capture of personal information data

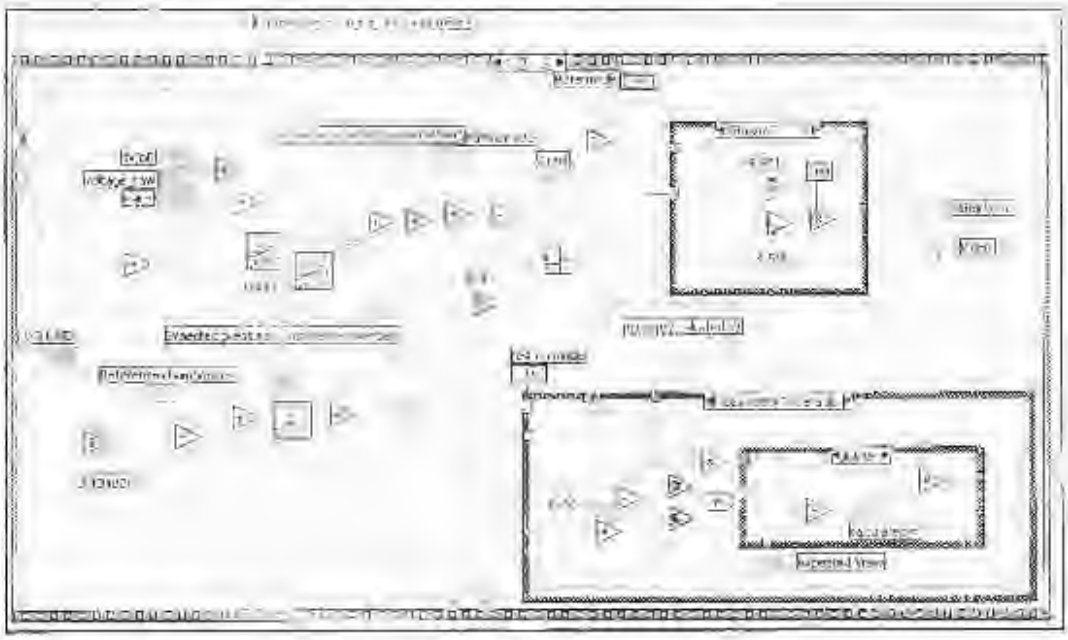

Figure E20. Block diagram of Basic information

Personal information is pre-captured from other devices and it will be keyed into to the "Basic info" sub-VI. The operator will be asked to enter the listed information of the subject:

- Height in cm (140-210)
- weight in Kg (35-120)
- Gender
- Age (17-91)
- Tidal Volume in liter

Range of the data for the above information has been set as above. Any mistyping of information will be indicated with an "error" sign to the operator. Notice that the range of the age is set to be from 17 to 91 due to the FRC predictions by Crapo et al. Body mass index (BMI) is also calculated to serve as a rough filter. A warning sign will be given when BMI is out of the normal range.

The arrangement of the front panel

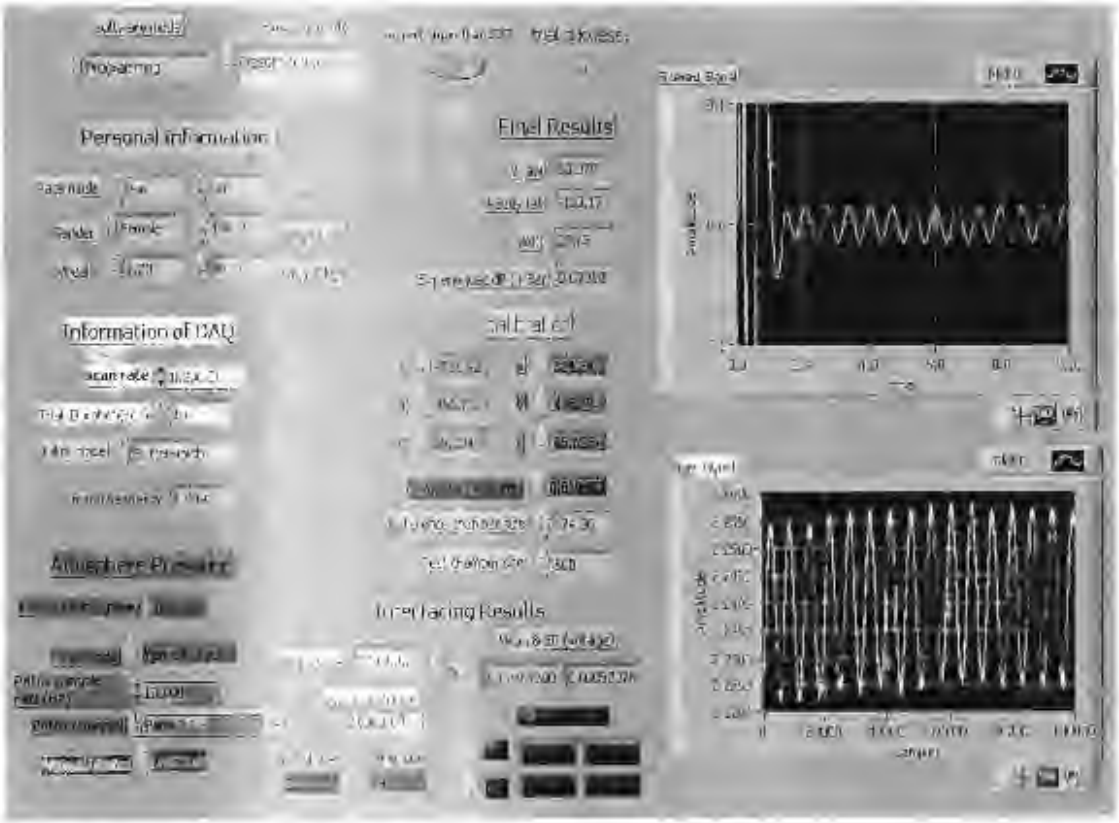

Figure E21. Arrangement of the front panels

The front panel consists of 4 diagrams and 6 groups of controls and indicators.

The four diagrams are as follows:

- Raw signal (showing the pressure signal) obtained from the DAQ card without any processing or filtering)
- First signal (showing the pressure signal after the average filter)
- Filtered signal (showing the data after the Butterworth filter (default) or the ideal filter after processing.
- Atmospheric pressure, showing the measured atmospheric pressure.

There are 6 main groups namely:

- Personal information
- Final results
- Information of DAQ
- Calibration
- Atmospheric pressure
- Interfacing result

Each group contains the corresponding controls and their indicators.
A description of the usage of these controls and indicators is included in the corresponding sections described previously.

Appendix F Test process

Appendix1 Ethics approval

Research Ethics Committee
Faculty of Health Science
E46 26 Old Main Building Groote
Schuur Hospital Observatory 7925
Queries Xolile Fula
Tel (021) 406 6492 Fax 406-6411
E-mail Xfula@curie.uct.ac.za

17 June 2003

REC REF: 220/2003

Dr WL Capper
Human Biology

Dear Dr Capper

BODY COMPOSITION ANALYSIS USING AIR DISPLACEMENT PLETHYSMOGRAPHY

Thank you for submitting your study to the Research Ethics Committee for reviewal.

It is a pleasure to inform you that the Committee has ***formally approved*** *the above mentioned study.*

Please quote the above Rec. reference number in all correspondence

Yours sincerely

PROF T ZAMOW
CHAIRPERSON

Appendix F2 Consent Form

Introduction of the studies

Body composition analysis is the process of estimating fat masses as a percentage of the body mass (%BF). This provides an important physical guide for doctors and sport researchers.

The aim of this study is to develop a method to establish a consistent, cost effective, comfortable, non-invasive and quick way to determine body composition.

Instruction of the trial study

In this study a scale will be used to determine your mass and a device based on air displacement plethysmography will be used to determine your body volume. The information will be recorded, from which your whole-body density is determined. Using this data, body fat and lean masses can then be calculated.

The whole testing procedure will take about 10 minutes. During the trial you will be required to wear a standard suit, which will be provided. While sitting inside the chamber you may be instructed to breathe though a disposable tube. There will not be any form of injection or invasive performances.

Your participation in this study is entirely voluntary and that if you refuse to participate or withdraw from participation at any time, there will be no prejudice to the quality of your subsequent clinical management and care.

I,_____ student/staff No: _____ ,
am fully aware of the above information and I am willing to participate in the trial.

Signed: _____ Date: _____

Appendix F3 Personal information form

Name: _____

Student/Staff No: _____

Male/Female: _____

Age: _____

Race: _____

Height: _____ **cm**

Weight: _____ **Kg**

Special comment:

_____

_____

_____

_____

_____

_____

_____

_____

_____

_____

_____

_____

Trial Done by: _____

Date of trial: _____

Appendix F4 Instructions of the trials for the testing subjects

Please read the following information. This will help you to understand the test procedure hence help us to obtain the most accuracy results.

1. Apply the provided ear plug to you ear. Take a few deep breaths then get into the chamber.

2. While you are in the chamber, do not hold you breath but try to breath as shallow as possible

3. You will also find a push button on your right hand side. That is for you to release yourself after the experiment or at anytime when you feel any sort of discomfort.

4. Once you get into the chamber. Place your feet under the seat. Note that there are sensors just above your legs; please make sure you not touching them as it could cause damage or affect the result of the experiment.

5. When the trial is finished the instructor will give an indication to you through the window.

6. You may now press the button and come out of the chamber. And the whole trial is competed.

7. Trials will be preformed twice on each subject to ensure its consistency.

Appendix F5 Practical considerations relating to the construction of the chamber

Introduction

During the design and construction process of the device; two ideas were investigated. This chapter covers the feasibility of putting them into practice. These ideas were:

- Air displacement using the human lung.
- Air displacement using a ventilator as a pressure driver.

Critical reasoning of these attempts

The main idea is to show that although these methods are theoretically sound, but impractical in real life situations.

Theoretically each source of error can be identified. An adjustment can be made to compensate for the error and these effects cannot be quantified without more assumptions. The result of these assumptions could lead to the measurement in a worse direction.

There are other many hidden factors that could cause total errors in the measurement.

Here is a list of possible factors:

- The lighting factor (fluorescent lights can affect the pressure sensor).
- Noise carried by the cable.
- The slipper factors of the DC motor (as this factor will make the frequency of change stroke not constant) over time and from day to day.
- Sound effects from the surroundings (such as noise from cars driving past nearby.)

The quantity of these noises varies from time to time and due to this common characteristic of these noises, the effect of this signal cannot be included in the theoretical model

Air displacement using the human lung

As explained in chapter four, during the trial studies, a known amount of air has to be displaced in order to generate a pressure change inside the chamber. This idea uses the breathing of the subject in the chamber to displace air from the chamber.

The method has the following major advantages:

- The lung volume of the subject could be considered to be outside the chamber; therefore it is not necessary to measure the lung volume.
- Since the subject breathes to the outside of the chamber, the humidity effect on the chamber will be minimized.
- Cost of the device will be reduced since a pressure drive is not required.

Setting up the device and results obtained from the trial studies.

A breathing tube has been connected between the chamber and a digital air flow sensor. On the other side of the chamber, the output connecting tube has been connected to a spirometer. The displacement of the air could thus be recorded at the same time as the relative pressure within the chamber. Trial studies were preformed.

(See appendix F7 for trial step to follow for this method.).

Results

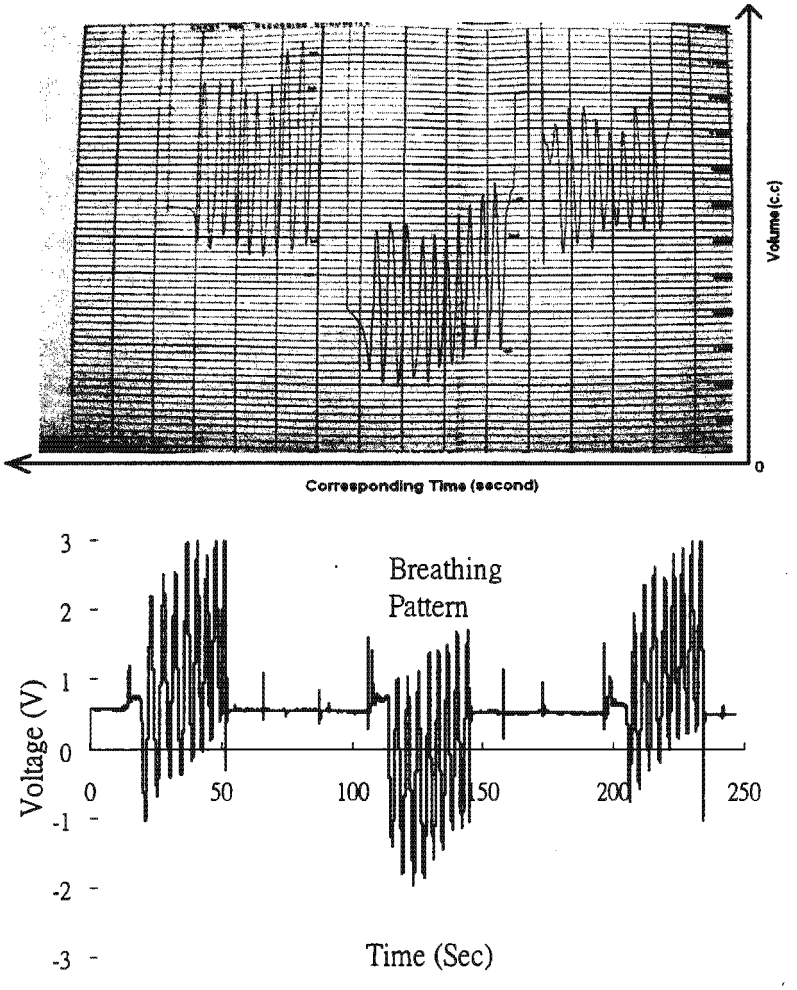

Figure F1. Volume displaced from breathing (top) and corresponding pressure (bottom)

For most of these measurements, the volume of the subject could only be estimated within ± 20 liters (figure8.3); due to the following major source of errors:

- The sensor resolution for volume measurement is only about 10ml. This is insufficient for ADP purposes.
- Signal to noise ratio is too small.
- The compartment of the air in the spirometer changes after few breaths, which affect the temperature and the humidity within the spirometer, hence the volume that was read from the spirometer can not reflect the true volume that can be used in the chamber. A more precise instrument will be needed in order to perform the task, hence more sources of error.

Principle findings

Although it has many advantages, using the lung as a pressure drive created a huge complexity to the measuring systems. It is thus preferable to have a constant and accurately known change in volume of the chamber rather than a variable change in volume which can only be measured to a limited accuracy. Training the subject for the trial also introduced an unpredictable factor. It could therefore be concluded that this is not a practical way of determine body composition.

Air displacement using a commercial ventilator as the pressure driver

According to above finding, I decided to use a constant pressure drive and chose a Bear 2 ventilator. This device was borrowed from the Respiratory ICU (C27) Groote Schuur Hospital, Cape Town South Africa. See the attached relevant documents of the ventilator.

The ventilator is calibrated weekly by trained specialists. The principle of the ventilator is that it delivers a relatively constant amount of air at an adjustable rate. It relies on the compliance of the patient's lung to exhale air in order to complete the respiration cycle. Therefore an artificial lung with either 1.5 or 2.0 litres capacity was placed inside the chamber and connected to the ventilator. Hence a constant amount of air can be displaced out of the chamber due to its fixed compliance. The volume of output air is measured to ensure it is constant and equal to the air input to the chamber by the ventilator.

Calibration studies were first introduced by setting different rates and amplitude of volume displaced in order to search for the best possible combination.
See appendix F8 for the relative settings.

Trial studies on different individuals were then performed. It was found that volume can be measured to within ±5L accuracy (see figure 8.5); but that larger errors occur during vivo studies.

Sources of error include:

- The ventilator requires time to warm up. (Time for the motor to get into a steady state).
- The air that the ventilator displaces is relatively constant compared to the human lung. However it is not designed to displace an absolute volume.
- With large subjects, the artificial lung tends to exhale the air faster due to a higher pressure. Hence it is difficult to distinguish between meaningful and unwanted signals (breathing, humidity).
- The ventilator is more than 15 years old.

Principle finding

The human subject claimed that they felt unconformable when using displacement of greater than 1.5 liters of air. With a rate slower than 10 cycles per minute a drift due to leakage becomes significant.

The ventilator provides a relatively accurate result compared to using a human lung for displacing the air, however it fails to provide a meaningful result in term of body composition analysis.

Conclusion

These three designs for air displacement have been investigated. None of them is able to measure the body volume to the level of accuracy (200ml) required for body composition analysis.

Although using subjects' own lungs as an air displacement device is simple and inexpensive, the air displacement with present equipment can only be determined to about 10ml. This results in larger variation in the calculated body volume. The ventilator is slightly more accurate in this regard but nevertheless not accurate enough.

An absolute constant pressure drive is needed, which can displace a known and constant volume of air in the chamber, regardless of the pressure inside the chamber.

When dealing with in vivo studies, it is essential to distinguish the signals that are either generated by the subject (temperature or humidity) or caused from the displacement from the pressure drive. Having a constant pressure drive allows us to filter out all unwanted signals.

These two methods described cannot provide accuracies high enough for practical use in body composition analysis.

Appendix F6 Theory of using the lung as a diaphragm for air displacement

Original formula: $V_{object} = P_{atm} \times \left(\frac{\Delta V}{\Delta P}\right) - P_{atm} \times \left(\frac{\Delta V_1}{\Delta P_1}\right)$

Using the human lung as a diaphragm ΔV, will provide a volume change as the subject breathes air in and out.

The inside pressure will be equal to atmospheric pressure as the door is closed. Once the person breaths in, the pressure will build up, and as he breathes out it will go down.

Determining the two chamber volume

The size of the empty test chamber is pre-determined by the water displacement method.

Pressure in the reference chamber is used as atmospheric pressure. Therefore the volume of the reference chamber is irrelevant.

The formula becomes

$$V_{object} = V_{chamber} - P_{atm} \times \left(\frac{\Delta V_1}{\Delta P_1}\right)$$

Where $\frac{\Delta V_1}{\Delta P_1}$ = ratio of change of volume to change in pressure for a test chamber containing a subject

Method of operation

1. Close the door.
2. Breath in and out.
3. Force breath in and hold for 3 seconds
4. Force breath out and hold for 3 seconds.
5. Open the door and introduce a calibration tool of known volume

Repeat the procedure again.

By comparing the two test results we are able to judge the accuracy of the measurement.

Temperature consideration

Air that is breathed in is warmed and humidified; hence it will occupy a larger volume in the lung than what is measured for ΔV_1 by the spirometer. This effect must be compensated for.

Appendix F7Trial steps for using lung to displace the air in the chamber

Please read the following information. This will help you to understand the test procedure hence help us to obtain the most accuracy results.

8. You will be given a "model breathing pattern". This will help you to learn how to breathe while inside the chamber, you will be given few chances to practice your breathing pattern

9. Take a few deep breaths then hold your breath, clamp your nose. Get into the chamber. Remember not to breathe into the chamber.

10. While you are inside the chamber you will find a pipe on your left hand side. You may only breathe though this pipe. Otherwise it could directly affect the result.

11. You will also find a push button on your right hand side. That is for you to release yourself after the experiment or at anytime when you feel discomfort.

12. Once you get into the chamber. Place your feet under the seat. Notice that there will be sensors just above your legs; please make sure you not touching them as it could also affect the result of the experiment.

13. Once the instructor has instructed you to start breathing though the pipe first breathe out and then breathe in. Try to avoid breathing too deeply neither too shallow.

14. After 8 cycles of breathing, you may press the button and come out of the chamber. The whole trial is then competed.

15. Trial will be preformed twice on each subject to ensure its consistency.

Appendix F8 Ventilator related information

Testing procedure for the chamber with the ventilator

1. Switch on the pressure sensor.
2. Open the "Labview" program.
3. Switch on the power for the magnetic lock of the door.
4. Pre-set the ventilator to standard configuration (check the ventilator configuration).
5. Switch on the ventilator. Turn the "peep" to set the proximal airway pressure gauge to about 40 mBar, hence the "plastic" lung is inflated before closing the door. (Peep stands for: positive end expiratory pressure).
6. Instruct the subject to step into the chamber and close the door.
7. The subject will breathe though the breathing pipe as instructed.
8. Adjust the "tidal volume" on the ventilator to 1 litre.
9. The collector for the breathing pipe on the chamber will be sealed; sampling and recording of the data will start.
10. The subject will be breathing into the chamber.
11. Follow the step to step instruction for software instruction (see appendix F11).
12. Remove the subject from the chamber and unseal the breathing pipe.
13. Check the data and save the data (see appendix F11).

Ventilator configuration

The I:E ratio=1:1

The I:E ratio represents the ratio of inspiratory time to expiratory time, from breath to breath.

In our case, we would like to keep the ratio at 1:1 so it have the same amount of time to breath in, as well as breath out.

The normal tidal volume=1 litre

The normal tidal volume represents the volume of the gas that is to be delivered to the "artificial lung".

The peep :(Proximal pressure to 20 mBar)

The peep is used to maintain a stable pressure inside "plastic lung", hence reducing the possible leakage of the chamber due to high pressures. Turn the peep up until the lung pressure is at 20.

Peak flow

Peak flow is calculated by the ratio of tidal volume time to normal rate time (factor of I:E ratio). In our case it would be 2(1+1) and the total peak flow equal 1times 30 times 2 =60 (LPM).

Appendix F9 Calibration procedure for the ADP Device

The operator will open the device and make sure the software mode is set to "perform a trial study" mode.

Estimating the size of the test chamber

During the first step, the PVC pipe from the pressure sensor is connected to the test chamber. The motor is then allowed to run. After the trial period, the values for the experienced pressure (ΔP) in the chamber is determined. This value is used to determine the chamber volume using the relationship between the changing volume and the change in pressure ($\frac{\Delta V}{\Delta P}$) (Note that this estimate contains errors; which are accommodated in the later calibration process)

Estimating the size of the reference chamber

The reference chamber is connected to the pressure sensor using a PVC pipe and the same process as above is followed. The size of the reference chamber is then calculated from the ($\frac{\Delta V}{\Delta P}$) relationship.

Determination of the offset of the device

The differential pressure transducer is connected between the test chamber and the reference chamber and a trial is performed. The result for the volume of the subject (V_B) becomes the new zero since there is no subject in the test chamber.

This offset value is used as the offset in the software. A second trial is obtained to check the offset is within 100ml from zero. If the result is not obtained within 100ml, the procedure will not be continued.

Determination of the coefficient in the curve fitting formula for the device

Put the calibration tool into the chamber. See the following table for the volume of inanimate subjects from a combination of calibration tools available.

Table F1

Combination of different volumes used in the calibration of the device

Calibration volume size (litres)	Combinations
60	60 litres brick of Styrofoam
74.85	60 +14.85 litre brick of Styrofoam
78.84	60 and 6×3.14 litres tube of styrofoam
87.41	60 +14.85 litres brick and 4×3.14 litres tube of styrofoam
90.55	60 +14.85 litres brick and 5×3.14 litres tube of styrofoam
93.69	60 +14.85 litres brick and 6×3.14 litres tube of styrofoam

Before starting the trial, make sure that "subject is bigger than 50" button is selected (This is designed since this is the volume where the pressure in the two chambers should cancel each other out. At this point, the signal to noise ratio will be very small, hence that any measurement around 50 litres should be avoided).

Change the atmospheric pressure (P_{atm}) mode to "manual input". (The number will be the first measurement from the barometer sensor). This is to execute the assumption of atmospheric pressure to remain constant during the whole calibration and trial period. The purpose is to reduce barometer random errors.

Two rounds of trials for each volume combination should be performed. For each volume, the variation between results must be less than 100ml. Once this is obtained, then the average of the experienced pressure (ΔP) of these two trials is used to represent the experienced pressure of the subject.

Once the ΔP's are determined for these subjects, the ratio of V_B to ΔP ($\frac{V_B}{\Delta P}$) is then plotted. A second order curve is fitted to the plotted points. The coefficient of this second order curve equation is used to be fed into the "ADP analysis.VI" sub-VI.

After successfully calibrating the device, two test trials should be performed by the user. The test trial result should be within 200ml of accuracy before performing an in vivo trial.

Appendix F10 Trial procedure of the ADP Device for the operator

1. Switch on the pressure sensor.
2. Check the position of the plunger mechanism.
3. Open the "Labview" program.
4. Switch on the power for the magnetic lock of the door.
5. Instruct the subject to step into the chamber and close the door.
6. The subject will be breathing into the chamber.
7. Follow the step by step instruction for software instruction (see appendix F11).
8. Start the software and the motor at the same time.
9. Remove the subject from the chamber and unseal the breathing pipe.
10. Check and save the data (see appendix F11).
11. Adjust the position of the plunger mechanism back to the starting position.

Appendix F11 Step by step instruction for operation of the software

1. Open Labview6.1.
2. Select "open VI" and open "ADP analysis.VI".
3. Select the software mode (default at "perform a trial study").
4. Select the test mode (default at "trial study).
5. Fill in the personal information sections on the front panel.

6. Press "run" to start the trial.
7. At the end of the trial, save the data into the desired name.

8. If trial is unsuccessful (indicator showing red),

8.1 Rerun the whole trial again.

If the software reports on wrong personal data input,

1. Correct the information.
2. Select the programming mode change the atmospheric pressure mode to manually input.
3. Use the indicated data from the pressure sensor as the manually input value.
4. Recall save the data.
5. Rerun the program.

If the trial is successful

1. Obtain the % body fat from the screen.
2. Obtain the BMI value from the screen.

Appendix G Further recommendation related

Appendix G1 Data sheet for PCI4451 and data sheet for Ashcroft sensor

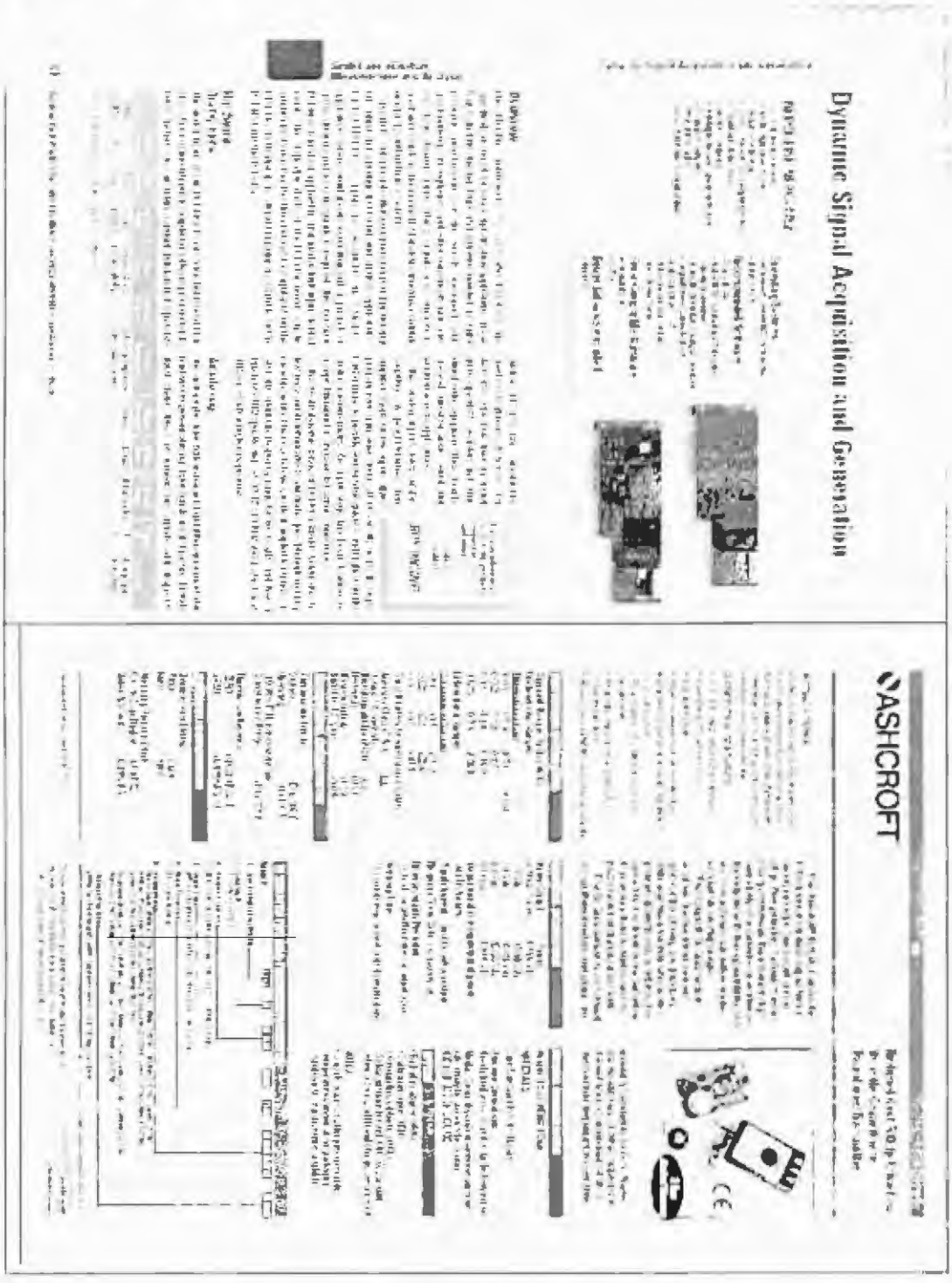

Appendix G2 Suggestions for further development

Stepper motor

For further development, the following components are required: Stepper motor, drive board and gear box.

The DC shunt motor used in the present design delivers 47lbs.ins (5.315N/m).

The following combinations are suggested which is sufficient for the interest of this project. See the following table for the basic description.

Table G1
Suggested specifications for further development

Components	Stepper motor	Drive board	Gear box
Supplier	R.S. Components		Microdyne
Stock number	340-3761	441-0287	N/A
Price	R3615-95	R6047-10	
Basic script	• 12 Volt HSX Hybrid Stepper Motor • 1.8 degree step angle (200steps/rev.) • Torque 7.8 N/m • Shaft Diameter. 9.525mm. x 28.6mm. • Motor current 4.5A/phase	6 Amp Bipolar Stepper Drive	86 x 86 Frame size with 3:1 ratio right angle box

The details of the stepper motor and its drive board can be obtained from R.S. components' (rswww.com) online catalogue.

Further request regarding to this gear box can be made to Microdyne Pty Ltd (www.microdyne.co.za).

Barometer

For suitable barometers see the following website for further information

- http://www.coastalenvironmental.com/cgi/index2.php?section=aviation&content=pdb
- http://www.driesen-kern.de/englischeseiten/products/miniaturedatalogger/plog125bengl.HTML

Both Web sites was last accessed on 2004/07/14.

Appendix H1 Engineering drawing for the chamber

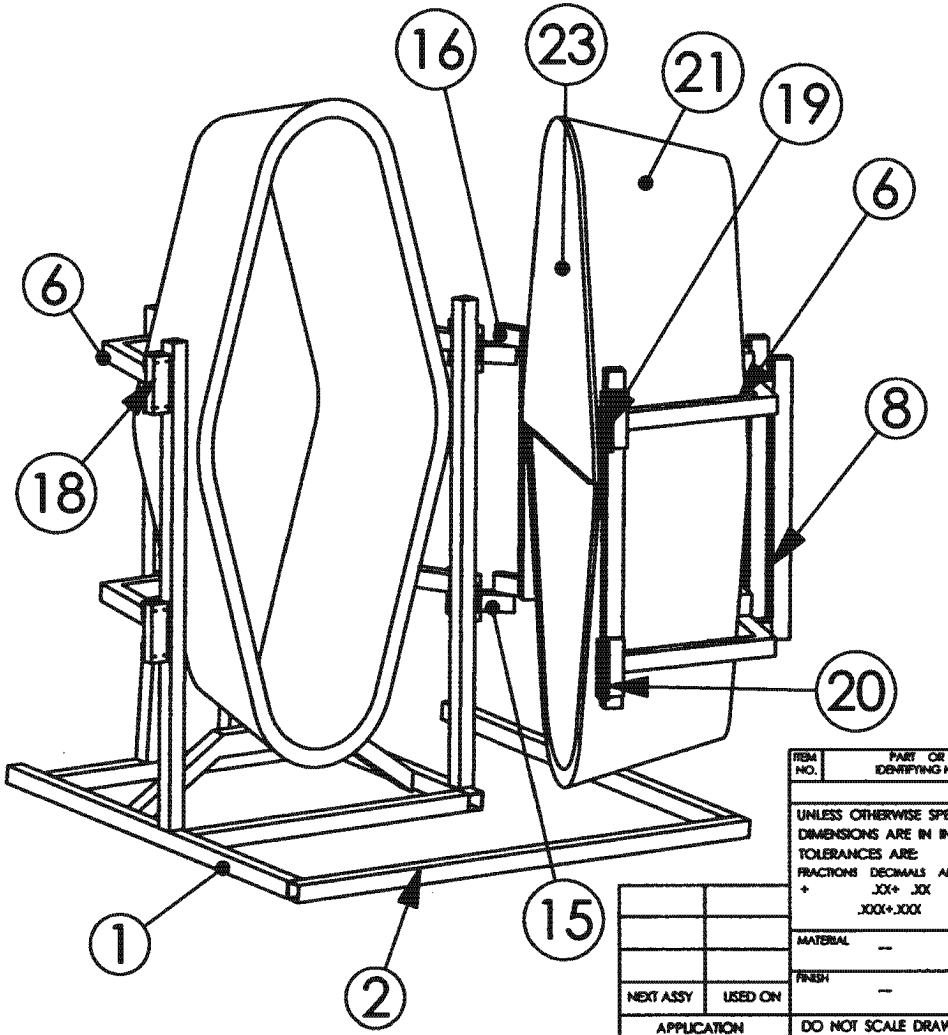

ITEM NO.	QTY.	PART NO.	DESCRIPTION
1	2	1300mm_tube_base	
2	1	1600mm_tube_base	
3	1	700mm_tube_base	
4	2	1100mm_tube_base	
5	1	U_bar_base	
6	4	U_bar	
7	8	40mm_tube	
8	4	800mm_tube	
9	2	1400mm_tube_right	
10	1	960mm_tube_left	
11	1	760mm_tube_Right_front	
12	2	500mm_tube_back	
13	2	Hinge_upper_fixed	
14	2	Hinge_upper_slider	
15	2	Hinge_lower	
16	2	Hinge_upper	
17	4	Magnet_support	
18	2	Magnet	
19	2	Magnet_Contact	
20	2	Contact_support	
21	2	Bath_tub	
22	1	Refferenc_chamber_base	
23	1	refference_chamber_front	

ITEM NO. | PART OR IDENTIFYING NO. | NOMENCLATURE OR DESCRIPTION | MATERIAL SPECIFICATION | QTY REQD

PARTS LIST

UNLESS OTHERWISE SPECIFIED DIMENSIONS ARE IN INCHES
TOLERANCES ARE:
FRACTIONS DECIMALS ANGLES
± .XX± .XX ± 1
.XXX±.XXX

MATERIAL —
FINISH —

NEXT ASSY | USED ON

APPLICATION | DO NOT SCALE DRAWING

CAD GENERATED DRAWING.
DO NOT MANUALLY UPDATE

APPROVALS	DATE
DRAWN	
CHECKED	
RESP ENG	
MFG ENG	
QUAL ENG	

UCT,BME - A.D.P. Analysis (Peter Ma)

Assembly of Chamber & Frame

SIZE A | DWG. NO. | REV.

Appendix H1 Engineering drawing for the chamber

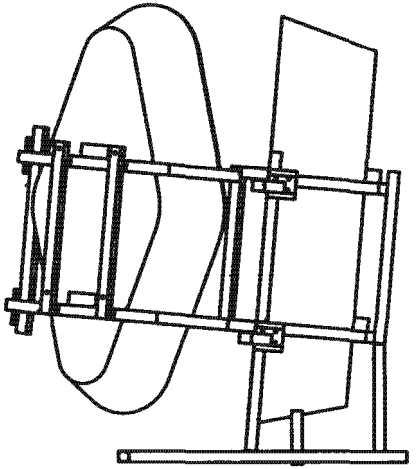

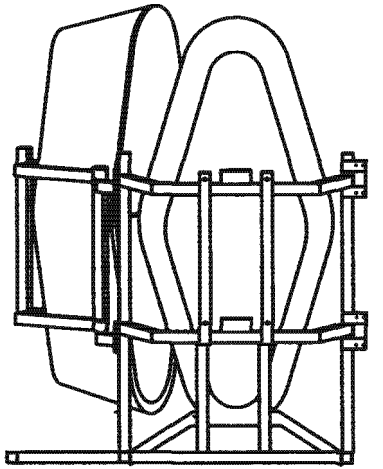

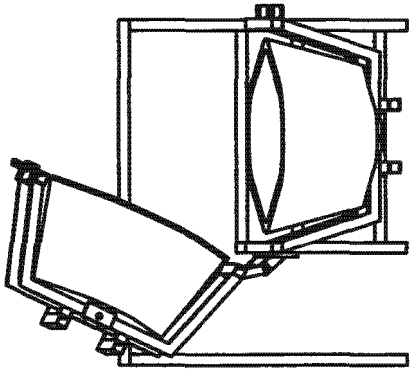

ITEM NO.	PART OR IDENTIFYING NO.	NOMENCLATURE OR DESCRIPTION	MATERIAL SPECIFICATION	QTY REQD

PARTS LIST

UNLESS OTHERWISE SPECIFIED
DIMENSIONS ARE IN INCHES
TOLERANCES ARE:
FRACTIONS DECIMALS ANGLES
± .XX± .XX ± 1
.XXX±.XXX

MATERIAL —

FINISH —

NEXT ASSY | USED ON

APPLICATION

DO NOT SCALE DRAWING

CAD GENERATED DRAWING.
DO NOT MANUALLY UPDATE

APPROVALS	DATE
DRAWN	
CHECKED	
RESP ENG	
MFG ENG	
QUAL ENG	

UCT,BME - A.D.P. Analysis (Peter Ma)

Chamber & Frame Assembly
(Orthographic view)

SIZE A | DWG. NO. | REV.

Appendix H1Engineering drawing for the chamber

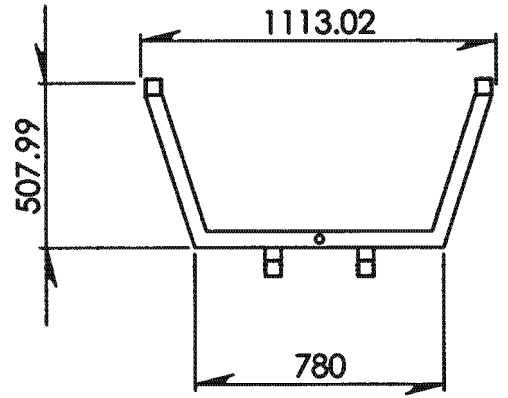

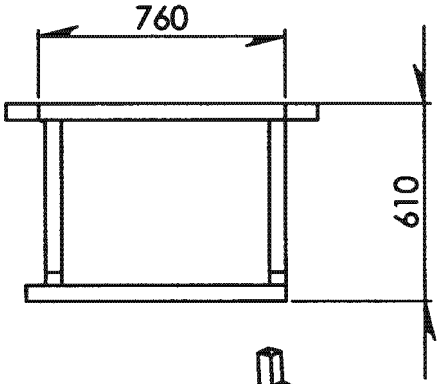

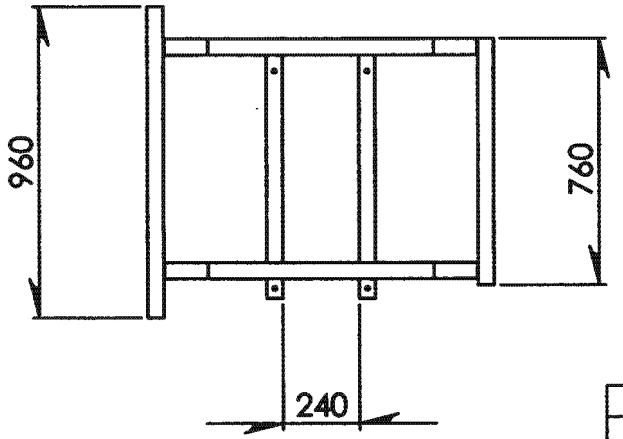

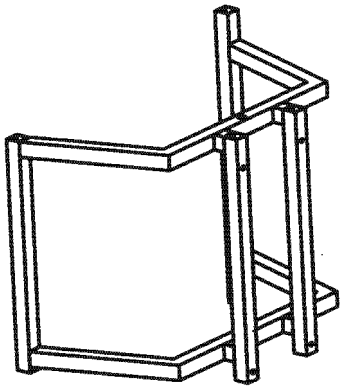

ITEM NO.	PART OR IDENTIFYING NO.	NOMENCLATURE OR DESCRIPTION	MATERIAL SPECIFICATION	QTY REQD

PARTS LIST

UNLESS OTHERWISE SPECIFIED DIMENSIONS ARE IN INCHES
TOLERANCES ARE:
FRACTIONS ± DECIMALS .XX± .XXX± ANGLES ± 1

MATERIAL ---

FINISH ---

DO NOT SCALE DRAWING

CAD GENERATED DRAWING. DO NOT MANUALLY UPDATE

APPROVALS	DATE
DRAWN	
CHECKED	
RESP ENG	
DWG ENG	
QUAL ENG	

UCT,BME - A.D.P. Analysis (Peter Ma)

Front Door Frame

NEXT ASSY	USED ON
APPLICATION	

SIZE A | DWG. NO. | REV.

Appendix H1Engineering drawing for the chamber

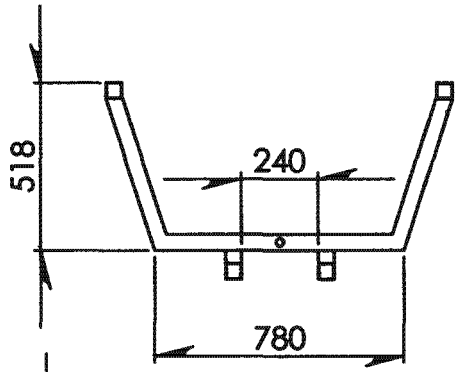

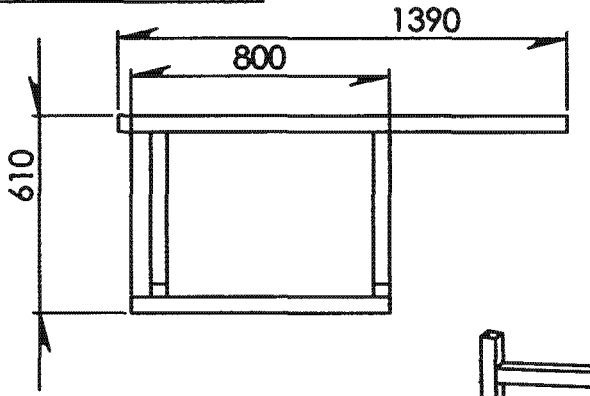

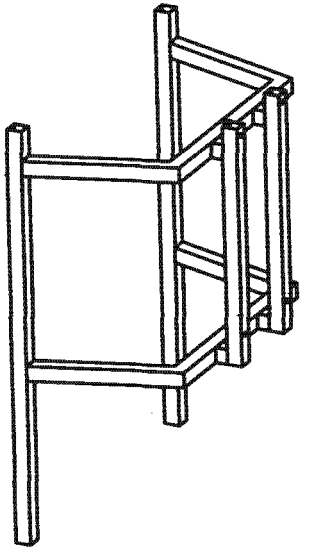

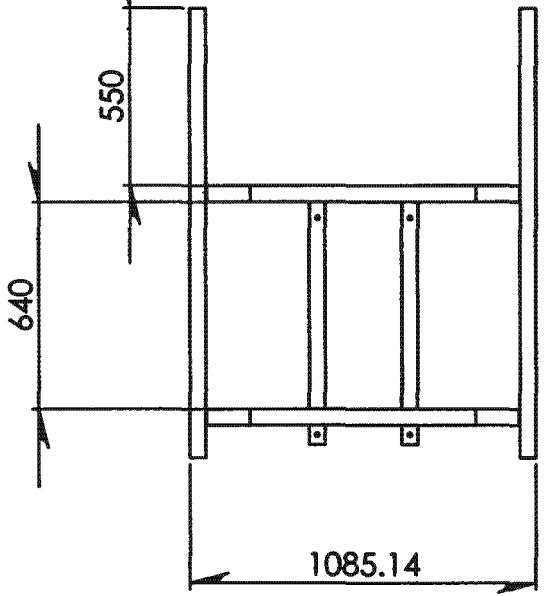

ITEM NO.	PART OR IDENTIFYING NO.	NOMENCLATURE OR DESCRIPTION	MATERIAL SPECIFICATION	QTY REQD

PARTS LIST

UNLESS OTHERWISE SPECIFIED DIMENSIONS ARE IN INCHES
TOLERANCES ARE:
FRACTIONS DECIMALS ANGLES
+ .XX+ .XX + 1
.XXX+.XXX

MATERIAL —

FINISH —

DO NOT SCALE DRAWING

CAD GENERATED DRAWING. DO NOT MANUALLY UPDATE

APPROVALS	DATE
DRAWN	
CHECKED	
RESP ENG	
MFG ENG	
QUAL ENG	

NEXT ASSY | USED ON

APPLICATION

UCT,BME - A.D.P. Analysis (Peter Ma)

Rear Door Frame

SIZE A | DWG. NO. | REV.

SCALE | CAD REF | SHEET OF

Appendix H1 Engineering drawing for the chamber

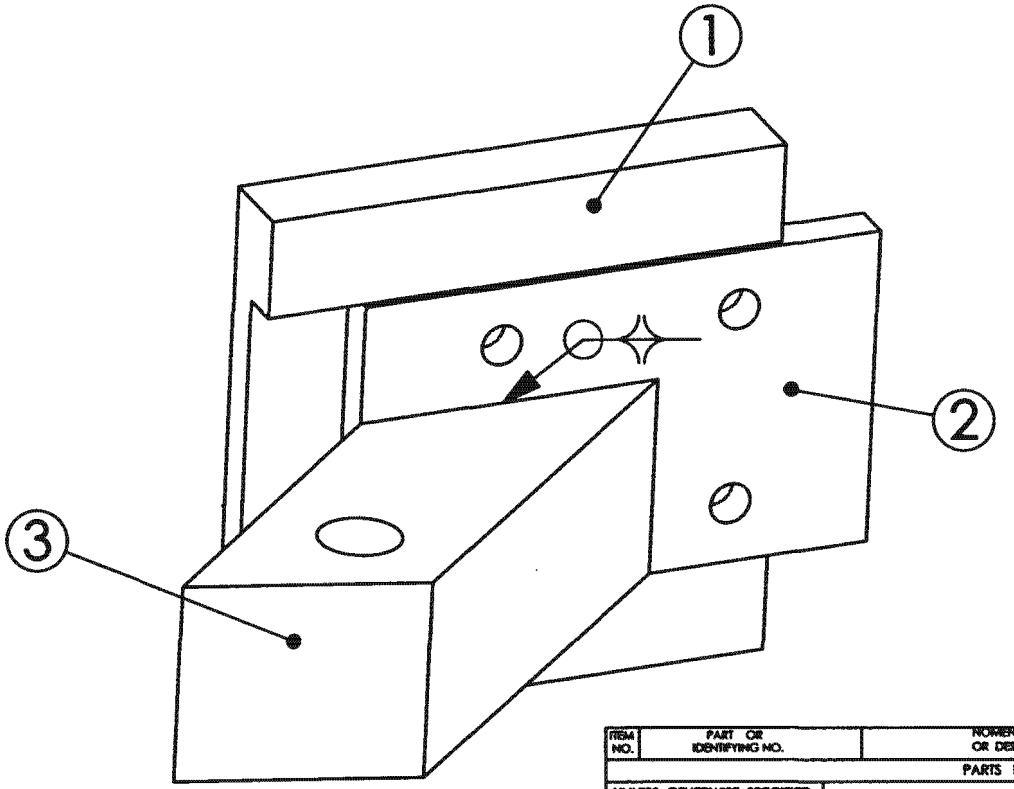

ITEM NO.	QTY.	PART NO.	DESCRIPTION
1	1	Hinge_upper_fixed	
2	1	Hinge_upper_slider	

ITEM NO.	PART OR IDENTIFYING NO.	NOMENCLATURE OR DESCRIPTION	MATERIAL SPECIFICATION	QTY REQD

PARTS LIST

UNLESS OTHERWISE SPECIFIED
DIMENSIONS ARE IN INCHES
TOLERANCES ARE:
FRACTIONS DECIMALS ANGLES
± .XX± .XX ± 1
.XXX±.XXX

MATERIAL —

FINISH —

DO NOT SCALE DRAWING

CAD GENERATED DRAWING.
DO NOT MANUALLY UPDATE

APPROVALS	DATE
DRAWN	
CHECKED	
RESP ENG	
MFG ENG	
QUAL ENG	

UCT.BME - A.D.P. Analysis (Peter Ma)

Hinge Assembly

SIZE	DWG. NO.	REV.
A		

NEXT ASSY	USED ON
APPLICATION	

Appendix H1Engineering drawing for the chamber

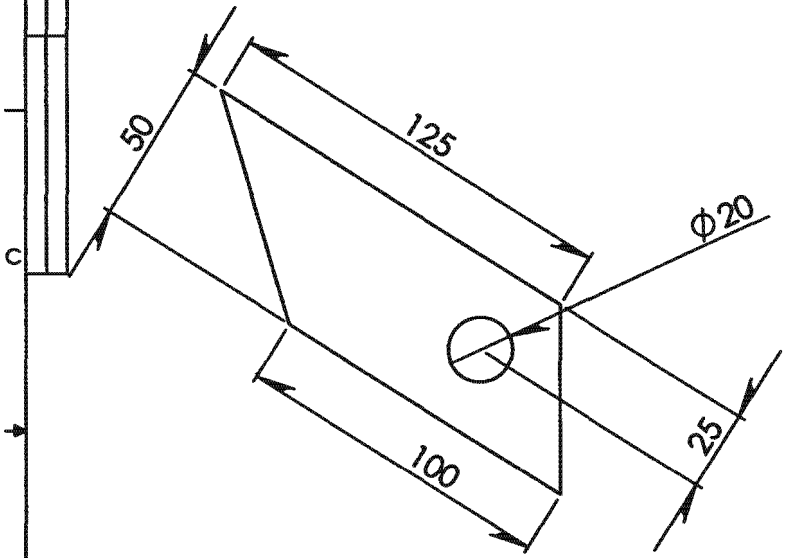

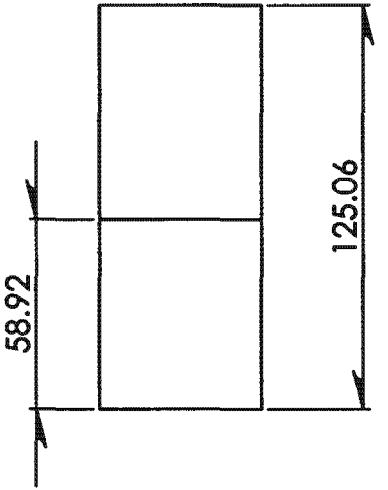

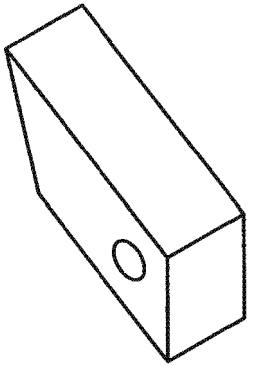

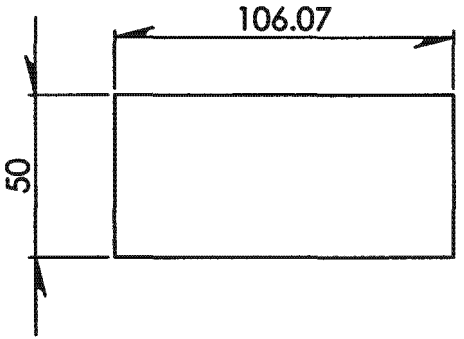

ITEM NO.	PART OR IDENTIFYING NO.	NOMENCLATURE OR DESCRIPTION	MATERIAL SPECIFICATION	QTY REQD

PARTS LIST

UNLESS OTHERWISE SPECIFIED DIMENSIONS ARE IN INCHES
TOLERANCES ARE:
FRACTIONS DECIMALS ANGLES
± .XX± .XX ± 1
.XXX±.XXX

MATERIAL ---

FINISH ---

DO NOT SCALE DRAWING

CAD GENERATED DRAWING, DO NOT MANUALLY UPDATE

APPROVALS	DATE
DRAWN	
CHECKED	
RESP ENG	
MFG ENG	
QUAL ENG	

UCT,BME - A.D.P. Analysis (Peter Ma)

Lower Hinge

NEXT ASSY	USED ON
APPLICATION	

SIZE	DWG. NO.	REV.
A		

Appendix H1Engineering drawing for the chamber

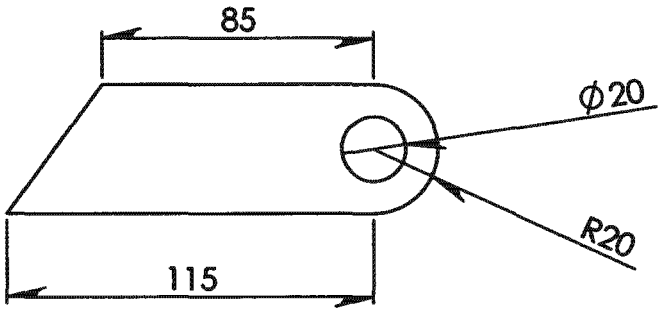

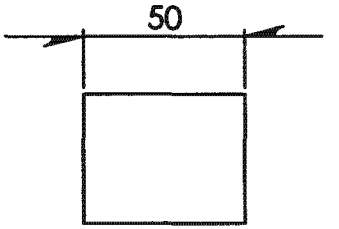

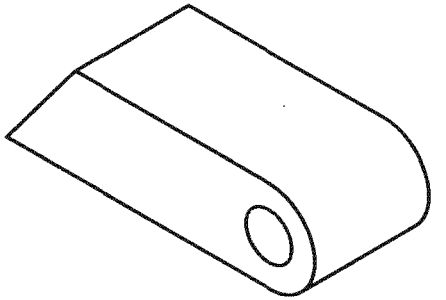

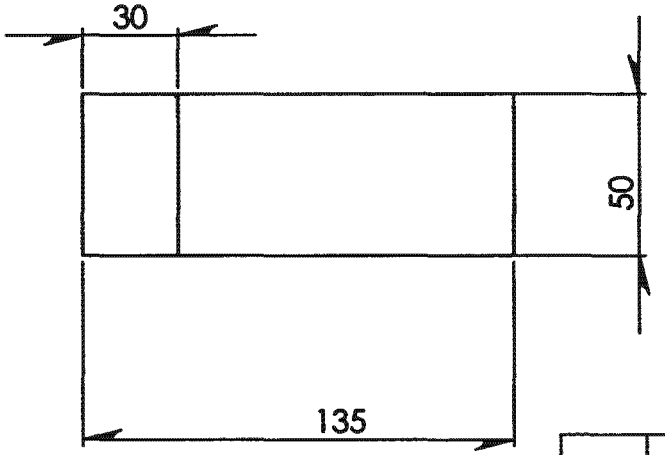

ITEM NO.	PART OR IDENTIFYING NO.	NOMENCLATURE OR DESCRIPTION	MATERIAL SPECIFICATION	QTY REQD

PARTS LIST

UNLESS OTHERWISE SPECIFIED
DIMENSIONS ARE IN INCHES
TOLERANCES ARE:
FRACTIONS DECIMALS ANGLES
± .XX± .XX ± 1
.XXX±.XXX

MATERIAL —

FINISH —

DO NOT SCALE DRAWING

CAD GENERATED DRAWING.
DO NOT MANUALLY UPDATE

APPROVALS	DATE
DRAWN	
CHECKED	
RESP ENG	
MFG ENG	
QUAL ENG	

UCT,BME - A.D.P. Analysis (Peter Ma)

Upper Hinge

NEXT ASSY	USED ON
APPLICATION	

SIZE	DWG. NO.	REV.
A		

SCALE: 1/4 SHEET 1 OF 1

Appendix H1Engineering drawing for the chamber

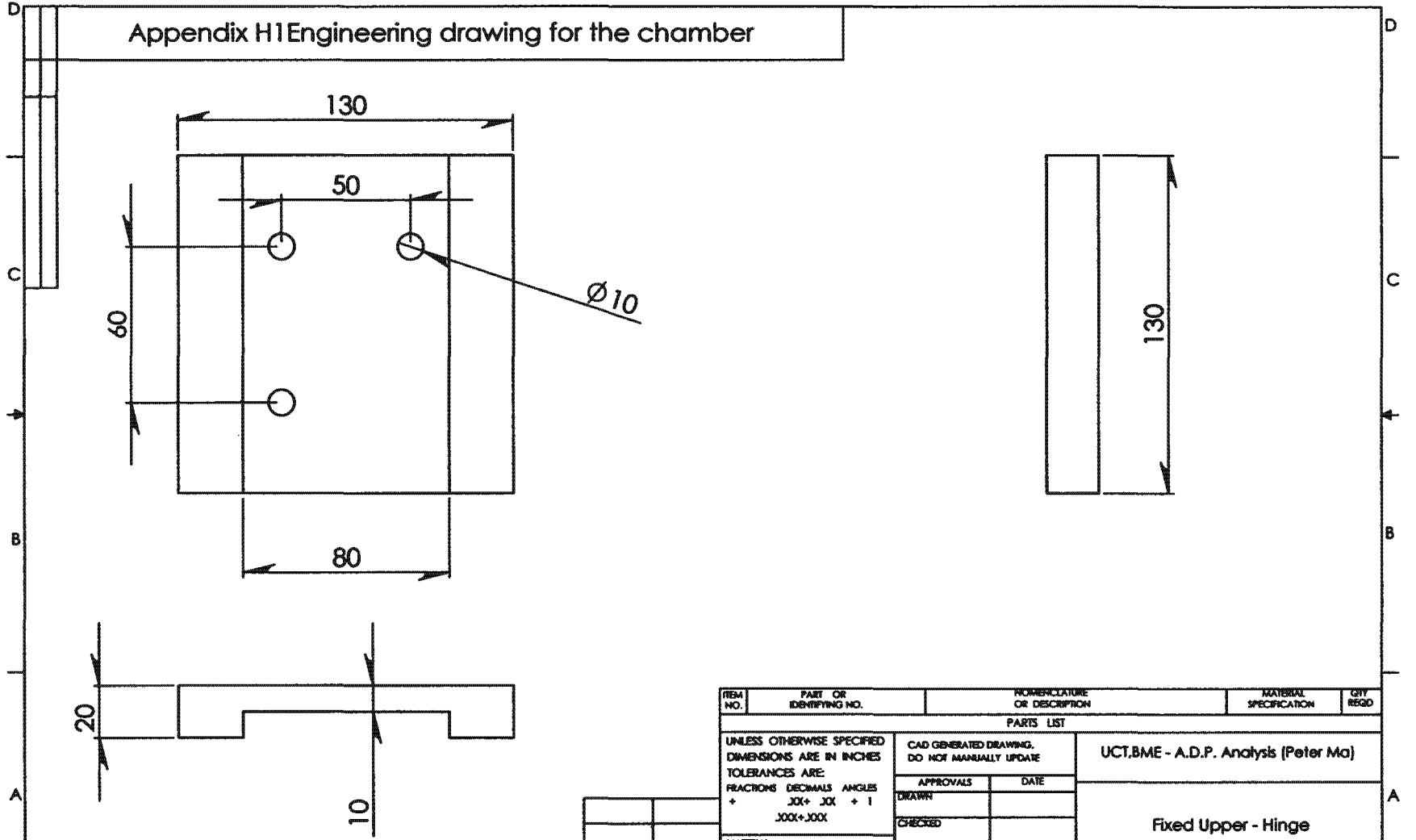

ITEM NO.	PART OR IDENTIFYING NO.	NOMENCLATURE OR DESCRIPTION	MATERIAL SPECIFICATION	QTY REQD

PARTS LIST

UNLESS OTHERWISE SPECIFIED DIMENSIONS ARE IN INCHES
TOLERANCES ARE:
FRACTIONS DECIMALS ANGLES
± .XX± .XX ± 1
.XXX±.XXX

MATERIAL —

FINISH —

DO NOT SCALE DRAWING

CAD GENERATED DRAWING. DO NOT MANUALLY UPDATE

APPROVALS	DATE
DRAWN	
CHECKED	
RESP ENG	
MFG ENG	
QUAL ENG	

UCT,BME - A.D.P. Analysis (Peter Ma)

Fixed Upper - Hinge

NEXT ASSY	USED ON

APPLICATION

SIZE A | DWG. NO. | REV.

Appendix H1Engineering drawing for the chamber

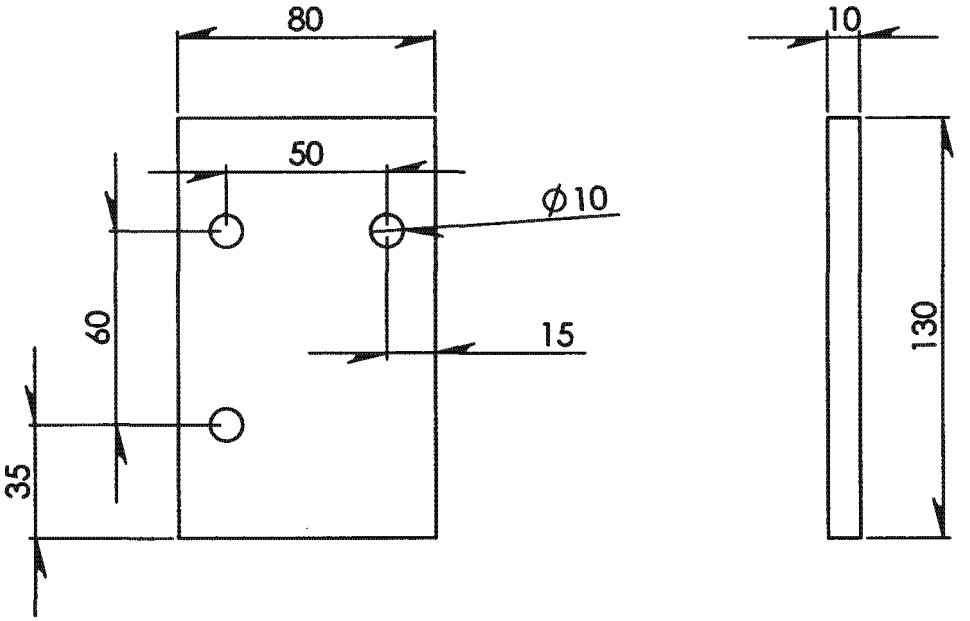

ITEM NO.	PART OR IDENTIFYING NO.	NOMENCLATURE OR DESCRIPTION	MATERIAL SPECIFICATION	QTY REQD
	PARTS LIST			

UNLESS OTHERWISE SPECIFIED DIMENSIONS ARE IN INCHES
TOLERANCES ARE:
FRACTIONS DECIMALS ANGLES
± .XX± .XX ± 1
.XXX±.XXX

MATERIAL —

FINISH —

DO NOT SCALE DRAWING

CAD GENERATED DRAWING.
DO NOT MANUALLY UPDATE

APPROVALS	DATE
DRAWN	
CHECKED	
RESP ENG	
MFG ENG	
QUAL ENG	

UCT,BME - A.D.P. Analysis (Peter Ma)

Sliding Upper Hinge

NEXT ASSY	USED ON

APPLICATION

SIZE A | DWG. NO. | REV.

Appendix H2 Engineering digram of the dual piston mechanism

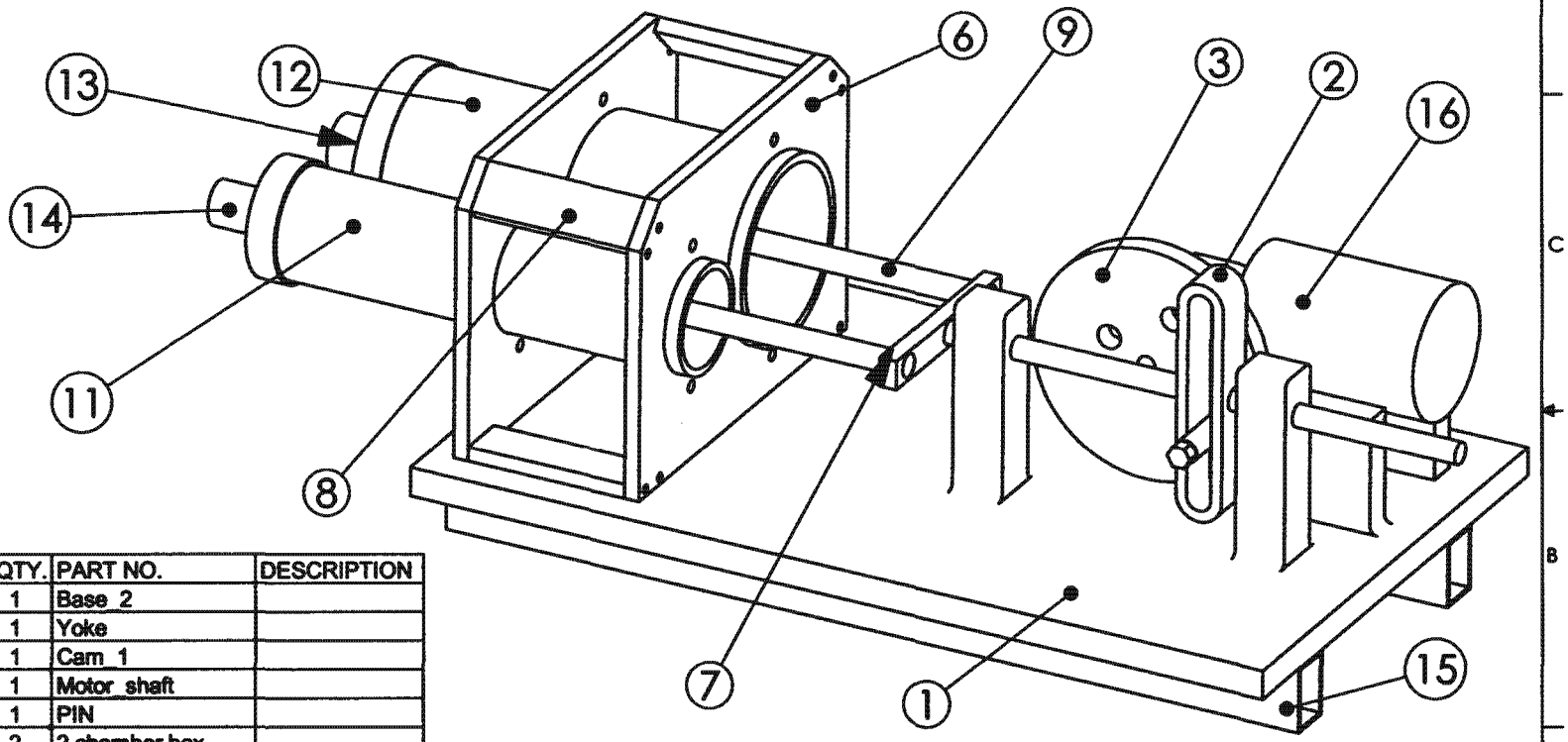

ITEM NO.	QTY.	PART NO.	DESCRIPTION
1	1	Base_2	
2	1	Yoke	
3	1	Cam_1	
4	1	Motor_shaft	
5	1	PIN	
6	2	2 chamber box	
7	1	2 chamber1	
8	4	2chamber box2	
9	1	2chamber2	
10	1	2 chamber2-1	
11	1	small chamber	
12	1	big chamber	
13	1	Piston_End	
14	1	Piston_End_small	
15	2	Al tube at base	
16	1	Motor	

ITEM NO.	PART OR IDENTIFYING NO.	NOMENCLATURE OR DESCRIPTION	MATERIAL SPECIFICATION	QTY REQD

PARTS LIST

UNLESS OTHERWISE SPECIFIED DIMENSIONS ARE IN INCHES
TOLERANCES ARE:
FRACTIONS DECIMALS ANGLES
± .XX± .XX ± 1
.XXX±.XXX

CAD GENERATED DRAWING. DO NOT MANUALLY UPDATE

APPROVALS	DATE
DRAWN	
CHECKED	
RESP ENG	
MFG ENG	
QUAL ENG	

MATERIAL —

FINISH —

DO NOT SCALE DRAWING

NEXT ASSY	USED ON
APPLICATION	

UCT,BME - A.D.P. Analysis (Peter Ma)

Motor & Piston mechanism Assembly

SIZE A | DWG. NO. | REV.

Appendix H2 Engineering digram of the dual piston mechanism

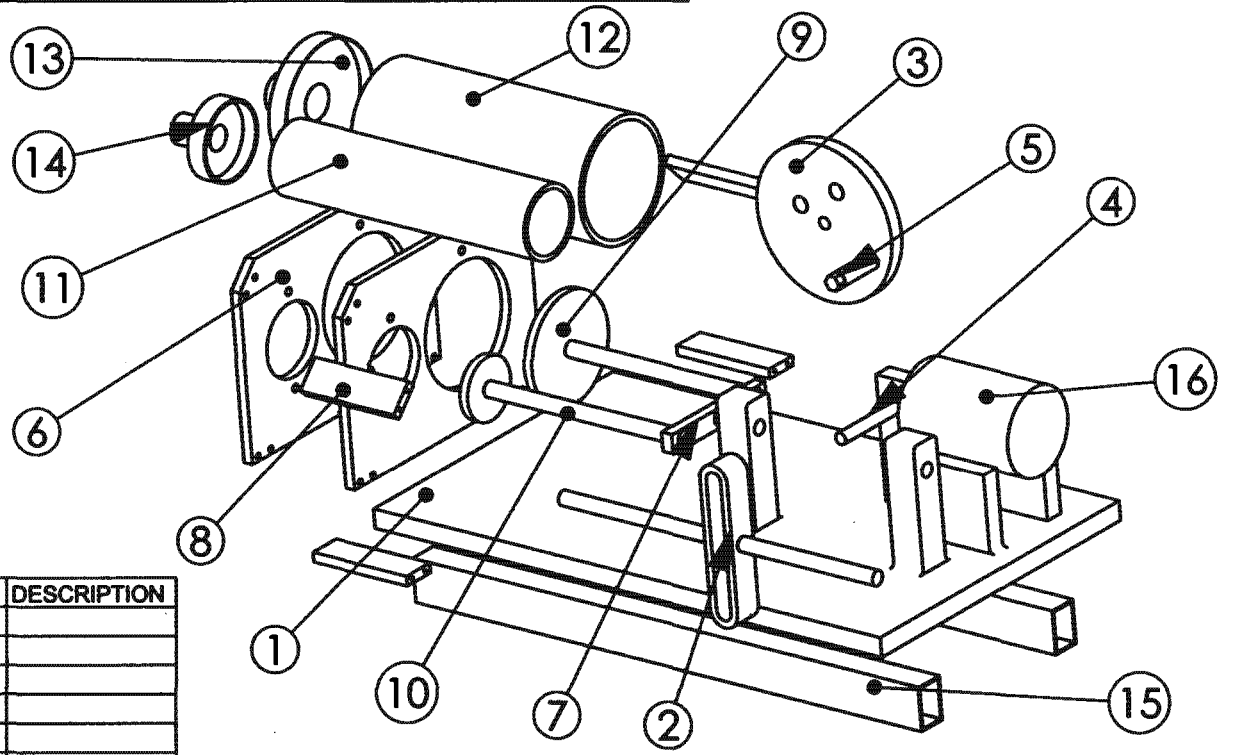

ITEM NO.	QTY.	PART NO.	DESCRIPTION
1	1	Base_2	
2	1	Yoke	
3	1	Cam_1	
4	1	Motor_shaft	
5	1	PIN	
6	2	2 chamber box	
7	1	2 chamber1	
8	4	2chamber box2	
9	1	2chamber2	
10	1	2 chamber2-1	
11	1	small chamber	
12	1	big chamber	
13	1	Piston_End	
14	1	Piston_End_small	
15	2	Al tube at base	
16	1	Motor	

ITEM NO.	PART OR IDENTIFYING NO.	NOMENCLATURE OR DESCRIPTION	MATERIAL SPECIFICATION	QTY REQD

PARTS LIST

UNLESS OTHERWISE SPECIFIED DIMENSIONS ARE IN INCHES
TOLERANCES ARE:
FRACTIONS ± DECIMALS .XX± .XXX ANGLES ± 1
.XXX±.XXX

MATERIAL —

FINISH —

DO NOT SCALE DRAWING

CAD GENERATED DRAWING. DO NOT MANUALLY UPDATE

APPROVALS	DATE
DRAWN	
CHECKED	
RESP ENG	
MFG ENG	
QUAL ENG	

NEXT ASSY	USED ON

APPLICATION

UCT,BME - A.D.P. Analysis (Peter Ma)

Motor & Piston Assembly
- Exploded view

SIZE A | DWG. NO. | REV.

Appendix H2 Engineering digram of the dual piston mechanism

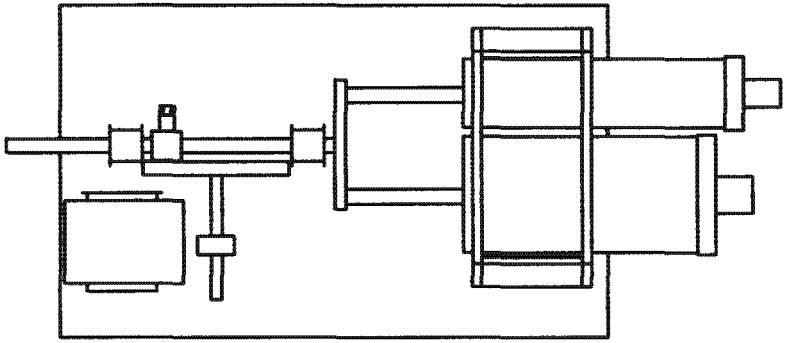

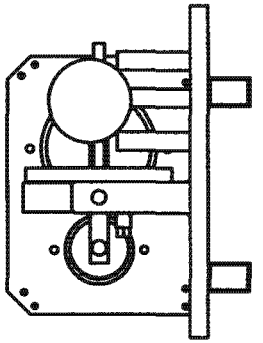

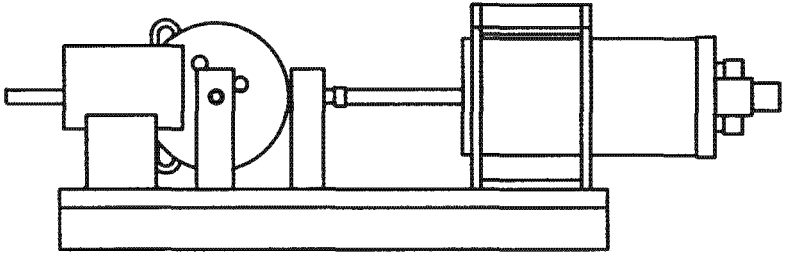

ITEM NO.	PART OR IDENTIFYING NO.	NOMENCLATURE OR DESCRIPTION	MATERIAL SPECIFICATION	QTY REQD
PARTS LIST				

UNLESS OTHERWISE SPECIFIED
DIMENSIONS ARE IN INCHES
TOLERANCES ARE:
FRACTIONS DECIMALS ANGLES
± .XX± .XX ± 1
.XXX±.XXX

MATERIAL —

FINISH —

DO NOT SCALE DRAWING

CAD GENERATED DRAWING.
DO NOT MANUALLY UPDATE

APPROVALS	DATE
DRAWN	
CHECKED	
RESP ENG	
MFG ENG	
QUAL ENG	

UCT,BME - A.D.P. Analysis (Peter Ma)

Motor & Piston mechanism
Assembly Orthographic View

NEXT ASSY	USED ON

APPLICATION

SIZE A | DWG. NO. | REV.

SCALE | WEIGHT | SHEET OF

Appendix H2 Engineering digram of the dual piston mechanism

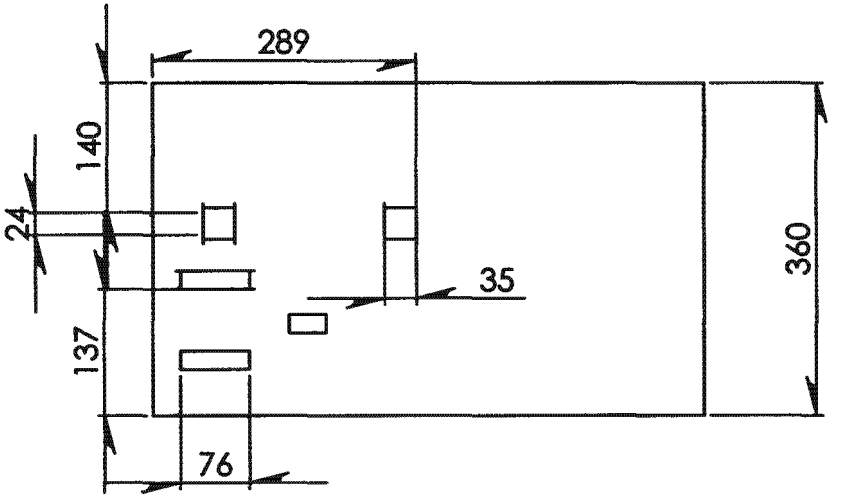

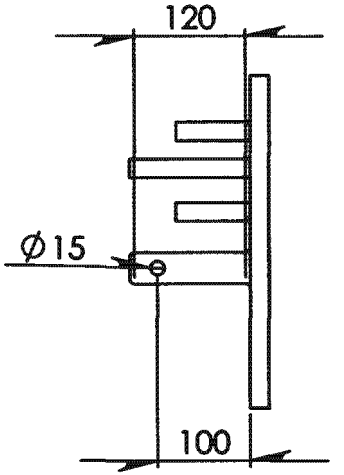

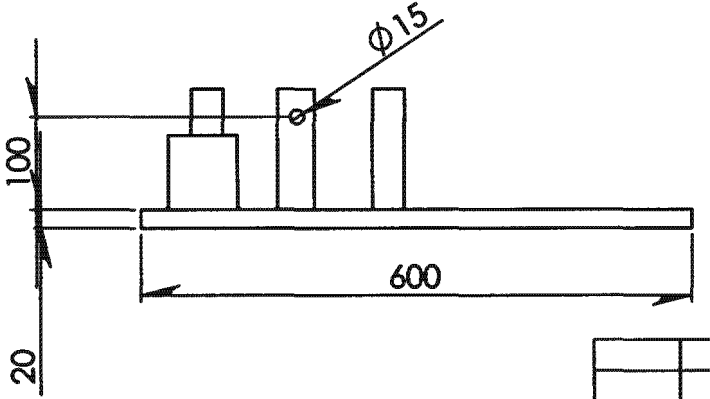

ITEM NO.	PART OR IDENTIFYING NO.	NOMENCLATURE OR DESCRIPTION	MATERIAL SPECIFICATION	QTY REQD
		PARTS LIST		

UNLESS OTHERWISE SPECIFIED DIMENSIONS ARE IN INCHES
TOLERANCES ARE:
FRACTIONS DECIMALS ANGLES
± .XX± .XX ± 1
.XXX±.XXX

MATERIAL —

FINISH —

DO NOT SCALE DRAWING

CAD GENERATED DRAWING.
DO NOT MANUALLY UPDATE

APPROVALS	DATE
DRAWN	
CHECKED	
RESP ENG	
MFG ENG	
QUAL ENG	

UCT,BME - A.D.P. Analysis (Peter Ma)

Base

NEXT ASSY	USED ON

APPLICATION

SIZE	DWG. NO.	REV.
A		

SCALE LOAD FILE SHEET OF

Appendix H2 Engineering digram of the dual piston mechanism

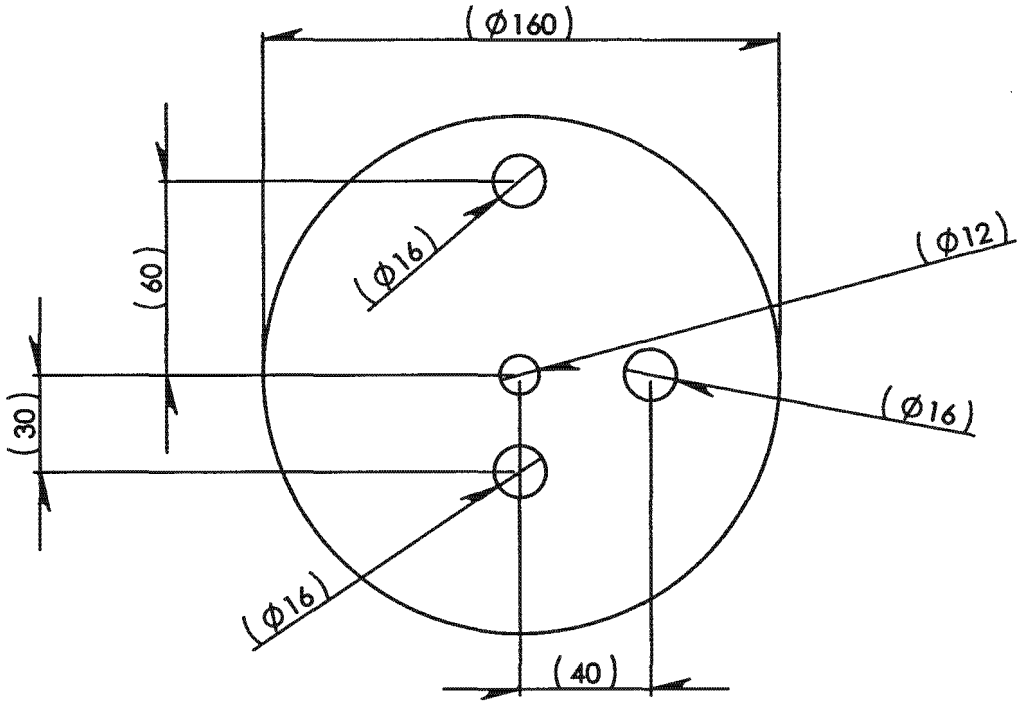

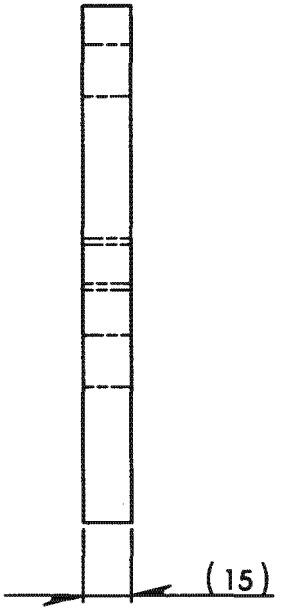

ITEM NO.	PART OR IDENTIFYING NO.	NOMENCLATURE OR DESCRIPTION	MATERIAL SPECIFICATION	QTY REQD
		PARTS LIST		

UNLESS OTHERWISE SPECIFIED
DIMENSIONS ARE IN INCHES
TOLERANCES ARE:
FRACTIONS DECIMALS ANGLES
± .XX± .XX ± 1
.XXX±.XXX

CAD GENERATED DRAWING.
DO NOT MANUALLY UPDATE

APPROVALS	DATE
DRAWN	
CHECKED	
RESP ENG	
MFG ENG	
QUAL ENG	

UCT,BME - A.D.P. Analysis (Peter Ma)

Cam

NEXT ASSY	USED ON

MATERIAL —

FINISH —

APPLICATION

DO NOT SCALE DRAWING

SIZE	DWG. NO.	REV.
A		

SCALE | CAD FILE | SHEET | OF

242

Appendix H2 Engineering digram of the dual piston mechanism

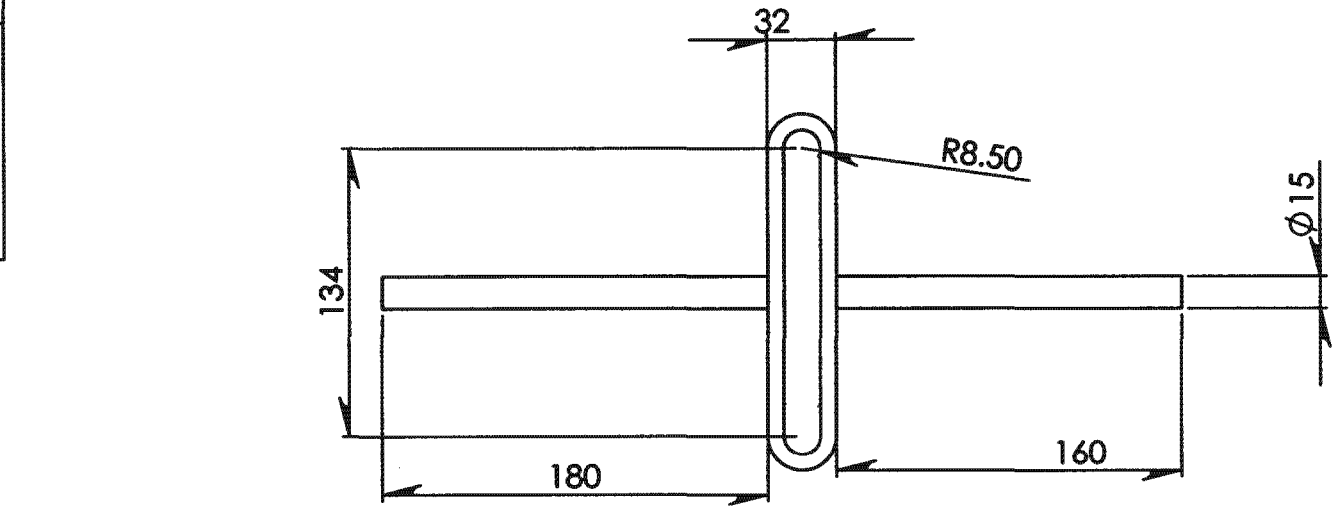

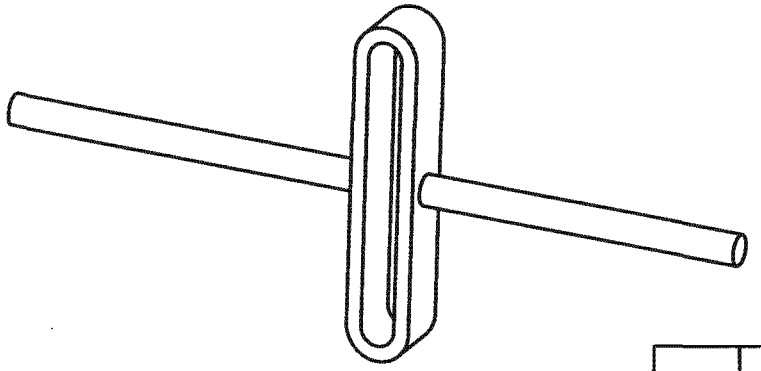

ITEM NO.	PART OR IDENTIFYING NO.	NOMENCLATURE OR DESCRIPTION	MATERIAL SPECIFICATION	QTY REQD

PARTS LIST

UNLESS OTHERWISE SPECIFIED DIMENSIONS ARE IN INCHES
TOLERANCES ARE:
FRACTIONS DECIMALS ANGLES
± .XX± .XX ± 1
.XXX±.XXX

CAD GENERATED DRAWING, DO NOT MANUALLY UPDATE

APPROVALS	DATE
DRAWN	
CHECKED	
RESP ENG	
MFG ENG	
QUAL ENG	

UCT,BME - A.D.P. Analysis (Peter Ma)

Yoke

NEXT ASSY	USED ON

MATERIAL ---

FINISH ---

APPLICATION

DO NOT SCALE DRAWING

SIZE A | DWG. NO. | REV.

SCALE | CAD FILE | SHEET | OF

Appendix H2 Engineering digram of the dual piston mechanism

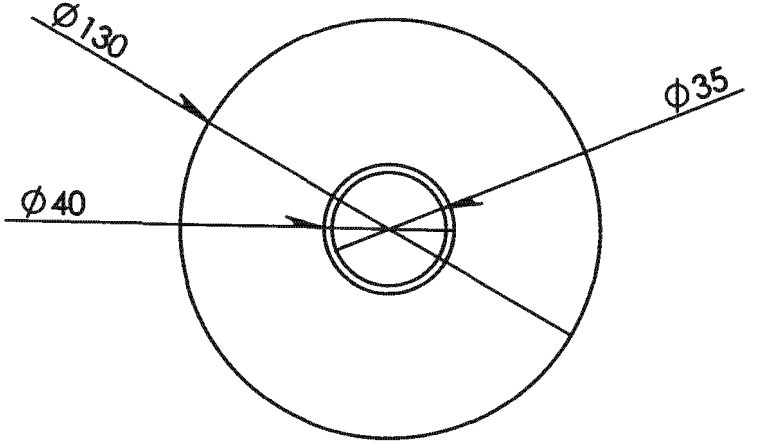

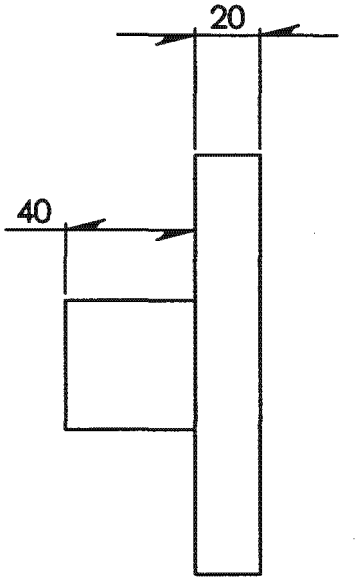

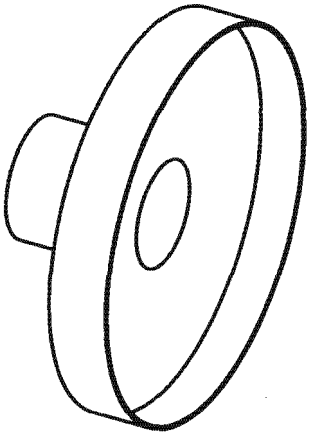

ITEM NO.	PART OR IDENTIFYING NO.	NOMENCLATURE OR DESCRIPTION	MATERIAL SPECIFICATION	QTY REQD

PARTS LIST

UNLESS OTHERWISE SPECIFIED DIMENSIONS ARE IN INCHES
TOLERANCES ARE:
FRACTIONS DECIMALS ANGLES
± .XX± .XX ± 1
.XXX±.XXX

MATERIAL —

FINISH —

DO NOT SCALE DRAWING

CAD GENERATED DRAWING. DO NOT MANUALLY UPDATE

APPROVALS	DATE
DRAWN	
CHECKED	
RESP ENG	
MFG ENG	
QUAL ENG	

NEXT ASSY	USED ON
APPLICATION	

UCT,BME - A.D.P. Analysis (Peter Ma)

Piston End Cap

SIZE	DWG. NO.	REV.
A		

Appendix H2 Engineering digram of the dual piston mechanism

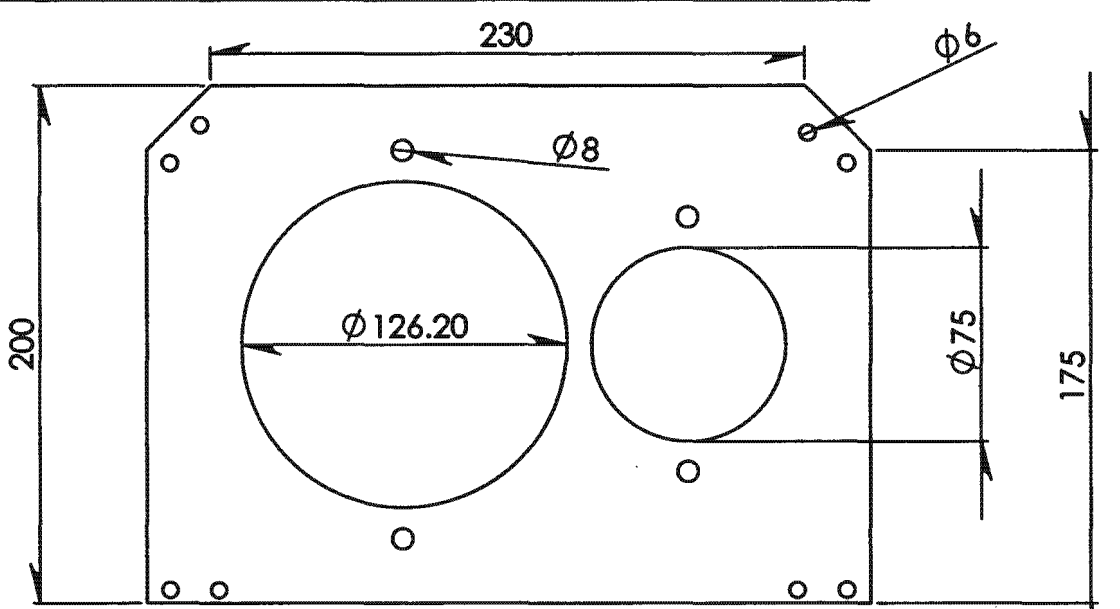

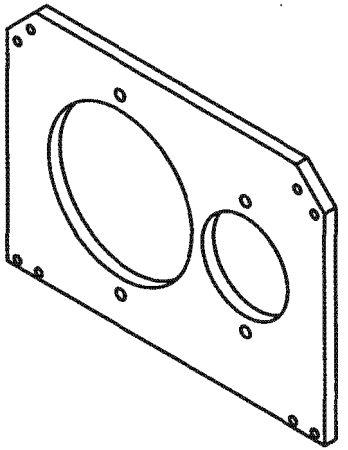

ITEM NO.	PART OR IDENTIFYING NO.	NOMENCLATURE OR DESCRIPTION	MATERIAL SPECIFICATION	QTY REQD

PARTS LIST

UNLESS OTHERWISE SPECIFIED DIMENSIONS ARE IN INCHES
TOLERANCES ARE:
FRACTIONS DECIMALS ANGLES
± .XX± .XX ± 1
.XXX±.XXX

MATERIAL —

FINISH —

DO NOT SCALE DRAWING

CAD GENERATED DRAWING, DO NOT MANUALLY UPDATE

APPROVALS	DATE
DRAWN	
CHECKED	
ENGR ENG	
MFG ENG	
QUAL ENG	

UCT,BME - A.D.P. Analysis (Peter Ma)

Piston box

NEXT ASSY	USED ON
APPLICATION	

SIZE A | DWG. NO. | REV.

Appendix H2 Engineering digram of the dual piston mechanism

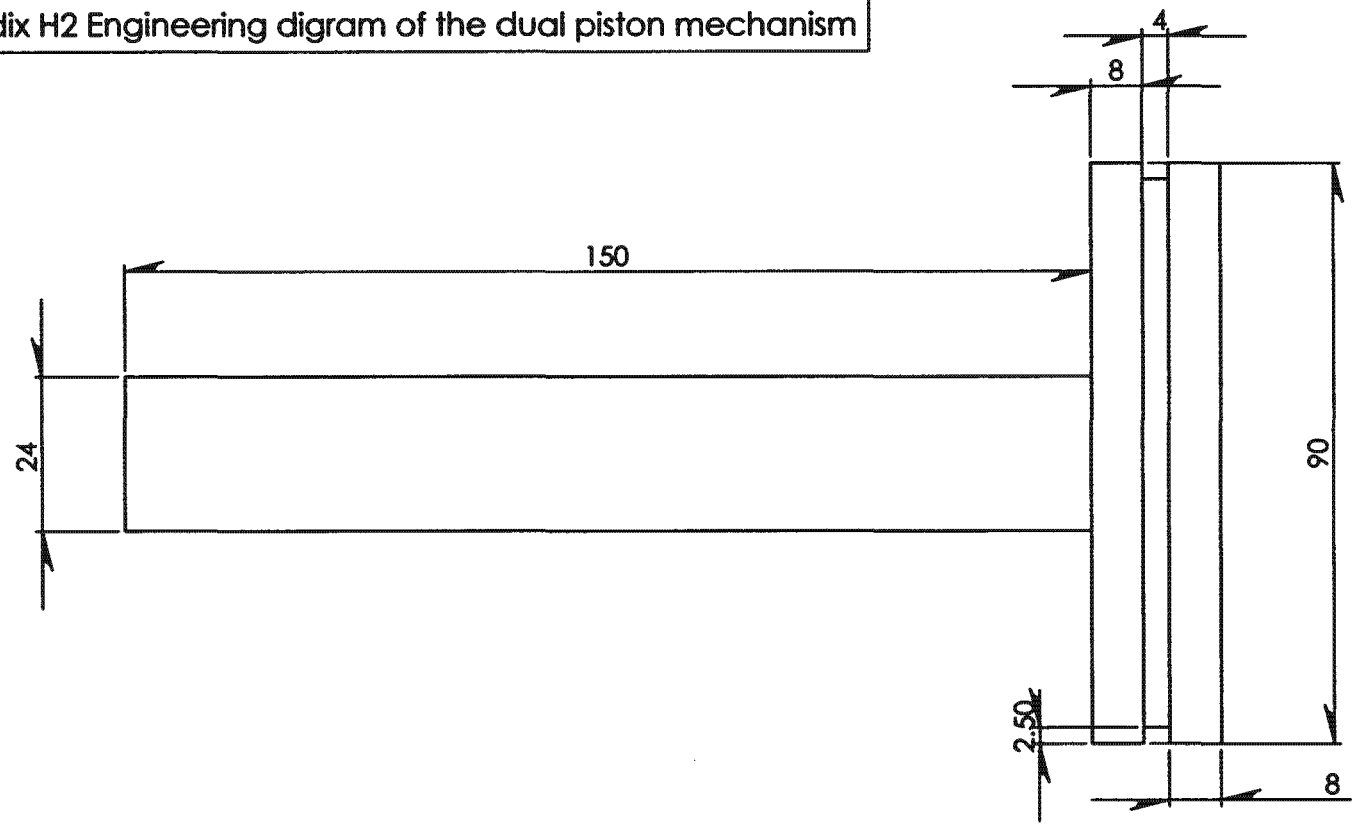

ITEM NO.	PART OR IDENTIFYING NO.	NOMENCLATURE OR DESCRIPTION	MATERIAL SPECIFICATION	QTY REQD

PARTS LIST

UNLESS OTHERWISE SPECIFIED DIMENSIONS ARE IN INCHES
TOLERANCES ARE:
FRACTIONS DECIMALS ANGLES
± .XX± .XX ± 1
.XXX±.XXX

MATERIAL —

FINISH —

DO NOT SCALE DRAWING

CAD GENERATED DRAWING. DO NOT MANUALLY UPDATE

APPROVALS	DATE
DRAWN	
CHECKED	
ENGR ENG	
MFG ENG	
QUAL ENG	

NEXT ASSY	USED ON

APPLICATION

UCT.BME - A.D.P. Analysis (Peter Ma)

Piston

SIZE A | DWG. NO. | REV.

SCALE | CAD FILE | SHEET | OF

Appendix I Hardware design elements; an ergonomics perspective

The following issues regarding the design of the hardware are proposed at various sections in the text:

1. The device should be designed in such a way that each component is interlinked but independent with each other i.e. each of the elements can be separately removed from the system.
2. As this is a health monitoring device rather than a life supporting device, the level of acceptance among its target subjects should also be considered
3. The seal should be evenly compressed, hence preventing any unknown leakages.

The following photos are used to illustrate how these ideas are put to practice.

Figure I1 Host connector between the chamber and the piston

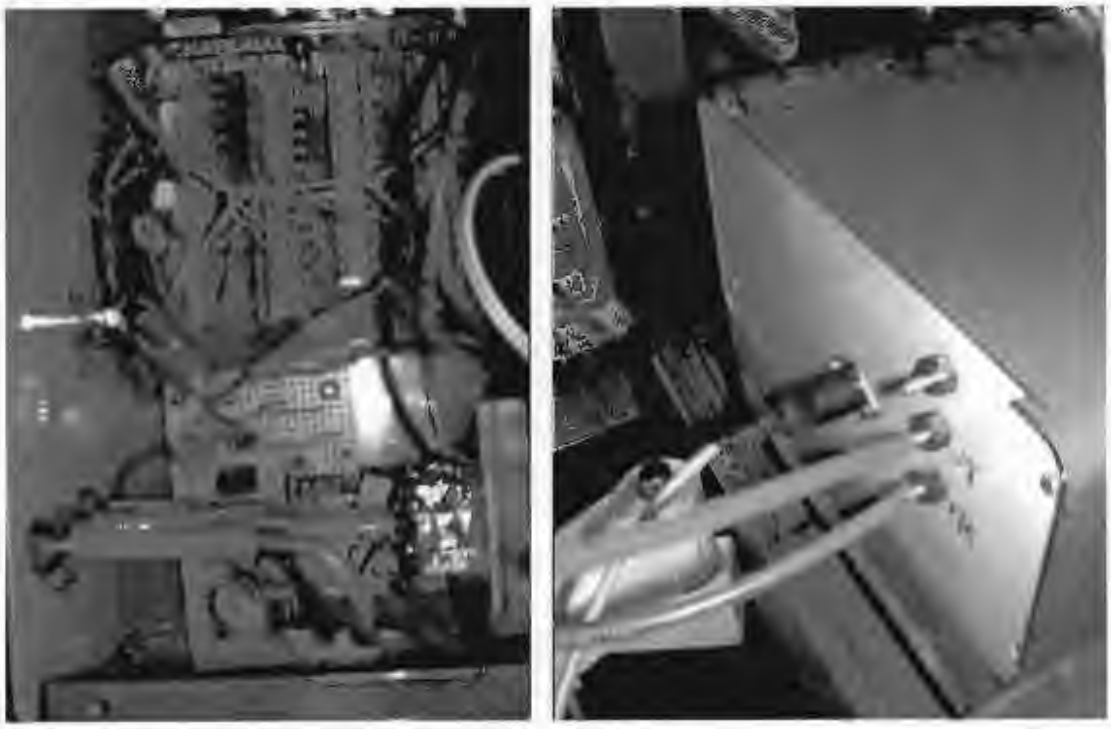

Figure I2 Tapered connecter for the PVC Pipe

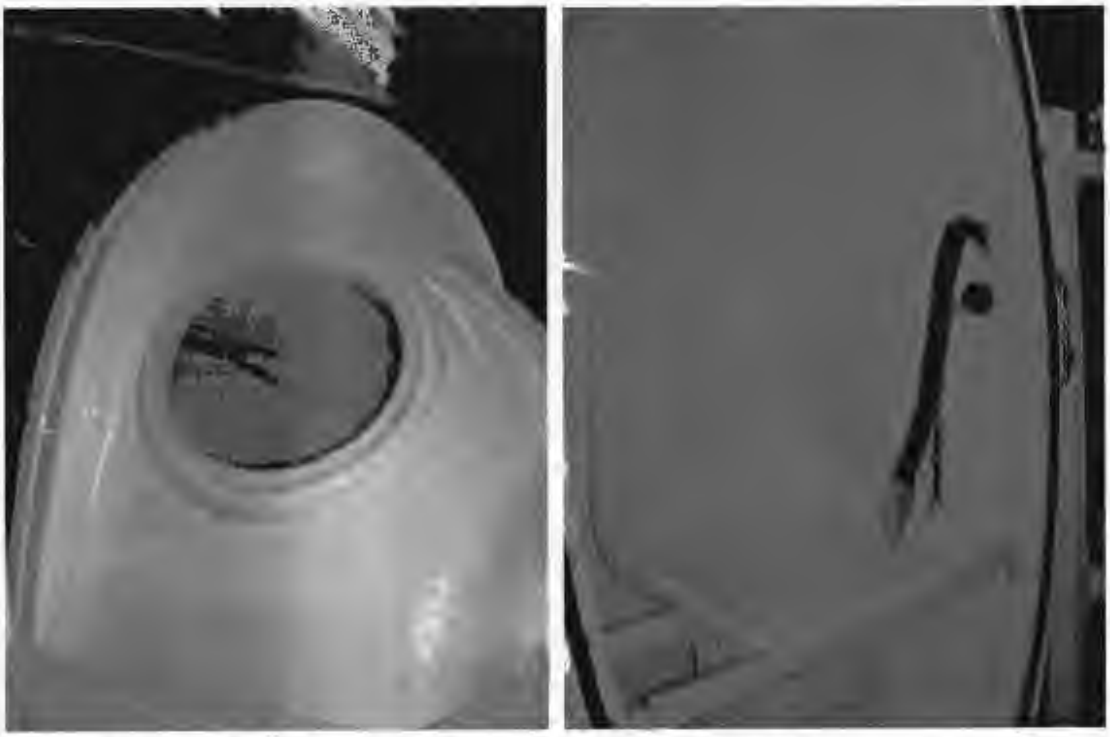

Figure I3 Window (left) and the Breathing pipe (right)

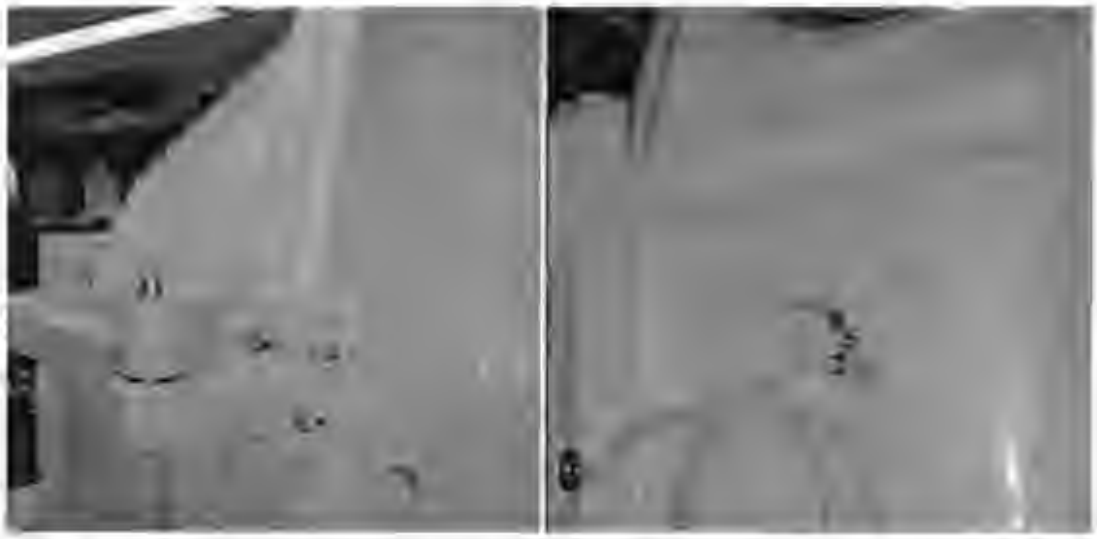

Figure I4 Door hinge (left) and the release valve for the leakage (right)

Figure I5 Clamp (left) and the safety switch (right)

All interfaces between elements were threaded and tapered. This ensures that the elements to be separated easily from each other and prevents any unknown leakages. The window, clamp and the safety switch add aesthetic value to the chamber allowing greater acceptance among subjects. The hinge design allows even compression of the airtight seal.